INDOOR POSITIONING MODEL BASED ON PEOPLE EFFECT AND RAY TRACING PROPAGATION

FIRDAUS

UNIVERSITI TEKNOLOGI MALAYSIA

INDOOR POSITIONING MODEL BASED ON PEOPLE EFFECT AND RAY TRACING PROPAGATION

FIRDAUS

A thesis submitted in fulfilment of the
requirements for the award of the degree of
Doctor of Philosophy

Razak Faculty of Technology and Informatics
Universiti Teknologi Malaysia

JULY 2020

DEDICATION

This thesis is dedicated to my mother and father,
Bapak Sabikun and Ibu Ina Sartinah,
Bapak Soendjojohadi and Ibu Sri Widajati.
Who taught me that the best type of knowledge
to have is that which can benefit life.
It is also dedicated to my wife and children,
Idha Arfianti, Asma, Husna, Hafshoh.
Who taught me to always struggle with love
and patience to achieve my dreams.

ACKNOWLEDGEMENT

First and foremost, I show gratitude to ALLAH the Almighty SWT who provided me with the strength, direction, and purpose throughout this study and throughout my life. I also wish to express my sincere appreciation to all those who have helped me—in one way or another—to complete this study.

My special thanks and appreciation go to my supervisor Dr. Noor Azurati Ahmad @ Salleh for all her patience, guidance, support and trust during the execution of this study. Through her guidance, I was able to overcome all the obstacles that I encountered in the difficult phases of my study. In fact, she always gave me immense hope every time I consulted with her on everything relating to my study and my life abroad. Not to forget, many thanks also to my second supervisor, Prof. Dr. Shamsul bin Sahibuddin, for his guidance and support. My thanks also go to all of the UTM staff, as well as the academic and administrative staff, for their kindness and cooperation in facilitating my study.

Finally, I wish to express my thanks to Universiti Teknologi Malaysia (UTM) and Universitas Islam Indonesia (UII) for funding this study.

ABSTRACT

WLAN-fingerprinting has been highlighted as the preferred technology in an Indoor Positioning System (IPS) due to its accurate positioning results and minimal infrastructure cost. However, the accuracy of IPS fingerprinting is highly influenced by the fluctuation in signal strength as a result of encountering obstacles. Many researchers have modelled static obstacles such as walls and ceilings, but hardly any have modelled the effect of people presence as an obstacle although the human body significantly impacts signal strength. Hence, the people presence effect must be considered to obtain highly accurate positioning results. Previous research proposed a model that only considered the direct path between the transmitter and the receiver. However, for indoor propagation, multipath effects such as reflection can also have a significant influence, but were not considered in past work. Therefore, this research proposes an accurate indoor positioning model that considers people presence using a ray tracing (AIRY) model in a dynamic environment which relies on existing infrastructure. Three solutions were proposed to construct AIRY: an automatic radio map using ray tracing (ARM-RT), a new human model in ray tracing (HUMORY), and a people effect constant for received signal strength indicator (RSSI) adaptation. At the offline stage, 30 RSSIs were recorded at each point using a smartphone to create a radio map database (523 points). The real-time RSSI was then compared to the radio map database at the online stage using MATLAB software to determine the user position (65 test points). The proposed model was tested at Level 3 of Razak Tower, UTM Kuala Lumpur (80 × 16 m). To test the influence of people presence, the number, position, and distance of the people around the mobile device (MD) were varied. The results showed that the closer the people were to the MD in both the Line of Sight (LOS) and Non-LOS position, the greater the decrease in RSSI, in which the increment number of people will increase the amount of reflection signals to be blocked. The signal strength reduction started from 0.5 dBm with two people and reached 0.9 dBm with seven people. In addition, the ray tracing model produced smaller errors on RSSI prediction than the multi-wall model when considering the effect of people presence. The k-nearest neighbour (KNN) algorithm was used to define the position. The initial accuracy was improved from 2.04 m to 0.57 m after people presence and multipath effects were considered. In conclusion, the proposed model successfully increased indoor positioning accuracy in a dynamic environment by overcoming the people presence effect.

ABSTRAK

WLAN-cap jari telah diserlahkan sebagai teknologi pilihan dalam Sistem Kedudukan Dalam Bangunan (IPS) kerana hasil penentuan kedudukan yang tepat dan kos infrastruktur yang minimum. Walau bagaimanapun, ketepatan pengecapan jari IPS sangat dipengaruhi oleh turun naik kekuatan isyarat akibat merentasi halangan. Ramai penyelidik telah menggunakan model halangan statik seperti dinding dan siling, tetapi hampir tidak ada yang memodelkan kesan kehadiran manusia sebagai halangan walaupun tubuh manusia secara signifikan mempengaruhi kekuatan isyarat. Oleh itu, kesan kehadiran manusia mesti dipertimbangkan untuk mendapatkan hasil kedudukan yang lebih tepat. Penyelidikan sebelum ini mencadangkan model yang hanya mempertimbangkan laluan lurus antara penghantar dan penerima. Walau bagaimanapun, untuk penyebaran dalam bangunan, kesan berbilang laluan seperti refleksi juga mempunyai pengaruh, tetapi tidak dipertimbangkan dalam kajian lepas. Oleh itu, penyelidikan ini mencadangkan model penentuan kedudukan dalam bangunan yang tepat yang menganggap kehadiran manusia menggunakan Model Surihan Sinar (AIRY), dalam persekitaran dinamik yang bergantung pada infrastruktur sedia ada. Tiga penyelesaian dicadangkan untuk membina AIRY: peta radio automatik menggunakan surihan sinar (ARM-RT), model manusia baru dalam penyurihan sinar (HUMORY), dan pemalar kesan manusia untuk penyesuaian penunjuk kekuatan isyarat yang diterima (RSSI). Pada peringkat luar talian, 30 RSSI direkodkan pada setiap titik menggunakan telefon pintar untuk membuat pangkalan data peta radio (523 titik). RSSI masa nyata kemudian dibandingkan dengan pangkalan data peta radio di peringkat dalam talian menggunakan perisian MATLAB untuk menentukan kedudukan pengguna (65 titik ujian). Model yang dicadangkan diuji di Tingkat 3, Menara Razak, UTM Kuala Lumpur (80m x 16m). Untuk menguji pengaruh kehadiran manusia, jumlah, kedudukan, serta jarak manusia di sekitar peranti mudah alih (MD) diubah. Hasil kajian menunjukkan bahawa semakin dekat seseorang itu dengan MD di kedua kedudukan garis nampak (LOS) dan bukan garis nampak (Non-LOS), semakin besar pengurangan RSSI di mana peningkatan bilangan manusia akan meningkatkan jumlah isyarat pantulan yang disekat. Pengurangan kekuatan isyarat bermula dari 0.5 dBm dengan dua orang dan mencapai 0.9 dBm dengan tujuh orang. Di samping itu, model surihan sinar menghasilkan ralat yang lebih kecil pada ramalan RSSI berbanding model berbilang dinding. Hal ini menunjukkan bahawa model penyurihan sinar meramalkan RSSI lebih baik daripada model berbilang dinding, terutama apabila memandang kesan kehadiran manusia. Algoritma KNN digunakan untuk menentukan kedudukan. Ketepatan awal ditingkatkan dari 2.04 m kepada 0.57 m setelah kehadiran manusia dan kesan berbagai laluan dipertimbangkan. Sebagai kesimpulan, model yang dicadangkan bejaya meningkatkan ketepatan kedudukan dalam bangunan dalam persekitaran yang dinamik dengan mengatasi kesan kehadiran manusia.

TABLE OF CONTENTS

LIST OF TABLES

LIST OF FIGURES

LIST OF ABBREVIATIONS

ANN	-	Artificial Neural Network
AIRY	-	Accurate Indoor Positioning System based on People Effect and Ray Tracing
AP	-	Access Point
ARM	-	Automatic Radio Map
GPS	-	Global Positioning System
IPS	-	Indoor Positioning System
KNN	-	K-Nearest Neighbour
LBS	-	Location-Based Service
LOS	-	Line of Sight
MD	-	Mobile Device
MRM	-	Manual Radio Map
MW	-	Multi-Wall
NLOS	-	Non-Line of Sight
PPE	-	People Presence Effect
RM	-	Radio Map
RSSI	-	Received Signal Strength Indicator
RT	-	Ray Tracing
SBR	-	Shooting and Bouncing Ray
UTM	-	Universiti Teknologi Malaysia
WLAN	-	Wireless Local Area Network
ARM-RT	-	Automatic Radio Map using Ray Tracing
HUMORY	-	Human Model in Ray Tracing

LIST OF SYMBOLS

S_i	-	RSS from available APs
L_i	-	Each site location
T_i	-	A tuple of (S_i, L_i)
d	-	Distance between the transceivers
PL	-	Path Loss
$\prod \overline{\overline{R_i}}$	-	Reflection coefficient
$\prod \overline{\overline{T_i}}$	-	Transmission coefficient
MSE	-	Mean Squared Error

LIST OF APPENDICES

CHAPTER 1

INTRODUCTION

1.1 Overview and Motivation

Location-based services (LBSs) are a significant permissive technology with a wide range of applications in human life (Horsmanheimo *et al.*, 2019). LBS are services that combine geographic location with other information to give more helpful services (Huang and Gartner, 2018). The LBS market is growing rapidly (Basiri *et al.*, 2015), with a market report estimating the LBS market to generate up to USD 77.84 billion revenue by 2021 (Markets and markets, 2016).

One of the main components of LBS is its positioning system—either indoor or outdoor. For outdoor positioning, Global Navigation Satellite Systems (GNSS) such as the Global Positioning System (GPS) and *Globalnaya Navigazionnaya Sputnikovaya Sistema* (GLONASS) have been used over a wide range of applications. GNNS is a worldwide position and time determination system that includes one or more satellite constellations, aircraft receivers, and system integrity monitoring, augmented as necessary to support the required navigation performance for the intended operation (Zhu *et al.*, 2018). GPS is a satellite navigation system operated by the United States whereas GLONASS is operated by the Russian Federation.

However, GPS cannot be used for indoor positioning because its signals cannot penetrate buildings. Due to GPS failure to work indoors, many researchers have attempted to build an alternative to GPS that can work indoors called the Indoor Positioning System (IPS) (Dardari *et al.*, 2015). When visiting a building for the first time such as an airport, an office building, an exhibition hall or a hypermarket, orientation may be difficult. Direction signs and static plans often do not provide the help one needs to find a specific location in time, resulting in stressful situations and

delays. According to ABI Research in 2015, IPS-based services have great economic potential, and are estimated to reach a market value of US$ 10 billion in 2020. Another report in 2016 by Markets and Markets estimated the global indoor location market to grow to $4,424.1 million by 2019, as shown in Figure 1.1 (Dasgupta and Singh, 2016). According to a Research and Markets report, the Global Indoor Positioning and Navigation market is expected to reach $54.60 billion by 2026.

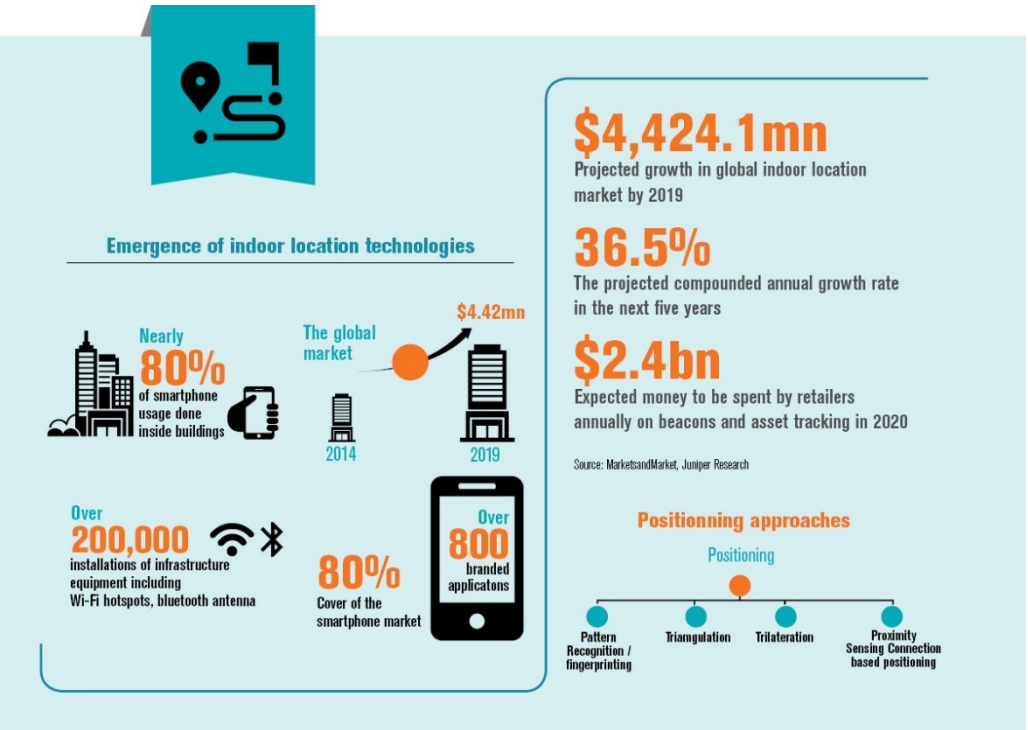

Figure 1.1 Infographic about the future of indoor location technologies

An IPS is any system that gives a precise position inside of buildings, such as a smart building (Turgut *et al.*, 2016), a hospital (Calderoni *et al.*, 2015), an airport, (Molina *et al.*, 2018), a subway (Stockx *et al.*, 2014), a construction site (Ma *et al.*, 2018), industrial sites (Cheng *et al.*, 2018), and university campuses (Golenbiewski *et al.*, 2018).

IPS uses many existing technologies such as radio frequencies (RFs) (Mier *et al.*, 2019), magnetic fields (Shu *et al.*, 2015), acoustic signals (Moutinho *et al.*, 2016), thermal sensors (Lu *et al.*, 2016), optical sensors (Mautz and Tilch, 2011) or other sensory information collected using a mobile device (MD) (Han *et al.*, 2016). Some examples of RF technology used in IPS, among others, are WLAN/Wi-Fi

(Zourmand *et al.*, 2018; Hsieh *et al.*, 2018), Bluetooth (Faragher and Harle, 2015), Zig Bee (Dong *et al.*, 2019), RFID (Tsirmpas *et al.*, 2015), frequency modulation (FM) (Popleteev, 2019), and Ultra-wideband (UWB) (Witrisal *et al.*, 2016). WLAN technology is commonly used in IPS because of its advantages, for example, radio waves can pass through obstacles like floors, walls, ceilings, and human bodies. Meanwhile, WLAN positioning systems can be implemented over a wide coverage area because it does not need any additional device.

One of the performance indicators of IPS is accuracy, which is the difference between the actual location and the estimated location (Rezazadeh *et al.*, 2018). There are many applications that require precise IPS, such as for emergency cases and patient monitoring. For example, it is essential for 911 to know the location of a caller as precisely as possible to control delays in emergency response. Delays in response can lead to a loss of lives. The emergency service has even defined a new standard called the "next-generation 911 (NG911)" (The National 911 Program, 2015; Sedlar *et al.*, 2019). In 2016, the United States (U.S.) National Aeronautics and Space Administration Jet Propulsion Laboratory (NASA JPL) cooperated with the Department of Homeland Security Science and Technology Directorate (S&T) to develop a high precision outdoor and indoor navigation and tracking system for emergency responders (U.S. Department of Homeland Security, 2016). An indoor navigation system that can track firefighters to within a meter is also in the works (Li *et al.*, 2018).

WLAN IPS has been highlighted as a preferred technology due to its accurate positioning results and minimal infrastructure cost (Yang and Shao, 2015). WLAN is a wireless local network standard (IEEE 802.11), a communication standard that is supported in most mobile phones. However, the WLAN signal is greatly influenced by environmental conditions, especially inside indoor areas because of the multipath effect, which can decrease signal accuracy. An example of a signal propagation model that considers multipath effects is the ray tracing model. This model requires an adaptive IPS that can adapt to the multipath effect and environmental changes, mainly the effect of people presence, to provide high-accuracy IPS.

1.2 Problem Background

Location detection techniques are categorised into three: proximity, triangulation, and fingerprint (Farid *et al.*, 2013). Proximity detection or connectivity-based techniques are simple to implement. The location of MD is defined based on the cell of origin (CoO) method with a known position and limited distance. Although this method is easy to implement, it has a large distance error, meaning that it cannot be adopted for WLAN-based IPS because the Access Point (AP) has a wide coverage (up to 100 m). Proximity techniques can be applied using RFID or Bluetooth, but which also have a limited range or coverage.

The triangulation technique uses the geometric properties of triangles to find the location of a target. The technique can be divided into two: lateration and angulation. The lateration technique is based on the measurement of the received radio signal strength (RSS), the signal phase, and the propagation-time such as the time of arrival (TOA), the time difference of arrival (TDOA), and the roundtrip time (RTT)(Makki *et al.*, 2015).

Fingerprinting is based on a pattern recognition technique that combines radio frequency (RF) with location information e.g. a label from the environment, to show the position of the MD. WLAN fingerprinting is usually conducted in two phases: offline and online. In the offline phase, a site survey is conducted to collect the value of the received signal strength indicator (RSSI) at many reference points (RPs) from all the detected access points (APs). In the online phase, a user samples or measures an RSSI vector at his/her position. Then, the system compares the received vector of the RSSI with the stored fingerprints in the radio map (RM) database. The position is then estimated based on the most similar "neighbours", which are the set of RPs with RSSI vectors that closely match the RSSI of the target (He and Chan, 2016).

WLAN-based RSSI Fingerprinting can provide highly accurate position estimates (Wang *et al.*, 2019). It also requires a low-cost investment, as shown in Table 1.1 (Potgantwar *et al.*, 2015; Basri and El Khadimi, 2016). On the other hand,

the large bandwidth makes the ultra-wideband (UWB) signal resistant to multipath problems and interference (Gao and Li, 2019), making UWB less influenced by the people presence effect, but it also requires a higher cost of investment.

Table 1.1 Comparison of indoor positioning technology, accuracy, cost, and people effect

Technology	**Accuracy**	**Cost**	**Channel Bandwidth**	**Interference caused by People Effect**
UWB	1 m–2 m	High	500 MHz–7.5 GHz	Low
RFID	1 m–2 m	Low	200 KHz; 500 KHz	High
Bluetooth	2 m–5 m	Low	1 MHz	High
WLAN	2 m–5 m	Low	22 MHz	High
Zigbee	1 m–3 m	High	0.3 MHz/0.6 MHz; 2 MHz	High

Manual radio map (RM) construction is labour intensive and time-consuming. Hence, automatic radio map generation was developed to reduce the time required to construct RM (Alshami, *et al.*, 2015; Du *et al.*, 2015; Lin *et al.*, 2015). An automatic radio map construction method is proposed using multi-sensors including inertial information, video data, and WIFI signals (Liu *et al.*, 2016). Then, a visual-based approach was proposed to construct a radio map in anonymous indoor environments (Liu *et al.*, 2017). On the other hand, Yu *et al.* (2016) and Li *et al.* (2018) constructed a system based on crowdsourcing. In Li *et al.'s* (2018) project, the users walked through a building to generate parts of road paths and then merging the PDR traces based on the similarity of the Wi-Fi fingerprints. These techniques did not need any prior knowledge of floor plans. These construction techniques were able to reduce the time required to construct RMs. However, it still required the user to exert significant effort to collect data using various sensors. New techniques have therefore been proposed based on indoor RF propagation models. This technique only requires information on the room layout and AP location as the system input. Alshami *et al.* (2015) and Caso and De Nardis (2017) used a Multi-wall signal path loss model to automatically generate a radio map. This technique quickly generated a radio map, but the model only considered the direct signal from the transmitter (AP) to the receiver (MD), whereas indirect signals such as reflection, which have a significant influence on indoor propagation, were not included.

The current research proposes a ray tracing model that considers multipath effects to obtain a more accurate radio map. The ray tracing technique obtains channel characteristics by identifying the contributions of individual multipath components (reflection, diffraction, and scattering) and calculates the composition of these components at the receiver. If we use all the multipath components, it will require high computational time (Hossain et al., 2019). Thus, in this research, we will only consider reflection in order to get low computational time and high accuracy.

Another problem faced in past studies is that the RSSI of WLAN is highly affected by environmental changes such as the effect of people presence, which will decrease position accuracy. Hence, environmental changes are still one of the main problems affecting WLAN positioning accuracy. Obstacles that could cause fluctuations in RSSI include walls, ceilings, and people (Farid *et al.*, 2013; He and Chan, 2016). Walls and ceilings have been discussed in Ubom *et al.* (2019), Saito and Omiya (2018), and Santana *et al.* (2016). The effect of people on signal strength was investigated in Slezak *et al.* (2018) for 60 GHz, in Alabish *et al.* (2018) for 18–22 GHz, and in Alshami *et al.* (2014) for 2.4 GHz. The result showed that people's presence in the Line of Sight (LOS) between the AP and the Mobile Device (MD) decreased the RSSI by 2 dBm to 5 dBm. This decline in the RSSI could result in a position error of more than 2 m. People holding a MD (user orientation problem) and people around the user could also block the WLAN signal from the APs depending on their position, in turn, reducing the RSSI value. Meanwhile, for Zig Bee, people's presence in the Line of Sight (LOS) decreased the RSSI by 3.97 dBm (Shukri *et al.*, 2016).

One of the main problems related to PPE is the position of the user holding a MD. This problem is known as the user orientation problem. To solve the user orientation problem, Liu and Wang (2015) collected four orientations of RM in the offline phase and used a KNN positioning algorithm in the online phase. Deng *et al.* (2018) also built a multi-orientation RM in the offline phase and employed a Rotation Matrix and the Principal Component Analysis (RMPCA) method. Their solution proved time-consuming because of the manual process involved, and the RSSI multi-vectors had to be collected at each node. The systems developed in the

study focused on the development of a multi-orientation RM database such that the system required a long time for collecting data for the database. Therefore, it is necessary to develop an adaptive system with a more efficient RM database to overcome the user orientation problem.

In addition to users who hold MDs, people around the users also affect the RSSI. People presence has the same effect as obstacles that block WLAN signals. The movement of humans in wireless networks is one of the major effects that cause significant variations in the received signal strength indicator (RSSI) (Booranawong *et al.*, 2019; Booranawong *et al.*, 2018). Alshami *et al.* (2015) presented experimental results showing that people's presence between the AP and the MD reduced the received signal strength by 2 dBm to 5 dBm. However, the study only discussed the effect of one or two people on the RSSI and only a single path signal propagation model was used to analyse the RSSI (Alshami *et al.*, 2017). However, multipath signals such as reflection also have a significant effect on indoor propagation, but these were not discussed. In fact, human tissues have a variety of relative permittivity values that influence the reflection signal (Zhekov *et al.*, 2019). The Foundation for Research on Information Technologies in Society in 2011 released the selected relative permittivity of main human tissues as shown in Table 1.2.

Table 1.2 Selected relative permittivity of some main human tissues

Tissue	**Relative permittivity**
Air	1
Blood	58.4
Fat	5.29
Muscle	52.8
Dry Skin	38.1
Wet Skin	42.9

Hence, this current research should consider the effect of many people around the user with different positions to improve the accuracy of the proposed IPS. In addition, this research should also consider modelling the human body in the ray

tracing multipath signal propagation model to analyse the effect of people presence on RSSI.

1.3 Problem Statement

One of the most popular methods in IPS is the WLAN Fingerprint because this technology has been widely installed inside buildings and provides a high level of accuracy (Yang and Shao, 2015). Although WLAN RSS fingerprinting is the most accurate positioning method, it still has a weakness, for example, constructing the RM is labour intensive and time-consuming, and the multipath signal is vulnerable to obstacle presence, such as walls, furniture, and people.

Many studies have modelled static obstacles such as walls and ceilings, but it is hard to find any research that has modelled the people presence effect. Human bodies absorb, reflect, and diffract WLAN signals, which, in turn, affect the value of RSSI. Thus, if offline mapping is performed when there are no people (or a few people) whereas positioning is performed when there are many people, the system can lose its reliability. The results have shown that, on average, the presence of human bodies increases the positioning error by 11% regardless of the algorithm used (Garcia-Villalonga and Perez-Navarro, 2015). Meanwhile, Alshami *et al.'s* (2015) experimental works showed that people's presence between a mobile device and the access point reduced the RSSI by 2 dBm to 5 dBm. This decline in RSSI could lead to a position error of more than 2 m.

Hence, there is a need to overcome the people presence effect to obtained highly accurate positioning results. In previous researches, as mentioned in Section 1.2, a propagation model was proposed that considered people presence based on a multi-wall model. However, only the direct path between the transmitter and the receiver was considered in the model, and every wall that crossed by this path was assumed to attenuate the passing ray by a constant amount. However, for indoor propagation, multipath effects (reflection, diffraction, and scattering), which were not considered in these studies, have a very significant influence. Therefore, there is a

need to develop a new indoor propagation model that considers multipath effects, such as the Ray Tracing model, to model the people presence effect and improve the accuracy of the Indoor Positioning System.

In this research, a new indoor positioning model that considers the people presence effect and multipath propagation based on a ray tracing model was proposed to improve the accuracy of WLAN fingerprinting IPS without the need to install a new device in the existing infrastructure.

1.4 Research Question

Based on the problem statement, the following research questions were derived:

i. What is the best way to develop and validate an accurate automatic radio map construction that considers ray tracing?
ii. How to develop and validate a human model that considered people presence effect on the received signal strength to enhance WLAN-fingerprinting Indoor Positioning based on ray tracing?
iii. How to develop and validate the proposed accurate indoor positioning model in a dynamic environment that also considers people presence effect and ray tracing?

1.5 Aim of the Study

This research proposes a new accurate indoor positioning model based on WLAN Fingerprinting using existing common devices that are already installed in a building (i.e. the Access Point). The proposed model has to adapt to the effect of environmental changes, especially the effect of people presence. The proposed model adopted a modified ray tracing radio propagation model to overcome the multipath effect.

1.6 Objective

The objectives of this research are as follows:

i. To develop and validate an accurate automatic radio map construction technique that considers ray tracing propagation
ii. To develop and validate a human model that considers the people presence effect on the received signal strength to enhance the proposed WLAN-fingerprinting Indoor Positioning System based on ray tracing propagation
iii. To develop and validate the proposed accurate indoor positioning model in a dynamic environment, which considers the effect of people presence effect and ray tracing.

1.7 Scope of Study

This research proposes a novel, accurate WLAN Fingerprinting indoor positioning model that considers the people presence effect and multipath propagation to improve positioning accuracy without adding any extra device. This model can determine the location of a MD accurately in a dynamic environment. Hence, this research is bounded by the following scope.

This research focused on indoor positioning while navigation, tracking, and other LBS fall out of the scope of study. WLAN fingerprinting was adopted as an indoor positioning method and the radio map was constructed using RSS from the available AP beacon.

The users carried the MD in their hand and used the Android Operating System with an internal WLAN adapter. Meanwhile, the access points (APs) were installed in a fixed and known position.

This research used the ray tracing propagation model to estimate the received signal strength. Accuracy and position errors were adopted as performance metrics to validate the proposed model. This research did not investigate human detection or any security or privacy issues.

1.8 Significance of the Study

Recently, LBS has proven to be a significant permissive technology with a wide range of applications. The performance of LBS is significantly affected by its IPS. By building an accurate IPS using existing devices (APs), the performance and coverage of LBS can be improved. The proposed system could be applied in an economic context (shopping centres, train stations, airports), as well as military, health (hospital, healthcare), and social aspects (people traffic management for emergency situations inside buildings).

Many applications require precise IPS such as emergency cases and patient monitoring. For example, 911 has defined a new standard called the “next generation 911 (NG911)” that includes a technique that recognises the precise position of the caller, while the U.S. Department of Homeland Security has developed a high precision outdoor and indoor navigation and tracking system for emergency responders. The U.S. Government is also developing an indoor navigation system that can track firefighters to within a meter.

IPS also plays an important role in the Internet of Things (IoT) (Ali *et al.*, 2019). One of the largest European Union projects on IoT (FP-7 Butler project) stated that location information is one of the key enabling technology in IoT. In the health sector, IoT manages numerous sensors mounted on a patient's body to monitor health conditions. If the patient's health condition deteriorates and he/she needs help immediately, then, the location of the patient would be vital to monitor. Hence, in cases such as these, an IPS with high accuracy is required.

1.9 Thesis Organisation

This thesis consists of six chapters that are organised as follows: Chapter 1 explains the overview and the motivation of this research such as the research questions, the objectives, the scope, and the limitations. The statement of the problem was formulated by highlighting the need for a new, accurate indoor

positioning model based on RSSI-WLAN Fingerprinting that could adapt to the people presence effect to improve the accuracy of the IPS without installing any extra devices in a dynamic environment.

Chapter 2 provides fundamental information about WLAN Fingerprinting, the path loss or radio propagation models, and related works on PPE in IPS. Chapter 3 presents the research methodology. It explains the research plan that contains three phases to achieve the desired objectives: 1) the Knowledge Building Phase, which aims to investigate the literature to develop the baseline; 2) the Development Phase in which an Accurate Indoor Positioning Model is designed and developed based on WLAN fingerprinting to improve the accuracy of IPS; and 3) the Validation Phase, which aims to validate the developed AIRY model. The development and validation phases are carried out to in parallel since AIRY has different components and the developed component must be validated before going to the next step.

Chapter 4 discusses the effects of people around the user on the RSSI and the proposed human model and the signal propagation model that consider people presence based on the ray tracing propagation model. Chapter 5 discusses the development of a highly accurate IPS that considers the people effect and was adopted from the ray tracing propagation model. Finally, Chapter 6 presents the conclusions to this study.

REFERENCES

Abed, A.K. and Abdel-Qader, I., 2018. Access Point Selection Using Particle Swarm Optimization in Indoor Positioning Systems. *NAECON 2018-IEEE National Aerospace and Electronics Conference*. 2018 IEEE, pp. 403–410.

Ajay, R.M., 2007. Advanced Cellular Networks: Planning and Optimization. *WIKEY and Sons, Nokia Networks, United Kingdom*.

Alabish, A., Kara, A. and Dalveren, Y., 2018. An Experimental Study towards Examining Human Body Movements in Indoor Wave Propagation at 18–22 GHz. *International Symposium on Networks, Computers and Communications (ISNCC)*. IEEE, pp. 1–4.

Ali, M.U., Hur, S. and Park, Y., 2019. Wi-Fi-based effortless indoor positioning system using IoT sensors. *Sensors*, 19(7), pp.1496-1515.

Alshami, I.H., Ahmad, N.A. and Sahibuddin, S., 2014. People effects on WLAN-Based IPS' accuracy experimental preliminary results. *Malaysian Software Engineering Conference (MySEC)*. IEEE, pp. 206–209.

Alshami, I.H., Ahmad, N.A. and Sahibuddin, S., 2015. People's Presence Effect on WLAN-Based IPS Accuracy. *Jurnal Teknologi*, 77(9), pp.173-178.

Alshami, I.H., Ahmad, N.A., Sahibuddin, S. and Firdaus, F., 2017. Adaptive Indoor Positioning Model Based on WLAN-Fingerprinting for Dynamic and Multi-Floor Environments. *Sensors*, 17(8), pp.1789-1817.

Alshami, I.H., Ahmad, N.A., Sahibuddin, S. and Yusof, Y.M., 2016. The effect of people presence on WLAN RSS is governed by influence distance. *3rd International Conference on Computer and Information Sciences (ICCOINS)*. IEEE, pp. 197–202.

Alshami, I.H., Salleh, N.A.A.@ and Sahibuddin, S., 2015. Automatic WLAN fingerprint radio map generation for accurate indoor positioning based on signal path loss model. *ARPN Journal of Engineering and Applied Sciences*, 10(23), pp.17930-17936.

Andrade, C.B. and Hoefel, R.P.F., 2010. IEEE 802.11 WLANs: A comparison on indoor coverage models. *23rd Canadian Conference on Electrical and Computer Engineering (CCECE)*. IEEE, pp. 1–6.

Askarzadeh, F.,Pahlavan, K., Geng, Y., Makarov, S.N., Ye,Y., Khan, U., 2016. Analyzing the effect of human body and metallic objects for indoor geolocation. 10th International Symposium on Medical Information and Communication Technology (ISMICT). IEEE, pp. 1–5.

Ayadi, M. and Zineb, A.B., 2014. Body Shadowing and Furniture Effects for Accuracy Improvement of Indoor Wave Propagation Models. *IEEE Transactions on Wireless Communications*, 13(11), pp.5999–6006.

Azpilicueta, L., Rawat, M., Rawat, K., Ghannouchi, F. M. and Falcone, F., 2014. A ray launching-neural network approach for radio wave propagation analysis in complex indoor environments. *IEEE Transactions on Antennas and Propagation*, 62(5), pp.2777–2786.

Azpilicueta, L., Falcone, F. and Janaswamy, R., 2017. A Hybrid Ray Launching-Diffusion Equation Approach for Propagation Prediction in Complex Indoor Environments. *IEEE Antennas and Wireless Propagation Letters*, 16, pp.214–217.

Bahl, P. and Padmanabhan, V.N., 2000. RADAR: An in-building RF-based user location and tracking system. *Nineteenth Annual Joint Conference of the IEEE Computer and Communications Societies.* IEEE, pp. 775–784.

Basiri, A., Moore, T., Hill, C. and Bhatia, P., 2015. Challenges of Location-Based Services Market Analysis: Current Market Description. In: Gartner, G. and Huang, H., (eds.) Lecture Notes in Geoinformation and Cartography. Springer International Publishing, pp. 273–282.

Basri, C. and El Khadimi, A., 2016. Survey on indoor localization system and recent advances of WIFI fingerprinting technique. *5th International Conference on Multimedia Computing and Systems (ICMCS)*. IEEE, pp. 253–259.

Bi, J., Wang, Y., Li, Z., Xu, S., Zhou, J., Sun, M., and Si, M., 2019. Fast radio map construction by using adaptive path loss model interpolation in large-scale building. *Sensors*, 19(3), p.712-730.

Booranawong, A., Jindapetch, N. and Saito, H., 2018. A system for detection and tracking of human movements using RSSI signals. *IEEE Sensors Journal*, 18(6), pp.2531–2544.

Booranawong, A., Sengchuai, K. and Jindapetch, N., 2019. Implementation and test of an RSSI-based indoor target localization system: Human movement effects on the accuracy. *Measurement*, 133, pp.370–382.

Borrelli, A., Monti, C., Vari, M. and Mazzenga, F., 2004. Channel models for IEEE 802.11 b indoor system design. *International Conference on Communications*. IEEE, pp. 3701–3705.

Brena, R.F., García-Vázquez, J.P., Galván-Tejada, C.E., Muñoz-Rodriguez, D., Vargas-Rosales, C., 2017. Evolution of indoor positioning technologies: A survey. *Journal of Sensors*, 19(3), pp.1–21.

Calderoni, L., Ferrara, M., Franco, A. and Maio, D., 2015. Indoor localization in a hospital environment using random forest classifiers. *Expert Systems with Applications*, 42(1), pp.125–134.

Casino, F., Azpilicueta, L., Lopez-Iturri, P., Aguirre, E., Falcone, F., Solanas, A., 2017. Optimized Wireless Channel Characterization in Large Complex Environments by Hybrid Ray Launching-Collaborative Filtering Approach. *IEEE Antennas and Wireless Propagation Letters*, 16, pp.780–783.

Caso, G., De Nardis, L., Lemic, F., Handziski, V., Wolisz, A., Di Benedetto, M.G., 2019. ViFi: Virtual Fingerprinting WiFi-based Indoor Positioning via Multi-Wall Multi-Floor Propagation Model. *IEEE Transactions on Mobile Computing*, pp.1–14.

Caso, G. and De Nardis, L., 2017. Virtual and oriented WiFi fingerprinting indoor positioning based on multi-wall multi-floor propagation models. *Mobile Networks and Applications*, 22(5), pp.825–833.

Cátedra, M.F., Gómez, J.M., Lozano, L. and Gonzalez, I., 2008. Application of GTD for location systems. *Radio Science,* 43(6), pp.1-10.

Chen, X., Tian, L., Tang, P. and Zhang, J., 2016. Modelling of Human Body Shadowing Based on 28 GHz Indoor Measurement Results. *IEEE 84th Vehicular Technology Conference (VTC-Fall)*, pp. 1–5.

Chen, Y.C., Chiang, J.R., Chu, H., Huang, P., Tsui, A.W., 2005. Sensor-assisted wi-fi indoor location system for adapting to environmental dynamics. *Proceedings of the 8th ACM international symposium on Modeling, analysis and simulation of wireless and mobile systems*. ACM, pp. 118–125.

Cheng, V.C., Hao, L.I., Ng, J.K. and Cheung, W.K., 2018. Fast Setup and Robust WiFi Localization for the Exhibition Industry. *IEEE 32nd International Conference on Advanced Information Networking and Applications (AINA)*. IEEE, pp. 472–479.

Chizhik, D., Valenzuela, R.A., Rodriguez, M. and Feick, R., 2016. Propagation into buildings: Theory vs. measurements. *IEEE International Symposium on Antennas and Propagation (APSURSI)*. IEEE, pp. 1455–1456.

Corte-Valiente, D., Gómez-Pulido, J.M., Gutiérrez-Blanco, O. and Castillo-Sequera, J.L., 2019. Localization Approach Based on Ray-Tracing Simulations and Fingerprinting Techniques for Indoor–Outdoor Scenarios. *Energies*, 12(15), pp.2943-2964.

Cotton, S.L., Chun, Y.J., Scanlon, W.G. and Conway, G.A., 2016. Path loss models for indoor off-body communications at 60 GHz. *IEEE International Symposium on Antennas and Propagation (APSURSI)*. IEEE, pp. 1441–1442.

Dalveren, Y., Alabish, A.H. and Kara, A., 2019. A simplified model for characterizing the effects of scattering objects and human body blocking indoor links at 28 GHz. *IEEE Access*, 7, pp.69687–69691.

Damosso, E., 1998. Digital mobile radio: COST 231 View on the evolution towards 3rd generation systems. *European Commission*, 18957, pp.234-238.

Dang, X., Si, X., Hao, Z. and Huang, Y., 2019. A Novel Passive Indoor Localization Method by Fusion CSI Amplitude and Phase Information. *Sensors*, 19(4), p.875.

Dardari, D., Closas, P. and Djuric, P.M., 2015. Indoor Tracking: Theory, Methods, and Technologies. *IEEE Transactions on Vehicular Technology*, 64(4), pp.1263–1278.

Dasgupta, A. and Singh, I., 2016. Inside A Big Building. *Geospatial World*, 6(16).

Davies, K.F., Jones, I.G. and Shapiro, J.L., 2018. A Bayesian Approach to Dealing with Device Heterogeneity in an Indoor Positioning System. *International Conference on Indoor Positioning and Indoor Navigation (IPIN)*. IEEE, pp. 1–8.

De Adana, F.S., Blanco, O.G., Diego, I.G., Arriaga, J.P., Cátedra, M.F., 2000. Propagation model based on ray tracing for the design of personal communication systems in indoor environments. *IEEE Transactions on Vehicular Technology*, 49(6), pp.2105–2112.

Deng, Z.-A., Qu, Z., Hou, C., Si, W., Zhang, C., 2018. WiFi positioning based on user orientation estimation and smartphone carrying position recognition. *Wireless Communications and Mobile Computing*, Vol.2018, pp.1-11.

Dong, Z.Y., Xu, W.M. and Zhuang, H., 2019. Research on ZigBee Indoor Technology Positioning Based on RSSI. *Procedia Computer Science*, 154, pp.424–429.

Du, Y., Yang, D. and Xiu, C., 2015. A Novel Method for Constructing a WIFI Positioning System with Efficient Manpower. *Sensors*, 15(4), pp.8358–8381.

El-Kafrawy, K., Youssef, M. and El-Keyi, A., 2011. Impact of the human motion on the variance of the received signal strength of wireless links. *IEEE 22nd International Symposium on Personal Indoor and Mobile Radio Communications (PIMRC),*. IEEE, pp. 1208–1212.

El-Kafrawy, K., Youssef, M., El-Keyi, A. and Naguib, A., 2010. Propagation modeling for accurate indoor WLAN RSS-based localization. *IEEE 72nd Vehicular Technology Conference Fall (VTC 2010-Fall)*. IEEE, pp. 1–5.

Fan, W.H., Yu, L., Wang, Z. and Xue, F., 2014. The effect of wall reflection on indoor wireless location based on RSSI. *IEEE International Conference on Robotics and Biomimetics (ROBIO)*. IEEE, pp. 1380–1384.

Fang, S.H., 2018. Robustness in Fingerprinting-Based Indoor Positioning Systems. *Positioning and Navigation in Complex Environments*. IGI Global, Vol 2018, pp. 88–141.

Fang, S.H., Wang, C.H. and Tsao, Y., 2015. Compensating for Orientation Mismatch in Robust Wi-Fi Localization Using Histogram Equalization. *IEEE Transactions on Vehicular Technology*, 64(11), pp.5210–5220.

Faragher, R. and Harle, R., 2015. Location Fingerprinting With Bluetooth Low Energy Beacons. *IEEE Journal on Selected Areas in Communications*, 33(11), pp.2418–2428.

Farid, Z., Nordin, R. and Ismail, M., 2013. Recent advances in wireless indoor localization techniques and system. *Journal of Computer Networks and Communications*, Vol.2013, pp.1-12.

Felsen, L.B. and Marcuvitz, N., 1994. *Radiation and Scattering of Waves*, John Wiley & Sons.

Feng, C., Au, W.S.A., Valaee, S. and Tan, Z., 2009. Orientation-aware indoor localization using affinity propagation and compressive sensing. *3rd IEEE International Workshop on Computational Advances in Multi-Sensor Adaptive Processing (CAMSAP)*. pp. 261–264.

Fet, N., Handte, M. and Marrón, P.J., 2013. A model for WLAN signal attenuation of the human body. *ACM international joint conference on Pervasive and ubiquitous computing*. ACM, pp. 499–508.

Frankenberg, E. and Jones, N.R., 2004. Self-rated health and mortality: does the relationship extend to a low income setting? *Journal of health and social behavior*, 45(4), pp.441–452.

Fuschini, F., Vitucci, E.M., Barbiroli, M., Falciasecca, G., Degli-Esposti, V., 2015. Ray tracing propagation modeling for future small-cell and indoor applications: A review of current techniques. *Radio Science*, 50(6), pp.469–485.

Gabriel, S., Lau, R.W. and Gabriel, C., 1996. The dielectric properties of biological tissues: III. Parametric models for the dielectric spectrum of tissues. *Physics in Medicine & Biology*, 41(11), p.2271.

Gao, H. and Li, X., 2019. Tightly-Coupled Vehicle Positioning Method at Intersections Aided by UWB. *Sensors*, 19(13), p.2867.

Garcia-Villalonga, S. and Perez-Navarro, A., 2015. Influence of human absorption of Wi-Fi signal in indoor positioning with Wi-Fi fingerprinting. *International Conference on.Indoor Positioning and Indoor Navigation (IPIN).* IEEE, pp. 1–10.

Ge, X. and Qu, Z., 2016. Optimization WIFI indoor positioning KNN algorithm location-based fingerprint. *7th IEEE International Conference on Software Engineering and Service Science (ICSESS)*. IEEE, pp. 135–137.

Geok, T.K., Hossain, F., Kamaruddin, M.N., Rahman, N.Z.A., Thiagarajah, S., Chiat, A.T.W., Liew, C.P., 2018. A Comprehensive Review of Efficient Ray-Tracing Techniques for Wireless Communication. *Int. J. Commun. Antenna Propag*, 8, pp.123–136.

Ghaddar, M., Talbi, L., Denidni, T.A. and Sebak, A., 2007. A conducting cylinder for modeling human body presence in indoor propagation channel. *IEEE Transactions on Antennas and Propagation*, 55(11), pp.3099–3103.

Ghosh, D., Roy, P., Chowdhury, C. and Bandyopadhyay, S., 2016. An ensemble of condition based classifiers for indoor localization. *IEEE International conference on advanced networks and telecommunications systems (ANTS)*. IEEE, pp. 1–6.

Golenbiewski, J., Tewolde, G.S. and Kwon, J., 2018. Evaluation of Indoor Positioning Technologies for Prototyping at Kettering University. *IEEE International Conference on Electro/Information Technology (EIT)*. IEEE, pp. 0509–0514.

Gómez, J., Tayebi, A., de Adana, F.S. and Gutiérrez, Ó., 2010. 3D Localisation method based on ray-tracing considering the presence of moving people. *Fourth European Conference Antennasand Propagation* (EuCAP). IEEE, pp. 1–4.

Grubisic, S. and Carpes Jr, W.P., 2014. An efficient indoor ray-tracing propagation model with a quasi-3D approach. *Journal of Microwaves, Optoelectronics and Electromagnetic Applications*, 13(2), pp.166–176.

Gu, Z., Chen, Z., Zhang, Y., Zhu, Y., Lu, M., Chen, A., 2016. Reducing fingerprint collection for indoor localization. *Computer Communications*, 83, pp.56–63.

Han, D., Jung, S. and Lee, S., 2016. A sensor fusion method for Wi-Fi-based indoor positioning. *ICT Express*, 2(2), pp.71–74.

Hatami, A. and Pahlavan, K., 2006. Comparative statistical analysis of indoor positioning using empirical data and indoor radio channel models. *3rd IEEE Consumer Communications and Networking Conference*. IEEE, pp. 1018–1022.

He, J., Li, S., Pahlavan, K. and Wang, Q., 2012. A realtime testbed for performance evaluation of indoor TOA location system. *IEEE International Conference on Communications (ICC)*. IEEE, pp. 482–486.

He, S. and Chan, S.-H.G., 2016. Wi-Fi fingerprint-based indoor positioning: Recent advances and comparisons. *IEEE Communications Surveys & Tutorials*, 18(1), pp.466–490.

He, S., Ji, B. and Chan, S.-H.G., 2016. Chameleon: Survey-free updating of a fingerprint database for indoor localization. *IEEE Pervasive Computing*, 15(4), pp.66–75.

He, S., Lin, W. and Chan, S.-H.G., 2016. Indoor localization and automatic fingerprint update with altered AP signals. *IEEE Transactions on Mobile Computing*, 16(7), pp.1897–1910.

Horsmanheimo, S., Lembo, S., Tuomimaki, L., Huilla, S., Honkamaa, P., Laukkanen, M., Kemppi, P., 2019. Indoor positioning platform to support 5G location based services. *IEEE International Conference on Communications Workshops (ICC Workshops)*. IEEE, pp. 1–6.

Hossain, F., Geok, T., Rahman, T., Hindia, M., Dimyati, K., Abdaziz, A., 2018. Indoor Millimeter-Wave Propagation Prediction by Measurement and Ray Tracing Simulation at 38 GHz. *Symmetry*, 10(10), pp464.

Hossain, F., Geok, T.K., Rahman, T.A., Hindia, M.N., Dimyati, K., Ahmed, S., Tso, C.P., Rahman, A., Ziela, N., 2019. An efficient 3-D ray tracing method: prediction of indoor radio propagation at 28 GHz in 5G network. Electronics, 8(3), pp.286.

Hosseinzadeh, S., Larijani, H., Curtis, K., Wixted, A., Amini, A., 2017. Empirical propagation performance evaluation of LoRa for indoor environment. *IEEE 15th International Conference on Industrial Informatics (INDIN)*. IEEE, pp. 26–31.

Hsieh, H.-Y., Prakosa, S.W. and Leu, J.-S., 2018. Towards the Implementation of Recurrent Neural Network Schemes for WiFi Fingerprint-Based Indoor Positioning. *IEEE 88th Vehicular Technology Conference (VTC-Fall)*. IEEE, pp. 1–5.

Hu, J., Liu, D., Yan, Z. and Liu, H., 2018. Experimental Analysis on Weight K-Nearest Neighbor Indoor Fingerprint Positioning. *IEEE Internet of Things Journal*.

Huang, H. and Gartner, G., 2018. *Current Trends and Challenges in Location-Based Services*, Multidisciplinary Digital Publishing Institute.

Iskander, M.F. and Yun, Z., 2002. Propagation prediction models for wireless communication systems. *IEEE Transactions on microwave theory and techniques*, 50(3), pp.662–673.

Islam, M.J., Reza, A.W., Noordin, K.A., Kausar, A., Ramiah, H., 2013. Efficient and accurate ray tracing method for indoor radio wave propagation prediction in presence of human body movement. *Journal of Electromagnetic Waves and Applications*, 27(12), pp.1566–1586.

Ji, Y., Biaz, S., Pandey, S. and Agrawal, P., 2006. ARIADNE: a dynamic indoor signal map construction and localization system. *Proceedings of the 4th international conference on Mobile systems, applications and services*. 2006 ACM, pp. 151–164.

Ji, Y. and Player, R., 2011. A 3-D indoor radio propagation model for WiFi and RFID. *Proceedings of the 9th ACM international symposium on Mobility management and wireless access*. 2011 ACM, pp. 27–34.

Jordan, S., Lim, L., Seubsman, S., Bain, C., Sleigh, A., Team, T.C.S., 2012. Secular changes and predictors of adult height for 86 105 male and female members of the Thai Cohort Study born between 1940 and 1990. *J Epidemiol Community Health*, 66(1), pp.75–80.

Kaemarungsi, K. and Krishnamurthy, P., 2012. Analysis of WLAN's received signal strength indication for indoor location fingerprinting. *Pervasive and mobile computing*, 8(2), pp.292–316.

Khafaji, A., Saadane, R., El Abbadi, J. and Belkasmi, M., 2008. Ray tracing technique based 60 GHz band propagation modelling and influence of people shadowing. *International Journal of Electrical, Computer, and Systems Engineering*, 2(2), pp.102–108.

Kim, Y., Shin, H., Chon, Y. and Cha, H., 2015. Crowdsensing-based Wi-Fi radio map management using a lightweight site survey. *Computer Communications*, 60, pp.86–96.

King, T., Kopf, S., Haenselmann, T., Lubberger, C., Effelsberg, W., 2006. COMPASS: A probabilistic indoor positioning system based on 802.11 and digital compasses. *1st international workshop on Wireless Network Testbeds, Experimental Evaluation & Characterization*. ACM, pp. 34–40.

Koda, Y., Yamamoto, K., Nishio, T. and Morikura, M., 2018. Measurement method of temporal attenuation by human body in off-the-shelf 60 GHz WLAN with HMM-based transmission state estimation. *Wireless Communications and Mobile Computing*, Vol. 2018, pp. 1-10.

Kouyoumjian, R.G. and Pathak, P.H., 1974. A uniform geometrical theory of diffraction for an edge in a perfectly conducting surface. *Proceedings of the IEEE*, 62(11), pp.1448–1461.

Krishnan, P., Krishnakumar, A.S., Ju, W.-H., Mallows, C., Gamt, S.N., 2004. A system for LEASE: Location estimation assisted by stationary emitters for indoor RF wireless networks. *INFOCOM 2004. Twenty-third AnnualJoint Conference of the IEEE Computer and Communications Societies*. 2004 IEEE, pp. 1001–1011.

Kunisch, J. and Pamp, J., 2008. Ultra-wideband double vertical knife-edge model for obstruction of a ray by a person. *2008 IEEE International Conference on Ultra-Wideband*. 2008 IEEE, pp. 17–20.

Lee, D.J. and Lee, W.C., 2000. Propagation prediction in and through buildings. *IEEE transactions on Vehicular Technology*, 49(5), pp.1529–1533.

Li, C., Zhao, J., Sun, Q., Gao, X., Sun, G., Zhu, C., 2019. NRSSD: Normalizing Received Signal Strength to Address Device Diversity Problem in Fingerprinting Positioning. *International Journal of Performability Engineering*, 15(3).

Li, D., Zhang, B. and Li, C., 2016. A Feature-Scaling-Based -Nearest Neighbor Algorithm for Indoor Positioning Systems. *IEEE Internet of Things Journal*, 3(4), pp.590–597.

Li, H., Ng, J.K., Cheng, V.C. and Cheung, W.K., 2018. Fast indoor localization for exhibition venues with calibrating heterogeneous mobile devices. *Internet of Things*, 3, pp.175–186.

Li, J., Xie, Z., Sun, X., Tang, J., Liu, H., Stankovic, J.A., 2018. An Automatic and Accurate Localization System for Firefighters. *2018 IEEE/ACM Third International Conference on Internet-of-Things Design and Implementation (IoTDI)*. 2018 IEEE, pp. 13–24.

Li, L., Shen, G., Zhao, C., Moscibroda, T., Lin, J.H., Zhao, F., 2014. Experiencing and handling the diversity in data density and environmental locality in an indoor positioning service. *Proceedings of the 20th annual international conference on Mobile computing and networking*. 11 September 2014 ACM, pp. 459–470.

Li, Z., Zhao, X. and Liang, H., 2018. Automatic construction of radio maps by crowdsourcing pdr traces for indoor positioning. *2018 IEEE International Conference on Communications (ICC)*. 2018 IEEE, pp. 1–6.

Lim, J.-S., Jang, W.-H., Yoon, G.-W. and Han, D.-S., 2013. Radio map update automation for WiFi positioning systems. *IEEE Communications Letters*, 17(4), pp.693–696.

Lim, S.Y., Yun, Z. and Iskander, M.F., 2018. Radio Propagation Modeling: A Unified View of the Ray-Tracing Image Method Across Emerging Indoor and Outdoor Environments. In: *The World of Applied Electromagnetics*. Springer, pp. 301–328.

Lim, T.O., Ding, L.M., Zaki, M., Suleiman, A.B., Fatimah, S., Siti, S., Tahir, A., Maimunah, A.H., 2000. Distribution of body weight, height and body mass index in a national sample of Malaysian adults. *Medical Journal of Malaysia*, 55(1), pp.108–128.

Lin, K.-S., Wong, A.K.-S., Wong, T.-L. and Lea, C.-T., 2015. Adaptive WiFi Positioning System with Unsupervised Map Construction. 2015 The Steering Committee of The World Congress in Computer Science, Computer Engineering and Applied Computing (WorldComp), p. 636.

Liu, H., Darabi, H., Banerjee, P. and Liu, J., 2007. Survey of wireless indoor positioning techniques and systems. *IEEE Transactions on Systems, Man, and Cybernetics, Part C (Applications and Reviews)*, 37(6), pp.1067–1080.

Liu, H.-H. and Yang, Y.-N., 2011. WiFi-based indoor positioning for multi-floor environment. *TENCON 2011-2011 IEEE Region 10 Conference*. 2011 IEEE, pp. 597–601.

Liu, J. and Wang, L., 2015. A WIFI radio signals based adaptive positioning scheme. *2015 IEEE Advanced Information Technology, Electronic and Automation Control Conference (IAEAC)*. December 2015 pp. 1132–1136.

Liu, T., Li, Q. and Zhang, X., 2016. Automatic Construction of Wi-Fi Radio Map Using Smartphones. *The International Archives of Photogrammetry, Remote Sensing and Spatial Information Sciences*, 41, p.309.

Liu, T., Zhang, X., Li, Q. and Fang, Z., 2017. A visual-based approach for indoor radio map construction using smartphones. *Sensors*, 17(8), p.1790.

Lott, M. and Forkel, I., 2001. A multi-wall-and-floor model for indoor radio propagation. *Vehicular Technology Conference, 2001. VTC 2001 Spring. IEEE VTS 53rd*. 2001 IEEE, pp. 464–468.

Lu, G., Yan, Y., Ren, L., Saponaro, P., Sebe, N., Kambhamettu, C., 2016. Where am i in the dark: Exploring active transfer learning on the use of indoor localization based on thermal imaging. *Neurocomputing*, 173, pp.83–92.

Lu, J.S., Steinbach, D., Cabrol, P. and Pietraski, P., 2012. Modeling human blockers in millimeter wave radio links. *ZTE communications*, 10(4), pp.23–28.

Luo, X., O'Brien, W.J. and Julien, C.L., 2011. Comparative evaluation of Received Signal-Strength Index (RSSI) based indoor localization techniques for construction jobsites. *Advanced Engineering Informatics*, 25(2), pp.355–363.

Ma, Z., Cai, S., Mao, N., Yang, Q., Feng, J., Wang, P., 2018. Construction quality management based on a collaborative system using BIM and indoor positioning. *Automation in Construction*, 92, pp.35–45.

MacCartney, G.R., Deng, S., Sun, S. and Rappaport, T.S., 2016. Millimeter-wave human blockage at 73 GHz with a simple double knife-edge diffraction model and extension for directional antennas. *2016 IEEE 84th Vehicular Technology Conference (VTC-Fall)*. 2016 IEEE, pp. 1–6.

Machaj, J., Brida, P. and Piché, R., 2011. Rank based fingerprinting algorithm for indoor positioning. *2011 International Conference on Indoor Positioning and Indoor Navigation*. 2011 IEEE, pp. 1–6.

Makki, A., Siddig, A., Saad, M. and Bleakley, C., 2015. Survey of WiFi positioning using time-based techniques. *Computer Networks*, 88, pp.218–233.

Mardeni, R. and Solahuddin, Y., 2012. Path loss model development for indoor signal loss prediction at 2.4 GHz 802.11 n network. *Microwave and Millimeter Wave Technology (ICMMT), 2012 International Conference on*. 2012 IEEE, pp. 1–4.

Markets and markets, 2016. *Location Based Services (LBS) and Real Time Location Systems (RTLS) Market by Location, Technology, Software, Hardware, Service and Application Area - Global Forecast to 2021*,

Mautz, R. and Tilch, S., 2011. Survey of optical indoor positioning systems. 2011 IEEE, pp. 1–7.

McKown, J.W. and Hamilton, R.L., 1991. Ray tracing as a design tool for radio networks. *IEEE Network*, 5(6), pp.27–30.

Meneses, F., Moreira, A., Costa, A. and Nicolau, M.J., 2019. Radio Maps for Fingerprinting in Indoor Positioning. In: *Geographical and Fingerprinting Data to Create Systems for Indoor Positioning and Indoor/Outdoor Navigation*. Elsevier, pp. 69–95.

Mier, J., Jaramillo-Alcázar, A. and Freire, J.J., 2019. At a Glance: Indoor Positioning Systems Technologies and Their Applications Areas. *International Conference on Information Technology & Systems*. 2019 Springer, pp. 483–493.

Millington, P.F. and Wilkinson, R., 2009. *Skin (Biological Structure and Function Books)*, Cambridge University Press, Cambridge.

Mohamed, M., Cheffena, M., Fontán, F.P. and Moldsvor, A., 2018. A Dynamic Channel Model for Indoor Wireless Signals: Working Around Interference Caused by Moving Human Bodies. *IEEE Antennas and Propagation Magazine*, 60(2), pp.82–91.

Molina, B., Olivares, E., Palau, C.E. and Esteve, M., 2018. A multimodal fingerprint-based indoor positioning system for airports. *IEEE Access*, 6, pp.10092–10106.

Moutinho, J.N., Araújo, R.E. and Freitas, D., 2016. Indoor localization with audible sound—Towards practical implementation. *Pervasive and Mobile Computing*, 29, pp.1–16.

Oussalah, M., Alakhras, M. and Hussein, M.I., 2015. Multivariable fuzzy inference system for fingerprinting indoor localization. *Fuzzy Sets and Systems*, 269, pp.65–89.

Oyie, N.O. and Afullo, T.J., 2018. Measurements and analysis of large-scale path loss model at 14 and 22 GHz in indoor corridor. *IEEE Access*, 6, pp.17205–17214.

Plouhinec, E. and Uguen, B., 2019. UTD Human Body Models Comparison based on dual Motion Capture and Radio Measurements. *IEEE-APS Topical Conference on Antennas and Propagation in Wireless Communications (APWC)*. IEEE, pp. 192–197.

Popleteev, A., 2019. Improving ambient FM indoor localization using multipath-induced amplitude modulation effect: A year-long experiment. *Pervasive and Mobile Computing*, 58, pp.1-14

Potgantwar, A., Kohli, J.K. and Shirke, P., 2015. Adaptive RSS based indoor positioning system using RFID and wireless technology. *Global Journal of Advanced Engineering Technologies*, 4(4), pp.436–446.

de Queiroz, A.D.C. and Trintinália, L.C., 2015. An analysis of human body shadowing models for ray-tracing radio channel characterization. *International Microwave and Optoelectronics Conference (IMOC)*. IEEE, pp. 1–5.

Rappaport, T.S., 1996. *Wireless communications: principles and practice*, prentice hall PTR New Jersey.

Rezazadeh, J., Subramanian, R., Sandrasegaran, K., Kong, X., Moradi, M., Khodamoradi, F., 2018. Novel iBeacon placement for indoor positioning in IoT. *IEEE Sensors Journal*, 18(24), pp.10240–10247.

Rezgui, Y., Pei, L., Chen, X., Wen, F., Han, C., 2017. An efficient normalized rank based SVM for room level indoor WiFi localization with diverse devices. *Mobile Information Systems,* Vol. 2017, pp. 1-20.

Rizos, C., Dempster, A.G., Li, B. and Salter, J., 2007. Indoor positioning techniques based on wireless LAN. 1st IEEE International Conference on Wireless Broadband and Ultra-Wideband Communications. IEEE, pp. 1-7

Rossi, J.P., Bic, J.C., Levy, A.J., Gabillett, Y., Rosen, M., 1991. A ray launching method for radio-mobile propagation in urban area. *Antennas and Propagation Society Symposium Digest*. IEEE, pp. 1540–1543.

Saeidi, C., Kamyab, M. and Fard, A., 2006. Fast Ray Tracing Propagation Prediction Model For Indoor Environments. *7th International Symposium on Antennas, Propagation & EM Theory*. IEEE, pp. 1–4.

Saito, K. and Omiya, M., 2018. A Computational Study of Indoor-to-Outdoor Propagation in Office Environment at 2.4 GHz and 5.2 GHz Bands. *IEEE International Workshop on Electromagnetics: Applications and Student Innovation Competition (iWEM)*. IEEE, pp. 1–2.

Salem, M., Ismail, M. and Misran, N., 2011, Validation of Three-Dimensional Ray-Tracing Algorithm for Indoor Wireless Propagations. *ISRN Communications and Networking*, vol 2011, pp.1-5.

Samama, N., 2019. *Indoor Positioning: Technologies and Performance*, John Wiley & Sons.

Sandby-Moller, J., Poulsen, T. and Wulf, H.C., 2003. Epidermal thickness at different body sites: relationship to age, gender, pigmentation, blood content, skin type and smoking habits. *Acta Dermato Venereologica*, 83(6), pp.410–413.

Santana, J.A., Macías, E., Suárez, Á., Marrero, D., Mena, V., 2016. Adaptive estimation of WiFi RSSI and its impact over advanced wireless services. *Mobile Networks and Applications*, pp.1–13.

Sasaki, M., Inomata, M., Yamada, W., Kita, N., Onizawa, T., Nakatsugawa, M., 2016. Path loss characteristics at multiple frequency bands from 0.8 to 37 GHz in indoor office. *10th European Conference on Antennas and Propagation (EuCAP)*. IEEE, pp. 1–4.

Schauer, L., Marcus, P. and Linnhoff-Popien, C., 2016. Towards feasible Wi-Fi based indoor tracking systems using probabilistic methods. *International Conference on Indoor Positioning and Indoor Navigation (IPIN)*. IEEE, pp. 1–8.

Sedlar, U., Winterbottom, J., Tavcar, B., Sterle, J., Cijan, J., Volk, M., 2019. Next Generation Emergency Services Based on the Pan-European Mobile Emergency Application (PEMEA) Protocol: Leveraging Mobile Positioning and Context Information. *Wireless Communications and Mobile Computing*, 2019.

Seidel, S.Y. and Rappaport, T.S., 1992. 914 MHz path loss prediction models for indoor wireless communications in multifloored buildings. *IEEE transactions on Antennas and Propagation*, 40(2), pp.207–217.

Shu, Y., Bo, C., Shen, G., Zhao, C., Li, L., Zhao, F., 2015. Magicol: Indoor Localization Using Pervasive Magnetic Field and Opportunistic WiFi Sensing. *IEEE Journal on Selected Areas in Communications*, 33(7), pp.1443–1457.

Shukri, S., Kamarudin, L.M., Cheik, G.C., Gunasagaran, R., Zakaria, A., Kamarudin, K., Zakaria, S.S., Harun, A., Azemi, S.N., 2016. Analysis of RSSI-based DFL for human detection in indoor environment using IRIS mote. *2016 3rd International Conference on Electronic Design (ICED)*. 2016 IEEE, pp. 216–221.

Slezak, C., Semkin, V., Andreev, S., Koucheryavy, Y., Rangan, S., 2018. Empirical effects of dynamic human-body blockage in 60 ghz communications. *IEEE Communications Magazine*, 56(12), pp.60–66.

Stockx, T., Hecht, B. and Schöning, J., 2014. SubwayPS: Towards Enabling Smartphone Positioning in Underground Public Transportation Systems. SIGSPATIAL International Conference on Advances in Geographic Information Systems. ACM, pp. 93-102

Sun, L., Zheng, Z., He, T. and Li, F., 2015. Multifloor Wi-Fi localization system with floor identification. *International Journal of Distributed Sensor Networks*, 11(7), p.131523.

Tayebi, A., Gomez Perez, J., Adana Herrero, F.M.S. de and Gutierrez, O., 2009. The application of ray-tracing to mobile localization using the direction of arrival and received signal strength in multipath indoor environments. *Progress In Electromagnetics Research*, 91, pp.1–15.

Torres-Sospedra, J. et al., 2018. Off-line evaluation of mobile-centric indoor positioning systems: The experiences from the 2017 IPIN competition. *Sensors*, 18(2), pp.487.

Trogh, J., Joseph, W., Martens, L. and Plets, D., 2019. An unsupervised learning technique to optimize radio maps for indoor localization. *Sensors*, 19(4), pp.752.

Tseng, P.-H. et al., 2017. Ray-Tracing-Assisted Fingerprinting Based on Channel Impulse Response Measurement for Indoor Positioning. *IEEE Transactions on Instrumentation and Measurement*, 66(5), pp.1032–1045.

Tsirmpas, C., Rompas, A., Fokou, O. and Koutsouris, D., 2015. An indoor navigation system for visually impaired and elderly people based on Radio Frequency Identification (RFID). *Information Sciences*, 320, pp.288–305.

Turgut, Z., Aydin, G.Z.G. and Sertbas, A., 2016. Indoor Localization Techniques for Smart Building Environment. *Procedia Computer Science*, 83, pp.1176–1181.

Ubom, E.A., Akpanobong, A.C. and Abraham, I.I., 2019. Characterization of Indoor Propagation Properties and Performance Evaluation for 2.4 Ghz Band Wi-Fi. *Available at SSRN 3391700*.

U.S. Department of Homeland Security, 2016. *Precision Outdoor and Indoor Navigation and Tracking for Emergency Responders (POINTER)*, NASA JPL.

Vahidnia, M.H., Malek, M.R., Mohammadi, N. and Alesheikh, A.A., 2013. A hierarchical signal-space partitioning technique for indoor positioning with WLAN to support location-awareness in mobile map services. *Wireless personal communications*, 69(2), pp.689–719.

Vega, C.P., Mediavilla, M.L. and Díez, M.C., 1997. Efectos del tráfico de personas sobre la atenuación en el canal de propagación en interiores. *Simposium de la Unión Internacional de Radio (URSI)*. pp. 1-4.

Viani, F., Polo, A. and Giarola, E., 2016. Exploiting EM simulation modelling for wireless indoor localization. *10th European Conference on Antennas and Propagation (EuCAP)*. IEEE, pp. 1–4.

Wang, H., Zhao, Z., Hu, J., Qu, Z., Feng, H., 2016. Study on improvement of fingerprint matching algorithm in wireless LAN based indoor positioning system. 2016 IEEE, pp. 275–280.

Wang, K., Yu, X., Xiong, Q., Zhu, Q., Lu, W., Huang, Y., Zhao, L., 2019. Learning to improve WLAN indoor positioning accuracy based on DBSCAN-KRF algorithm from RSS fingerprint data. *IEEE Access*.

Wang, L. and Wong, W.C., 2014. A Novel RSS model and Power-bias Mitigation Algorithm in fingerprinting-based Indoor Localization in Wireless Local Area Networks. *20th European Wireless Conference*. pp. 1–7.

Wang, Q., Zhao, X., Li, S., Wang, M., Sun, S., Hong, W., 2017. Attenuation by a human body and trees as well as material penetration loss in 26 and 39 GHz

millimeter wave bands. *International Journal of Antennas and Propagation*. Hindawi Vol. 2017, pp.1-8.

Wang, T.-M., Tseng, P.-H., Chan, Y.-C. and Lin, D.-B., 2015. A ray-tracing based fingerprinting for indoor positioning. *Intl Conf on Scalable Computing and Communications.* IEEE, pp. 1859–1863.

Wilson, R., 2002. Propagation losses through common building materials 2.4 GHz vs 5 GHz. *Magis Networks Inc.: San Diego, CA, USA*.

Witrisal, K., Hinteregger, S., Kulmer, J., Leitinger, E., Meissner, P., 2016. High-accuracy positioning for indoor applications: RFID, UWB, 5G, and beyond. *IEEE International Conference on RFID (RFID)*. IEEE, pp. 1–7.

Wu, C., Yang, Z. and Liu, Y., 2018. Adaptive Radio Map Updating. In: *Wireless Indoor Localization*. Springer, pp. 83–107.

Wu, D., Xu, Y. and Ma, L., 2009. Research on RSS based indoor location method. *Pacific-Asia Conference on Knowledge Engineering and Software Engineering*. IEEE, pp. 205–208.

Xia, S., Liu, Y., Yuan, G., Zhu, M., Wang, Z., 2017. Indoor fingerprint positioning based on Wi-Fi: An overview. *ISPRS International Journal of Geo-Information*, 6(5), p.135.

Xue, W., Qiu, W., Hua, X. and Yu, K., 2017. Improved Wi-Fi RSSI measurement for indoor localization. *IEEE Sensors Journal*, 17(7), pp.2224–2230.

Yadav, R.K., Bhattarai, B., Gang, H.-S. and Pyun, J.-Y., 2019. Trusted K Nearest Bayesian Estimation for Indoor Positioning System. *IEEE Access*, 7, pp.51484–51498.

Yamada, N., Tanaka, Y. and Nishikawa, K., 2005. Radar cross section for pedestrian in 76GHz band. *European Microwave Conference.* IEEE, pp. 4–7.

Yang, C. and Shao, H.-R., 2015. WiFi-based indoor positioning. *IEEE Communications Magazine*, 53(3), pp.150–157.

Yaw, K.C., 2012. Measurement of dielectric material properties. *Rohde & Schwarz*.

Yin, J., Yang, Q. and Ni, L., 2005. Adaptive Temporal Radio Maps for Indoor Location Estimation. *Third IEEE International Conference on Pervasive Computing and Communications*. IEEE, pp. 85–94.

Yin, J., Yang, Q. and Ni, L.M., 2008. Learning adaptive temporal radio maps for signal-strength-based location estimation. *IEEE Transactions on Mobile Computing*, 7(7), pp.869–883.

Yu, N., Xiao, C., Wu, Y. and Feng, R., 2016. A radio-map automatic construction algorithm based on crowdsourcing. *Sensors*, 16(4), pp.504-535.

Yun, Z. and Iskander, M.F., 2015. Ray tracing for radio propagation modeling: principles and applications. *IEEE Access*, 3, pp.1089–1100.

Zafari, F., Gkelias, A. and Leung, K.K., 2019. A survey of indoor localization systems and technologies. *IEEE Communications Surveys & Tutorials*.

Zhang, S., Guo, J., Wang, W. and Hu, J., 2018. Indoor 2.5 D Positioning of WiFi Based on SVM. *Ubiquitous Positioning, Indoor Navigation and Location-Based Services (UPINLBS)*. IEEE, pp. 1–7.

Zhang, Wei, Liu, K., Zhang, Weidong, Zhang, Y., Gu, J., 2016. Deep neural networks for wireless localization in indoor and outdoor environments. *Neurocomputing*, 194, pp.279–287.

Zhao, X., Wang, Q., Li, S., Geng, S., Wang, M., Sun, S., Wen, Z., 2016. Attenuation by human bodies at 26-and 39.5-GHz millimeter wavebands. *IEEE Antennas and Wireless Propagation Letters*, 16, pp.1229–1232.

Zhekov, S.S., Franek, O. and Pedersen, G.F., 2019. Dielectric Properties of Human Hand Tissue for Handheld Devices Testing. *IEEE Access*, 7, pp.61949–61959.

Zhou, R. and Sang, N., 2012. Enhanced Wi-Fi Fingerprinting with Building Structure and User Orientation. *8th International Conference on Mobile Ad-hoc and Sensor Networks (MSN)*. pp. 219–225.

Zhu, N., Marais, J., Bétaille, D. and Berbineau, M., 2018. GNSS position integrity in urban environments: A review of literature. *IEEE Transactions on Intelligent Transportation Systems*, 19(9), pp.2762–2778.

Ziri-Castro, K.I., Scanlon, W.G. and Evans, N.E., 2005. Prediction of variation in MIMO channel capacity for the populated indoor environment using a radar cross-section-based pedestrian model. *IEEE Transactions on Wireless Communications*, 4(3), pp.1186–1194.

Zourmand, A., Sheng, N.W., Hing, A.L.K. and AbdulRehman, M., 2018. Human Counting and Indoor Positioning System Using WiFi Technology. *IEEE International Conference on Automatic Control and Intelligent Systems (I2CACIS)*. IEEE, pp. 142–147.

APPENDIX A
Experimental Setup

Table A.1 Experiment to manually construct a radio map in a simple building

Experiment No.	A1
Title	Manual Radio Map (RM) Construction
Subtitle	Simple Building
Aim	Creating a radio map database for a simple building
Location	Auditorium of Faculty of Industrial Technology, Universitas Islam Indonesia, Yogyakarta Size: 13 m x 17 m
Device	3 Access Points (APs) : Linksys WAP300N 1 Mobile Device (MD) : Xiaomi Redmi note 3 Android Application to record RSS
Procedure	1. Grid the testbed, divide into 221 points, with a 1 m distance between points 2. Give a position label (x,y) to each point 3. Configure APs and MD 4. Record RSSI using MD to create manual RM (30 beacons per point and to calculate the median)

Table A.2 Experiment to manually construct a radio map in a complex building

Experiment No.	A2
Title	Manual Radio Map (RM) Construction
Subtitle	Complex Building
Aim	Creating a radio map database for a complex building
Location	Level 3, Razak Building, Universiti Teknologi Malaysia, Kuala Lumpur. Size: 80 m × 16 m
Device	3 Access Points (APs) : Linksys WAP300N 1 Mobile Device (MD) : Xiaomi Redmi Note 3 Android Application to record RSS
Procedure	1. Grid the testbed, divide into 523 points, with a 1 m distance between points 2. Give a position label (x,y) to each point 3. Configure APs and MD 4. Record RSSI using MD to create manual RM (30 beacons per point and calculate the median)

In this case, a simple building means that the building only has one room, which, in this experiment, was the Auditorium of Faculty of Industrial Technology, Universitas Islam Indonesia, Yogyakarta, as shown in Figure A.1 and Figure A.2.

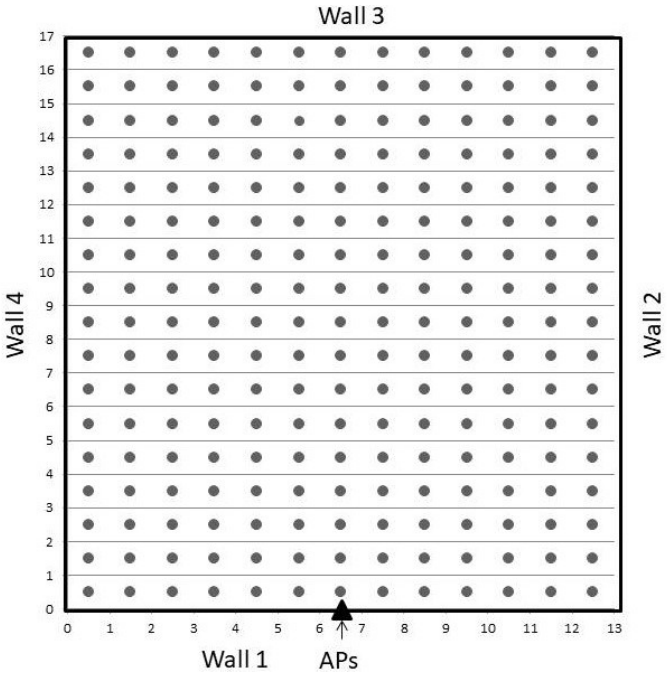

Figure A.1. Layout of the Auditorium of the Faculty of Industrial Technology

Figure A.2. Photo of the Auditorium of the Faculty of Industrial Technology

A complex building means a building with many rooms. In this experiment, the complex building was the 3rd floor of Razak Tower, Universiti Teknologi Malaysia, Kuala Lumpur, as shown in Figure A.3 and Figure A.4.

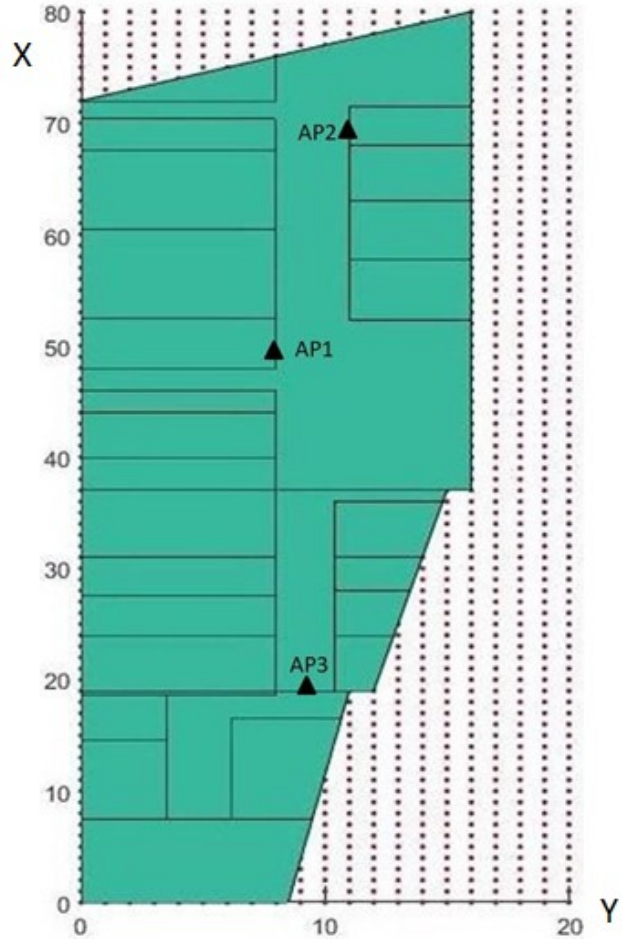

Figure A.3. Layout of Razak Tower Level 3

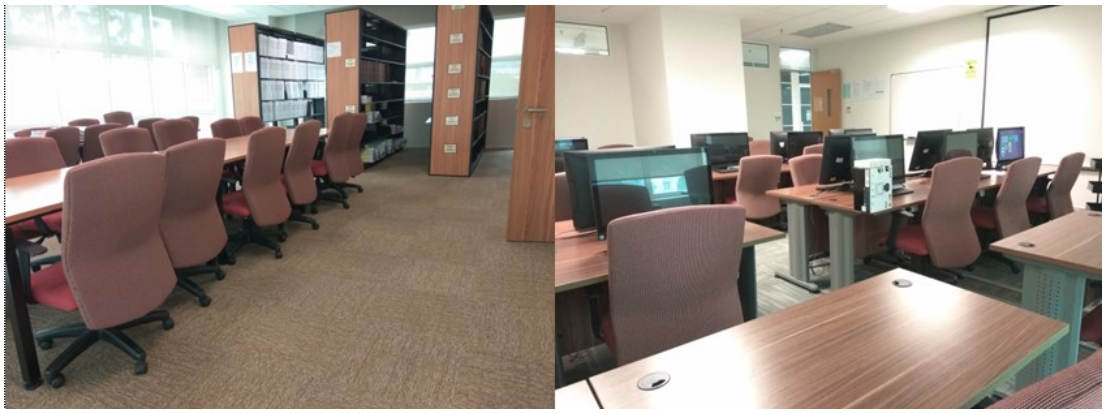

Figure A.4. Photos of Certain Rooms in Razak Tower Level 3

Table A.3 Automatic Radio Map (RM) Construction using the Multi-Wall Propagation Model

Experiment No.	A3
Title	Automatic Radio Map (RM) Construction without People Effect
Subtitle	Multi-Wall Model
Aim	Creating an automatic multi-wall radio map (MWRM) database
Location	Computer Simulation using MATLAB
Device	1 Laptop : Dell Inspiron 14 5000 Series (Core i7) Software : MATLAB
Procedure	1. Write the program script based on the multi-wall propagation model 2. Define the layout and parameters of the building 3. Run the simulation 4. Compare the results to MRM and calculate the Mean Squared Error (MSE)

Table A.4 RSSI Prediction considering People Effect using the Multi-Wall Propagation Model

Experiment No.	A4
Title	RSSI Prediction considering People Effect
Subtitle	Multi-Wall Propagation Model
Aim	Predicting RSSI in certain points considering people around that point
Location	Computer Simulation using MATLAB
Device	1 Laptop : Dell Inspiron 14 5000 Series (Core i7) Software : MATLAB R2016a
Procedure	1. Write the program script based on the multi-wall propagation model 2. Define the layout and parameters of the building 3. Define the people model (shape and parameters) 4. Run the simulation 5. Compare the results to the measurement data from Experiments A5, A6, and A7

Table A.5 Effect of People in the Line of Sight (LOS) between AP and MD on RSS

Experiment No.	A5
Title	Effect of People on RSS
Subtitle	People Position on Line of Sight (LOS) between AP and MD
Aim	To know the effect of one person on RSS in LOS position and its pattern
Location	Auditorium of Faculty of Industrial Technology, Universitas Islam Indonesia, Yogyakarta Size: 13 m × 17 m
Device	3 Access Points (APs) : Linksys WAP300N 1 Mobile Device (MD) : Xiaomi Redmi Note 3 Android Application to record RSS
Procedure	1. Set APs and MD with variation in AP height, h(AP1) = 1 m, h(AP2) = 2 m, h(AP3) = 3 m, and h(MD) = 1 m. Distance between AP1 and MD is 10 m. 2. One person stands between AP and MD in the LOS position, with variation in people distance from MD. 3. MD records RSS, 30 beacons in each position.

Table A.6 Effect of One Person in the Non Line of Sight (NLOS) around MD

Experiment No.	A6
Title	Effect of People on RSS
Subtitle	One person on Non-Line of Sight (NLOS) Position around MD
Aim	To know the effect of one person on RSS in NLOS position and its pattern
Location	Auditorium of Faculty of Industrial Technology, Universitas Islam Indonesia, Yogyakarta Size: 13 m × 17 m
Device	3 Access Points (APs) : Linksys WAP300N 1 Mobile Device (MD) : Xiaomi Redmi Note 3 Android Application to record RSS
Procedure	1. Set APs and MD with variation in AP height, h(AP1) = 1 m, h(AP2) = 2 m, h(AP3) = 3 m, and h(MD) = 1 m. Distance between AP1 and MD is 10 m. 2. One person stands around MD in the NLOS position, with variation in the distance from MD (1 m, 2 m, 3 m). 3. MD records RSS, 30 beacons in each position.

Figure A.5. RSSI measurement to determine the effect of many people (Experiment A7)

Table A.7 Effect of Many People in the Non-Line of Sight (NLOS) Position around MD

Experiment No.	A7
Title	Effect of People on RSS
Subtitle	Many People in the Non-Line of Sight (NLOS) Position around MD
Aim	To determine the effect of many people in the NLOS position on RSS and its pattern
Location	Auditorium of Faculty of Industrial Technology, Universitas Islam Indonesia, Yogyakarta Size: 13 m × 17 m
Device	3 Access Points (APs) : Linksys WAP300N 1 Mobile Device (MD) : Xiaomi Redmi Note 3 Android Application to record RSS
Procedure	1. Set APs and MD with variation in AP height, h(AP1) = 1 m, h(AP2) = 2 m, h(AP3) = 3 m, and h(MD) = 1 m. Distance between AP1 and MD is 10 m. 2. Many people stand around MD in the NLOS position, with variation in distance to MD (1 m, 2 m, 3 m). 3. MD records RSS, 30 beacons in each position.

Table A.8 Automatic Radio Map (RM) Construction using the Ray Tracing Propagation Model

Experiment No.	A8
Title	Automatic Radio Map (RM) Construction without People Effect
Subtitle	Ray Tracing Propagation Model
Aim	Creating an automatic ray tracing radio map (RTRM) database
Location	Computer Simulation using MATLAB
Device	1 Laptop : Dell Inspiron 14 5000 Series (Core i7) Software : MATLAB
Procedure	1. Write the program script based on the Ray Tracing propagation model 2. Define the layout and parameters of the building 3. Run the simulation 4. Compare results to the MRM and calculate the Mean Squared Error (MSE)

Table A.9 RSSI Prediction considering People Effect based on the Ray Tracing Propagation Model

Experiment No.	A9
Title	RSSI Prediction considering People Effect
Subtitle	Ray Tracing Propagation Model
Aim	Predicting RSSI at a certain point considering people around that point
Location	Computer Simulation using MATLAB
Device	1 Laptop : Dell Inspiron 14 5000 Series (Core i7) Software : MATLAB R2016a
Procedure	1. Write the program script based on the ray tracing propagation model 2. Define the layout and parameters of the building 3. Define the people model (shape and parameters) 4. Run the simulation 5. Compare the results to the measurement data from Experiments A5, A6, and A7

Table A.10 Testing the accuracy of the system using the manual radio map

Experiment No.	A10
Title	Testing the accuracy of the system without the influence of people
Subtitle	Manual Radio Map (MRM)
Aim	Calculate the accuracy of the system using the manual radio map
Location	Computer Simulation using MATLAB R2016a
Device	1 Laptop : Dell Inspiron 14 5000 Series (Core i7) Software : MATLAB R2016a
Procedure	1. Write the localisation program script based on the KNN algorithm 2. Measure the RSSI vectors at 65 nodes in the building as input 3. Run the simulation using MRM 4. Find the accuracy of the system

Table A.11 Testing the accuracy of the system using the multi-wall automatic radio map

Experiment No.	A11
Title	Testing the accuracy of the system without the influence of people
Subtitle	Automatic Radio Map using Multi-Wall Model (ARM-MW)
Aim	Calculate the accuracy of the system using the automatic radio map based on the multi-wall model
Location	Computer Simulation using MATLAB R2016a
Device	1 Laptop : Dell Inspiron 14 5000 Series (Core i7) Software : MATLAB R2016a
Procedure	1. Write the localisation program script based on KNN 2. Measure the RSSI vectors at 65 nodes in the building as input 3. Run the simulation using ARM-MW 4. Find the accuracy of the system

Table A.12 Testing the accuracy of the system using the ray tracing automatic radio map

Experiment No.	A12
Title	Testing the accuracy of the system without the influence of people
Subtitle	Automatic Radio Map using the Ray Tracing Model (ARM-RT)
Aim	Calculate the accuracy of the system using the automatic radio map based on the ray tracing model
Location	Computer Simulation using MATLAB R2016a
Device	1 Laptop : Dell Inspiron 14 5000 Series (Core i7) Software : MATLAB R2016a
Procedure	1. Write the localisation program script based on KNN algorithm 2. Measure the RSSI vectors at 65 nodes in the building as input 3. Run the simulation using ARM-RT 4. Find the accuracy of the system

Table A.13 Testing the effect of people presence (LOS) on IPS accuracy

Experiment No.	A13
Title	Testing the effect of people presence on IPS accuracy
Subtitle	People in the LOS position
Aim	Calculate the accuracy of the system when there are people in the LOS position
Location	Computer Simulation using MATLAB R2016a
Device	1 Laptop : Dell Inspiron 14 5000 Series (Core i7) Software : MATLAB R2016a
Procedure	1. Write the localisation program script based on the KNN algorithm 2. Perform the adaptation of 65 RSSI vectors, the same ones used in the experiment in Section 5.2, and use as input 3. Run the simulation using 3 radio map databases: MRM, ARM-MW, and ARM-RT 4. Find the accuracy of the system

Table A.14 Testing the effect of people presence (NLOS) on IPS accuracy

Experiment No.	A14
Title	Testing the effect of people presence on IPS accuracy
Subtitle	People in the NLOS position
Aim	Calculate the accuracy of the system when there are people in the NLOS position
Location	Computer Simulation using MATLAB R2016a
Device	1 Laptop : Dell Inspiron 14 5000 Series (Core i7) Software : MATLAB R2016a
Procedure	1. Write the localisation program script based on the KNN algorithm 2. Perform the adaptation of 65 RSSI vectors, the same ones used in the experiment in Section 5.2, and use as input 3. Run the simulation using 3 radio map databases: MRM, ARM-MW, and ARM-RT 4. Find the accuracy of the system

Table A.15 Testing the accuracy of the proposed model (AIRY)

Experiment No.	A15
Title	Testing the accuracy of the proposed model (AIRY)
Subtitle	-
Aim	Calculate the accuracy of the proposed model (AIRY)
Location	Computer Simulation using MATLAB R2016a
Device	1 Laptop : Dell Inspiron 14 5000 Series (Core i7) Software : MATLAB R2016a
Procedure	1. Write the localisation program script based on the KNN algorithm 2. Measure the RSSI vectors at 65 nodes with people around the nodes in the building, and use as input 3. Run the simulation using the ARM-RT radio map database and find the initial position 4. Calculate the accuracy (initial accuracy) 5. Perform adaptation on the 65 RSSI vectors, the same ones used in Step 2 of this experiment based on people in both positions (LOS/ NLOS) 6. Run the simulation using the ARM-RT radio map database and find the position (accurate position) 7. Find the accuracy of the system (accurate accuracy) 8. Compare the initial accuracy and the accurate accuracy

APPENDIX B
Pseudocode of Algorithms

Algorithm 1: Automatic Radio Map Multi-Wall ARM MW Generation

Input: $Floors\ No, Rooms\ No, Walls\ List, People\ List, AccessPoints\ List$

Output: $Point\ Dynamic\ Radio\ Map\ (PDRM)$

1: $Create\ Reference\ Point\ List\ (RP)$
2: ***For*** $x \leftarrow RSP.x\ to\ REP.x$ ***do***
3: ***For*** $y \leftarrow RSP.y\ to\ REP.y$ ***do***
4: $rp.x \leftarrow (REP.x - RSP.x)/2$
5: $rp.y \leftarrow (REP.y - RSP.y)/2$
6: $rplabel = (x, y)$
7: $RP.add(rp + rplabel)$
8: ***End*** For
9: ***End*** For
10: $Create\ Room\ Dynamic\ Radio\ Map\ List\ (FDRM)$
11: ***For*** $each\ RP\ in\ Reference\ Point\ List$ ***do***
12: ***For*** $each\ AP\ in\ AccessPoints\ List$ ***do***
13: $d \leftarrow EuclideanDistance(RP, AP)$
14: $id \leftarrow Influnce\ distance(RP, AP)$
15: $Walls\_between\ (wb) = 0$
16: $People\ in\ Influence\ Distance\ (pid) = 0$
17: ***For*** $each\ Wall\ in\ Walls\ List$ ***do***
18: ***If*** $\left(Wall\ intersect\ LOS_{between(RP,AP)}\right)$ ***then***
19: $wb = wb + 1$
20: ***End*** If
21: ***End*** For
22: ***For*** $each\ Person\ in\ People\ List$ ***do***
23: ***If*** $(person\ location\ between\ (RP, AP)\ and \leq id)$ ***then***
24: $pid = pid + 1$
25: ***End*** If
26: ***End*** For
27: $rss \leftarrow -34 - 22 * log10(d) - wb * 3 - pid * 2 - random(-1,1)$
28: $PDRM.add(rss + RP.rplabel)$
29: ***End*** For
30: ***End*** For
31: ***Return*** $RDRM$

Algorithm 2: Automatic Radio Map Ray Tracing ARM RT Generation

Input: *Building Map, Relative Permittivity List, AccessPoints List*

Output: *Automatic Radio Map Ray Tracing (ARM RT)*

1: *Defining a Finite Panel (Walls)*
2: *3D Formation of the Structure*
3: *Calculating Fresnel Coefficients for Walls*
4: ***For*** $i \leftarrow 1$ *to size* $(wall.xyz1,1)$ ***do***
5: *find reflection and transmission Fresnell coefficient for each wall*
6: ***End*** *For*
7: *Meshing the Boundary Volume and Assign the RX height*
8: *Calculating the Distance of* $TX(s)$ *from every mesh node* RXi
9: ***For*** $i \leftarrow 1$ *to* ***do***
10: *find the distance*
11: ***End*** *For*
12: *Equating the Panels* $(Walls)$ *in 3D*
13: *finding projection of TX on each panel*
14: *calculating the reflection* $(mirror)$ *of TX across each panel*
15: *Calculating the 2nd Image of TX across each wall*
16: *Calculating LOS Components*
17: *Calculating Multipath & Reflection Components*
18: *find the reflection coefficient*
19: *count the walls between reflection paths*
20: *find the antenna gain and beam departure angle*
21: *calculating the anggle of arrival*
22: *find the walls between TX to reflection point*
23: *find finite walls between reflection point and RX*
24: *find number of walls between reflection paths*
25: *calculating the received signal at RX from reflection point on wall j*
26: *calculating 2nd reflection*
27: *Drawing the Maps*
28: *LOS Propagation Map Only* (a)
29: *1st Reflection Propagation Map Only* (b)
30: *2nd Reflection Propagation Map Only* (c)
31: *LOS and Propagation Map* $= a + b + c$
32: ***Return*** *ARMRT*

Algorithm 3: RSSI Adaptation

Input: *Initial RSSI, People Location, AP Location, Initial Position*

Output: *Adapted RSSI*

1: *Get Initial RSSI (Ri)and People Location*
2: *Get Initial Location and AP Location*
3: ***For*** *each Ri* ***do***
4: ***If*** *(there is no people)* ***then***
5: $Ra = Ri$
6: ***End*** *If*
7: ***If*** *(there is people in LOS position)* ***then***
8: $Ra = Ri + 5$
9: ***End*** *If*
10: ***If*** *(there is people in NLOS position)* ***then***
11: $Ra = Ri + 0.5$
12: ***End*** *If*
13: ***End*** *For*

APPENDIX C
Manual Radio Map Database of the Simple Building

Median of RSSI (dBm)			Position	
AP1	AP2	AP3	x	y
-50	-49	-50	1	1
-48	-49	-50	1	2
-48	-49	-51	1	3
-52	-47	-49	1	4
-52	-47	-48	1	5
-52	-47	-47	1	6
-52	-46	-48	1	7
-52	-46	-48	1	8
-45	-44	-49	1	9
-45	-44	-48	1	10
-46	-45	-48	1	11
-44	-46	-45	1	12
-45	-49	-44	1	13
-43	-45	-44	1	14
-45	-45	-42	1	15
-43	-45	-45	1	16
-45	-44	-45	1	17
-49	-48	-49	2	1
-52	-48	-48	2	2
-52	-47	-51	2	3
-52	-47	-48	2	4
-48	-47	-52	2	5
-48	-47	-48	2	6
-51	-48	-48	2	7
-51	-45	-45	2	8
-46	-49	-45	2	9
-45	-46	-44	2	10
-45	-44	-45	2	11
-47	-42	-43	2	12
-47	-46	-43	2	13
-42	-44	-42	2	14
-42	-42	-42	2	15
-41	-43	-40	2	16
-39	-42	-40	2	17
-51	-49	-51	3	1
-48	-49	-51	3	2
-48	-48	-50	3	3
-50	-48	-50	3	4
-48	-47	-49	3	5
-46	-48	-49	3	6

Median of RSSI (dBm)			Position	
AP1	AP2	AP3	x	y
-47	-48	-48	3	7
-50	-47	-47	3	8
-48	-47	-46	3	9
-49	-44	-44	3	10
-49	-45	-44	3	11
-49	-44	-43	3	12
-41	-41	-44	3	13
-46	-40	-43	3	14
-45	-46	-43	3	15
-39	-40	-41	3	16
-42	-40	-41	3	17
-54	-51	-49	4	2
-54	-51	-52	4	3
-51	-50	-49	4	4
-51	-47	-49	4	5
-46	-47	-48	4	6
-45	-46	-47	4	7
-46	-47	-47	4	8
-48	-48	-46	4	9
-51	-44	-45	4	10
-48	-46	-45	4	11
-46	-38	-43	4	12
-46	-43	-42	4	13
-46	-41	-44	4	14
-41	-39	-40	4	15
-40	-40	-41	4	16
-38	-35	-39	4	17
-53	-50	-52	5	2
-51	-48	-50	5	3
-47	-48	-48	5	4
-47	-49	-47	5	5
-47	-49	-46	5	6
-47	-48	-45	5	7
-48	-48	-44	5	8
-48	-47	-44	5	9
-46	-45	-44	5	10
-47	-42	-44	5	11
-46	-45	-44	5	12
-46	-40	-45	5	13
-42	-39	-42	5	14

Median of RSSI (dBm)			Position	
AP1	AP2	AP3	x	y
-42	-37	-41	5	15
-39	-37	-41	5	16
-39	-37	-40	5	17
-50	-51	-50	6	2
-50	-51	-50	6	3
-50	-51	-50	6	4
-50	-47	-49	6	5
-46	-47	-48	6	6
-48	-47	-48	6	7
-49	-48	-47	6	8
-49	-48	-47	6	9
-49	-50	-46	6	10
-45	-46	-44	6	11
-45	-45	-44	6	12
-45	-42	-43	6	13
-42	-40	-40	6	14
-42	-38	-39	6	15
-36	-39	-39	6	16
-34	-34	-38	6	17
-54	-51	-50	7	2
-53	-51	-48	7	3
-48	-50	-47	7	4
-46	-50	-46	7	5
-46	-46	-46	7	6
-45	-46	-45	7	7
-46	-47	-45	7	8
-50	-44	-45	7	9
-50	-50	-47	7	10
-50	-42	-44	7	11
-45	-45	-43	7	12
-45	-45	-43	7	13
-42	-43	-41	7	14
-41	-39	-40	7	15
-36	-33	-38	7	16
-33	-34	-39	7	17
-53	-50	-51	8	2
-53	-49	-51	8	3
-49	-49	-49	8	4
-51	-49	-48	8	5
-47	-49	-48	8	6
-46	-48	-46	8	7
-51	-46	-49	8	8
-51	-46	-44	8	9

Median of RSSI (dBm)			Position	
AP1	AP2	AP3	x	y
-48	-45	-46	8	10
-48	-43	-47	8	11
-48	-43	-44	8	12
-44	-43	-44	8	13
-40	-38	-40	8	14
-40	-37	-40	8	15
-36	-34	-39	8	16
-33	-37	-38	8	17
-54	-50	-54	9	2
-49	-50	-50	9	3
-48	-48	-50	9	4
-50	-48	-49	9	5
-47	-47	-49	9	6
-48	-47	-48	9	7
-48	-46	-47	9	8
-48	-46	-47	9	9
-48	-45	-46	9	10
-49	-43	-46	9	11
-47	-41	-45	9	12
-44	-41	-40	9	13
-44	-40	-39	9	14
-42	-40	-39	9	15
-35	-35	-40	9	16
-38	-39	-40	9	17
-50	-48	-52	10	2
-54	-50	-56	10	3
-48	-50	-50	10	4
-47	-50	-49	10	5
-47	-50	-49	10	6
-45	-47	-48	10	7
-51	-47	-48	10	8
-51	-47	-47	10	9
-49	-47	-46	10	10
-48	-49	-45	10	11
-45	-45	-44	10	12
-42	-41	-43	10	13
-46	-41	-42	10	14
-38	-40	-41	10	15
-40	-40	-41	10	16
-37	-39	-40	10	17
-55	-51	-51	11	2
-52	-51	-51	11	3
-51	-50	-50	11	4

Median of RSSI (dBm)			Position	
AP1	AP2	AP3	x	y
-46	-50	-49	11	5
-46	-50	-49	11	6
-44	-45	-48	11	7
-51	-45	-48	11	8
-45	-49	-48	11	9
-48	-43	-46	11	10
-48	-47	-45	11	11
-48	-44	-45	11	12
-40	-44	-44	11	13
-41	-43	-44	11	14
-46	-43	-43	11	15
-42	-42	-43	11	16
-43	-41	-42	11	17
-51	-49	-51	12	1
-47	-50	-50	12	2
-47	-50	-50	12	3
-46	-50	-49	12	4
-47	-50	-49	12	5
-46	-50	-48	12	6
-46	-49	-48	12	7
-46	-48	-47	12	8

Median of RSSI (dBm)			Position	
AP1	AP2	AP3	x	y
-46	-50	-47	12	9
-52	-45	-48	12	10
-47	-45	-45	12	11
-44	-45	-45	12	12
-46	-45	-46	12	13
-43	-42	-43	12	14
-44	-42	-45	12	15
-49	-48	-50	13	1
-49	-48	-50	13	2
-49	-48	-49	13	3
-49	-49	-49	13	4
-49	-49	-48	13	5
-49	-49	-48	13	6
-47	-49	-48	13	7
-47	-49	-48	13	8
-45	-44	-48	13	9
-46	-45	-47	13	10
-46	-45	-46	13	11
-45	-44	-46	13	12
-46	-44	-46	13	13
-46	-43	-45	13	14

APPENDIX D
Manual Radio Map Database of the Complex Building

No.	RSSI (dBm)			Position	
	AP1	AP2	AP3	X	Y
1	-86	-80	-69	2	15
2	-86	-82	-71	2	14
3	-85	-82	-65	2	13
4	-85	-82	-66	2	12
5	-79	-82	-63	2	11
6	-82	-79	-65	2	10
7	-85	-82	-61	2	9
8	-78	-78	-63	2	8
9	-85	-82	-69	3	15
10	-85	-82	-64	3	14
11	-83	-82	-70	3	13
12	-83	-82	-62	3	12
13	-80	-82	-69	3	11
14	-76	-82	-66	3	10
15	-80	-80	-65	3	9
16	-78	-80	-66	3	8
17	-86	-75	-64	3	7
18	-86	-82	-70	4	14
19	-81	-82	-64	4	13
20	-81	-82	-70	4	12
21	-82	-82	-65	4	11
22	-82	-82	-60	4	10
23	-85	-82	-59	4	9
24	-79	-82	-59	4	8
25	-75	-78	-63	4	7
26	-89	-82	-69	5	15
27	-87	-82	-64	5	14
28	-79	-82	-61	5	13
29	-80	-80	-67	5	12
30	-84	-81	-60	5	11
31	-87	-81	-64	5	10
32	-82	-78	-62	5	9
33	-72	-77	-64	5	8
34	-71	-77	-64	5	7
35	-83	-81	-70	6	13
36	-83	-81	-64	6	12
37	-81	-77	-61	6	11
38	-80	-82	-66	6	10
39	-79	-75	-60	6	9
40	-80	-79	-62	6	8

No.	RSSI (dBm)			Position	
	AP1	AP2	AP3	X	Y
41	-71	-82	-62	6	7
42	-84	-82	-63	7	15
43	-84	-82	-69	7	14
44	-83	-82	-65	7	13
45	-83	-77	-63	7	12
46	-81	-77	-60	7	11
47	-83	-79	-63	7	10
48	-84	-82	-64	7	9
49	-79	-76	-64	7	8
50	-71	-81	-64	7	7
51	-81	-80	-59	8	12
52	-80	-77	-57	8	11
53	-83	-81	-58	8	10
54	-81	-76	-57	8	9
55	-80	-78	-56	8	8
56	-78	-77	-54	8	7
57	-77	-81	-62	9	12
58	-77	-79	-58	9	11
59	-79	-79	-66	9	10
60	-71	-80	-61	9	9
61	-78	-79	-60	9	8
62	-77	-78	-58	9	7
63	-76	-81	-57	10	12
64	-76	-81	-54	10	11
65	-76	-79	-64	10	10
66	-77	-79	-52	10	9
67	-78	-78	-52	10	7
68	-79	-73	-54	10	6
69	-79	-78	-61	11	12
70	-77	-82	-58	11	11
71	-79	-79	-60	11	10
72	-74	-77	-52	11	9
73	-76	-79	-50	11	8
74	-76	-80	-51	11	7
75	-78	-79	-60	11	6
76	-76	-78	-53	12	12
77	-76	-80	-60	12	11
78	-80	-79	-60	12	10
79	-74	-83	-55	12	9
80	-73	-83	-54	12	8

No.	RSSI (dBm)			Position	
	AP1	AP2	AP3	X	Y
81	-71	-76	-57	12	7
82	-70	-79	-56	12	6
83	-78	-81	-60	13	11
84	-78	-78	-61	13	10
85	-78	-76	-54	13	9
86	-71	-79	-54	13	8
87	-70	-76	-48	13	7
88	-73	-76	-52	13	6
89	-76	-79	-59	14	11
90	-79	-79	-58	14	10
91	-71	-77	-55	14	9
92	-68	-81	-50	14	8
93	-67	-75	-51	14	7
94	-69	-73	-51	14	6
95	-70	-79	-62	15	15
96	-69	-78	-58	15	14
97	-72	-78	-58	15	13
98	-71	-80	-56	15	12
99	-70	-79	-58	15	11
100	-69	-80	-56	15	10
101	-72	-77	-56	15	9
102	-71	-77	-52	15	8
103	-73	-76	-48	15	7
104	-72	-74	-53	15	6
105	-78	-81	-56	16	15
106	-75	-79	-58	16	14
107	-75	-79	-56	16	13
108	-74	-79	-54	16	12
109	-73	-79	-51	16	11
110	-72	-79	-57	16	10
111	-72	-77	-54	16	9
112	-71	-77	-48	16	8
113	-71	-75	-51	16	7
114	-68	-73	-53	16	6
115	-76	-78	-56	17	15
116	-77	-81	-57	17	14
117	-77	-82	-58	17	13
118	-78	-80	-56	17	12
119	-80	-82	-51	17	11
120	-74	-78	-50	17	10
121	-73	-78	-49	17	9
122	-68	-77	-49	17	8
123	-67	-76	-55	17	7

No.	RSSI (dBm)			Position	
	AP1	AP2	AP3	X	Y
124	-67	-79	-51	17	6
125	-78	-79	-63	18	15
126	-78	-77	-64	18	14
127	-75	-77	-64	18	13
128	-78	-78	-55	18	12
129	-79	-79	-51	18	11
130	-77	-80	-53	18	10
131	-78	-80	-54	18	9
132	-65	-80	-53	18	6
133	-76	-78	-56	19	15
134	-75	-78	-56	19	14
135	-76	-77	-55	19	13
136	-77	-78	-51	19	12
137	-77	-75	-52	19	11
138	-78	-79	-52	19	10
139	-66	-77	-46	19	7
140	-68	-80	-47	19	6
141	-76	-78	-57	20	15
142	-79	-76	-53	20	14
143	-75	-75	-58	20	13
144	-78	-79	-56	20	12
145	-77	-76	-54	20	11
146	-75	-78	-48	20	10
147	-71	-77	-47	20	9
148	-63	-77	-47	20	7
149	-67	-76	-46	20	6
150	-75	-76	-49	20	5
151	-77	-81	-51	20	4
152	-73	-79	-60	21	15
153	-74	-80	-54	21	14
154	-77	-82	-58	21	13
155	-76	-78	-56	21	12
156	-73	-75	-55	21	11
157	-76	-78	-51	21	10
158	-73	-76	-45	21	9
159	-66	-72	-49	21	7
160	-65	-77	-50	21	6
161	-75	-84	-52	21	5
162	-77	-76	-56	21	4
163	-77	-82	-57	22	15
164	-74	-78	-63	22	14
165	-78	-79	-56	22	13
166	-75	-78	-52	22	12

No.	RSSI (dBm)			Position	
	AP1	AP2	AP3	X	Y
167	-74	-76	-57	22	11
168	-69	-74	-54	22	10
169	-75	-76	-51	22	9
170	-70	-79	-52	22	7
171	-64	-74	-46	22	6
172	-72	-81	-53	22	5
173	-78	-79	-56	22	4
174	-79	-79	-61	23	15
175	-76	-79	-60	23	14
176	-76	-79	-60	23	13
177	-76	-78	-58	23	12
178	-73	-80	-57	23	11
179	-70	-76	-51	23	10
180	-74	-75	-51	23	9
181	-68	-72	-53	23	7
182	-68	-76	-55	23	6
183	-73	-81	-55	23	5
184	-77	-83	-59	23	4
185	-60	-73	-59	24	7
186	-66	-70	-56	24	6
187	-76	-78	-60	25	15
188	-74	-78	-59	25	14
189	-74	-79	-56	25	13
190	-74	-79	-56	25	12
191	-76	-78	-51	25	11
192	-76	-80	-57	25	10
193	-75	-78	-58	25	9
194	-63	-76	-55	25	7
195	-65	-74	-59	25	6
196	-69	-78	-61	26	15
197	-69	-78	-63	26	14
198	-74	-77	-59	26	13
199	-70	-75	-55	26	12
200	-76	-77	-55	26	11
201	-70	-77	-54	26	10
202	-63	-76	-54	26	7
203	-63	-76	-56	26	6
204	-74	-78	-64	27	15
205	-74	-78	-57	27	14
206	-77	-78	-62	27	13
207	-76	-78	-60	27	12
208	-73	-77	-56	27	11
209	-71	-78	-53	27	10

No.	RSSI (dBm)			Position	
	AP1	AP2	AP3	X	Y
210	-65	-73	-59	27	7
211	-63	-77	-54	27	6
212	-71	-75	-62	28	15
213	-74	-75	-62	28	14
214	-77	-74	-68	28	13
215	-71	-77	-59	28	12
216	-76	-78	-65	28	11
217	-72	-76	-63	28	10
218	-72	-72	-59	28	9
219	-60	-78	-62	28	7
220	-61	-76	-61	28	6
221	-69	-75	-63	29	15
222	-68	-75	-62	29	14
223	-69	-75	-65	29	13
224	-68	-74	-65	29	12
225	-69	-73	-67	29	11
226	-72	-76	-60	29	10
227	-63	-74	-65	29	9
228	-66	-70	-60	29	7
229	-58	-71	-60	29	6
230	-70	-72	-68	29	5
231	-71	-75	-62	29	4
232	-71	-74	-62	29	3
233	-67	-75	-62	30	15
234	-69	-75	-66	30	14
235	-69	-74	-62	30	13
236	-65	-73	-63	30	12
237	-71	-73	-63	30	11
238	-71	-77	-66	30	10
239	-69	-76	-63	30	9
240	-64	-78	-59	30	7
241	-57	-70	-58	30	6
242	-72	-73	-62	30	5
243	-70	-80	-61	30	4
244	-62	-72	-64	30	3
245	-64	-72	-60	31	6
246	-59	-73	-63	32	7
247	-62	-66	-60	32	6
248	-69	-74	-64	32	5
249	-66	-74	-68	32	4
250	-61	-77	-66	33	7
251	-64	-75	-61	33	6
252	-71	-76	-67	33	5

No.	RSSI (dBm)			Position	
	AP1	AP2	AP3	X	Y
253	-63	-73	-69	33	4
254	-64	-72	-71	33	3
255	-68	-74	-72	33	2
256	-60	-74	-61	34	7
257	-58	-71	-62	34	6
258	-68	-73	-68	34	5
259	-62	-73	-63	34	4
260	-66	-74	-63	34	3
261	-66	-74	-67	34	2
262	-60	-67	-61	35	7
263	-61	-75	-62	35	6
264	-63	-66	-67	35	5
265	-66	-74	-71	35	4
266	-59	-76	-69	35	3
267	-63	-76	-65	35	2
268	-58	-68	-66	36	7
269	-65	-68	-72	36	5
270	-63	-76	-72	36	4
271	-62	-68	-63	36	3
272	-52	-69	-70	37	7
273	-55	-71	-71	37	4
274	-58	-69	-64	38	7
275	-53	-67	-62	39	7
276	-53	-67	-65	40	7
277	-51	-66	-70	41	7
278	-50	-65	-63	42	7
279	-50	-65	-71	43	7
280	-52	-65	-72	44	7
281	-53	-63	-72	45	7
282	-52	-65	-77	46	7
283	-66	-73	-77	47	13
284	-63	-69	-76	47	12
285	-61	-69	-77	47	11
286	-56	-69	-77	47	10
287	-55	-65	-68	47	9
288	-59	-65	-66	47	8
289	-62	-65	-65	47	7
290	-61	-66	-74	47	6
291	-64	-63	-67	47	5
292	-64	-63	-67	47	4
293	-61	-68	-74	47	3
294	-63	-68	-70	47	2
295	-62	-66	-75	47	1

No.	RSSI (dBm)			Position	
	AP1	AP2	AP3	X	Y
296	-57	-63	-74	48	7
297	-60	-62	-75	48	6
298	-61	-66	-72	48	5
299	-57	-68	-72	48	4
300	-62	-61	-76	48	3
301	-59	-67	-76	48	2
302	-61	-63	-75	48	1
303	-60	-64	-76	49	7
304	-59	-65	-68	49	6
305	-65	-63	-71	49	5
306	-63	-65	-75	49	4
307	-60	-62	-73	49	3
308	-64	-65	-71	49	2
309	-61	-67	-77	49	1
310	-61	-60	-67	50	7
311	-61	-64	-66	50	6
312	-62	-64	-72	50	5
313	-66	-67	-74	50	4
314	-58	-73	-67	50	3
315	-66	-67	-74	50	2
316	-66	-73	-77	50	1
317	-59	-59	-66	51	7
318	-63	-65	-68	51	6
319	-61	-64	-69	51	5
320	-66	-69	-65	51	4
321	-65	-66	-76	51	3
322	-67	-73	-76	51	2
323	-67	-70	-75	51	1
324	-66	-43	-67	52	7
325	-76	-62	-77	53	15
326	-78	-59	-81	53	14
327	-75	-65	-82	53	13
328	-76	-63	-81	53	12
329	-74	-58	-81	53	11
330	-73	-55	-77	53	10
331	-56	-57	-74	53	7
332	-63	-58	-73	53	6
333	-63	-62	-78	53	4
334	-64	-67	-81	53	2
335	-69	-67	-76	53	1
336	-75	-58	-79	54	15
337	-74	-58	-79	54	14
338	-73	-59	-73	54	13

No.	RSSI (dBm)			Position	
	AP1	AP2	AP3	X	Y
339	-73	-61	-73	54	12
340	-72	-59	-73	54	11
341	-72	-60	-72	54	10
342	-66	-53	-78	54	9
343	-68	-58	-78	54	7
344	-69	-58	-78	54	6
345	-68	-69	-79	54	4
346	-66	-69	-77	54	3
347	-66	-66	-77	54	2
348	-66	-64	-78	54	1
349	-76	-64	-75	55	15
350	-77	-60	-75	55	14
351	-71	-58	-75	55	13
352	-67	-61	-75	55	12
353	-74	-59	-75	55	11
354	-72	-58	-76	55	10
355	-68	-56	-77	55	9
356	-62	-57	-74	55	7
357	-68	-57	-76	55	6
358	-70	-68	-79	55	4
359	-61	-64	-75	55	3
360	-70	-65	-73	55	2
361	-61	-64	-79	55	1
362	-76	-58	-75	56	15
363	-75	-57	-76	56	14
364	-76	-59	-75	56	13
365	-76	-58	-75	56	12
366	-72	-63	-75	56	11
367	-70	-58	-75	56	10
368	-71	-63	-75	56	9
369	-62	-57	-77	56	7
370	-61	-57	-76	56	6
371	-63	-64	-78	56	4
372	-62	-69	-79	56	3
373	-63	-64	-76	56	2
374	-62	-61	-76	56	1
375	-72	-63	-76	57	15
376	-71	-59	-75	57	14
377	-75	-58	-75	57	13
378	-74	-62	-75	57	12
379	-72	-64	-76	57	11
380	-74	-59	-76	57	10
381	-72	-55	-76	57	9

No.	RSSI (dBm)			Position	
	AP1	AP2	AP3	X	Y
382	-62	-57	-72	57	7
383	-60	-58	-72	57	6
384	-66	-65	-75	57	4
385	-64	-69	-80	57	3
386	-64	-68	-75	57	2
387	-64	-62	-76	57	1
388	-73	-59	-77	58	15
389	-72	-57	-77	58	14
390	-74	-56	-76	58	13
391	-74	-60	-75	58	12
392	-73	-62	-76	58	11
393	-72	-53	-76	58	10
394	-75	-56	-76	58	9
395	-66	-58	-77	58	7
396	-61	-58	-75	58	6
397	-72	-64	-76	59	15
398	-75	-64	-76	59	14
399	-75	-54	-75	59	13
400	-73	-56	-74	59	12
401	-71	-54	-75	59	11
402	-67	-54	-75	59	10
403	-61	-52	-78	59	7
404	-69	-61	-85	59	6
405	-76	-62	-77	60	15
406	-76	-62	-78	60	14
407	-75	-57	-78	60	13
408	-75	-58	-79	60	12
409	-72	-61	-79	60	11
410	-68	-55	-79	60	10
411	-74	-59	-80	60	9
412	-63	-57	-76	60	7
413	-61	-57	-76	60	6
414	-75	-58	-78	61	15
415	-72	-57	-79	61	14
416	-73	-53	-79	61	13
417	-70	-54	-78	61	12
418	-72	-52	-78	61	11
419	-73	-54	-77	61	10
420	-68	-60	-77	61	9
421	-65	-56	-78	61	7
422	-66	-54	-76	61	6
423	-77	-52	-80	62	15
424	-76	-60	-79	62	14

No.	RSSI (dBm)			Position	
	AP1	AP2	AP3	X	Y
425	-69	-60	-78	62	13
426	-76	-56	-78	62	12
427	-72	-56	-78	62	11
428	-68	-56	-79	62	10
429	-73	-53	-79	62	9
430	-67	-53	-78	62	7
431	-64	-53	-78	62	6
432	-72	-53	-79	63	15
433	-75	-61	-80	63	14
434	-69	-50	-78	63	13
435	-73	-53	-78	63	12
436	-68	-57	-77	63	11
437	-68	-61	-79	63	10
438	-63	-52	-78	63	7
439	-64	-52	-76	63	6
440	-78	-55	-80	64	15
441	-76	-62	-79	64	14
442	-72	-52	-79	64	13
443	-74	-57	-78	64	12
444	-74	-56	-78	64	11
445	-64	-52	-78	64	7
446	-67	-53	-77	64	6
447	-72	-54	-79	64	4
448	-75	-56	-80	64	3
449	-72	-56	-79	64	2
450	-72	-56	-78	64	1
451	-77	-52	-80	65	15
452	-78	-49	-78	65	14
453	-75	-49	-81	65	13
454	-77	-48	-81	65	12
455	-78	-47	-80	65	11
456	-75	-49	-79	65	10
457	-73	-48	-83	65	9
458	-68	-52	-78	65	7
459	-64	-52	-77	65	6
460	-71	-54	-79	65	4
461	-75	-56	-80	65	3
462	-77	-53	-78	65	2
463	-70	-54	-77	65	1
464	-76	-55	-80	66	15
465	-76	-57	-81	66	14
466	-75	-48	-76	66	13
467	-78	-50	-78	66	12

No.	RSSI (dBm)			Position	
	AP1	AP2	AP3	X	Y
468	-78	-52	-78	66	11
469	-69	-53	-77	66	10
470	-74	-53	-78	66	9
471	-66	-51	-78	66	7
472	-67	-51	-74	66	6
473	-73	-55	-82	66	4
474	-76	-56	-82	66	3
475	-76	-59	-84	66	2
476	-72	-54	-83	66	1
477	-80	-63	-78	67	15
478	-75	-54	-81	67	14
479	-73	-51	-81	67	13
480	-74	-51	-81	67	12
481	-75	-47	-80	67	11
482	-72	-54	-79	67	10
483	-70	-48	-78	67	9
484	-68	-45	-79	67	7
485	-71	-48	-77	67	6
486	-74	-50	-84	67	4
487	-81	-55	-86	67	3
488	-78	-51	-85	67	2
489	-72	-53	-81	67	1
490	-65	-48	-75	68	7
491	-67	-44	-79	68	6
492	-63	-46	-79	69	7
493	-65	-52	-75	69	6
494	-71	-48	-83	69	4
495	-73	-52	-81	69	3
496	-80	-53	-84	69	2
497	-81	-59	-80	69	1
498	-80	-43	-82	70	12
499	-79	-42	-82	70	11
500	-78	-40	-85	70	10
501	-76	-48	-82	70	9
502	-75	-44	-80	70	8
503	-65	-43	-78	70	7
504	-65	-50	-80	70	6
505	-66	-49	-83	70	4
506	-73	-48	-84	70	3
507	-75	-52	-86	70	2
508	-74	-52	-85	71	7
509	-64	-48	-76	71	6
510	-67	-49	-79	71	5

No.	RSSI (dBm)			Position	
	AP1	AP2	AP3	X	Y
511	-73	-55	-86	71	4
512	-81	-55	-85	71	3
513	-76	-55	-85	71	2
514	-74	-56	-87	71	1
515	-76	-53	-83	72	11
516	-76	-54	-83	72	10
517	-75	-53	-82	72	9
518	-71	-50	-76	72	7
519	-68	-53	-75	72	6

No.	RSSI (dBm)			Position	
	AP1	AP2	AP3	X	Y
520	-75	-54	-75	72	5
521	-79	-56	-86	72	4
522	-76	-51	-83	73	11
523	-74	-50	-85	73	10
524	-78	-53	-84	73	9
525	-78	-58	-84	74	11
526	-76	-59	-84	74	10
527	-79	-56	-84	74	9

APPENDIX E
Automatic Radio Map-Ray Tracing (ARM-RT) Database of the Complex Building

No	RSSI (dBm)		
	AP1	AP2	AP3
1	-83.08	-81.43	-74.33
2	-81.69	-84.33	-73.59
3	-78.92	-81.5	-74.79
4	-78.27	-79.62	-76.47
5	-80.83	-81.68	-79.03
6	-77.74	-78.26	-65.71
7	-77.56	-79.93	-65.68
8	-78.39	-80.04	-65.71
9	-81.99	-81.84	-73.55
10	-82.26	-80.88	-81.6
11	-77.73	-81.46	-73.78
12	-78.47	-80.3	-75.3
13	-79.55	-80.5	-78.55
14	-78.07	-81.16	-65.22
15	-78.54	-79.52	-65.18
16	-77.8	-79.66	-65.22
17	-85.34	-75.19	-75.3
18	-82.12	-79.93	-80.44
19	-80.13	-81.75	-72.84
20	-78.46	-76.6	-74.77
21	-78.35	-79.57	-76.96
22	-80.73	-81.34	-64.67
23	-78.7	-79.01	-64.63
24	-76.84	-78.09	-64.67
25	-77.23	-77.23	-64.78
26	-82.18	-82.27	-71.76
27	-81.43	-80.83	-72.72
28	-78.93	-80.85	-71.96
29	-76.79	-76.64	-73.61
30	-78.33	-79.65	-76.42
31	-80.54	-80.81	-81.83
32	-78.23	-78.36	-64.06
33	-76.27	-78.47	-64.11
34	-76.41	-79.79	-64.24
35	-78.17	-81.65	-79.88
36	-78.42	-76.17	-72.49
37	-76.53	-77.03	-74.94
38	-81.08	-80.51	-81.2
39	-78.76	-78.8	-63.43
40	-77.7	-78.62	-63.48
41	-76.11	-79.22	-63.66
42	-79.31	-82.93	-70.12
43	-80.96	-81.65	-70.71
44	-79.97	-81.19	-78.54
45	-77.41	-75.98	-71.37
46	-74.85	-77.91	-74.32
47	-80.43	-81.12	-78.74
48	-77.02	-79.68	-62.78
49	-78.16	-78.01	-62.84
50	-75.97	-79.81	-63.04
51	-76.61	-78.03	-70.08
52	-74.94	-79.45	-72.68
53	-79.01	-78.77	-77.91
54	-75.66	-79.59	-61.95
55	-76.42	-79.01	-62.01
56	-74.34	-80.75	-62.19
57	-75.08	-78.26	-68.98
58	-74	-78.61	-71.23
59	-78.48	-78.99	-75.67
60	-75.8	-78.79	-61.17
61	-76.34	-79.5	-61.24
62	-73.51	-79.95	-61.45
63	-74.05	-80.42	-67.5
64	-73.97	-79.64	-69.82
65	-76.99	-79.66	-74.83
66	-75.08	-79.91	-60.31
67	-73.12	-80.03	-60.67
68	-82.6	-75.84	-67.45
69	-75.61	-80.17	-59.79
70	-74.94	-78.14	-67.89
71	-77.09	-78.26	-72.71
72	-75.74	-79.24	-59.37
73	-75.1	-79.19	-59.49
74	-72.79	-80.33	-59.83
75	-80.26	-76.45	-66.19
76	-73.62	-79.93	-59.21
77	-73.37	-78.75	-66.81
78	-76.57	-79.2	-70.95
79	-75.1	-78.67	-58.61
80	-74.73	-78.35	-58.77

81	-72.65	-79.91	-59.22
82	-73.98	-79.78	-59.89
83	-73.51	-78.56	-64.63
84	-75.78	-78.67	-68.96
85	-74.38	-78.57	-57.49
86	-73.92	-78.74	-57.68
87	-72.16	-80.04	-58.26
88	-73.45	-78.17	-59.16
89	-72.68	-78.4	-56.85
90	-73.12	-75.68	-66.58
91	-73.66	-78.64	-56.55
92	-72.71	-78.91	-56.8
93	-72.61	-79.76	-57.6
94	-73.24	-76.81	-58.41
95	-74.36	-79.18	-63.13
96	-73.5	-78.89	-62
97	-78.04	-79.9	-61.48
98	-73.64	-78.5	-56.95
99	-72.74	-78.44	-55.71
100	-73	-75.31	-64.49
101	-73.17	-78.54	-55.5
102	-72.49	-78.93	-55.91
103	-72.71	-78.64	-56.72
104	-72.48	-78.54	-58.38
105	-74.3	-76.77	-63.52
106	-73.24	-77.94	-61.86
107	-74.51	-77.87	-60.79
108	-72.82	-76.2	-56.78
109	-71.91	-76.58	-55.44
110	-72.54	-75.45	-62.34
111	-72.66	-78	-54.89
112	-72.67	-79.48	-55.2
113	-71.73	-79.7	-56.93
114	-71.81	-76.57	-58.87
115	-74.46	-76.01	-64.73
116	-73.28	-83.07	-63.03
117	-73.35	-77.81	-61.2
118	-72.1	-75.85	-57.52
119	-72.29	-78.49	-55.32
120	-71.83	-75.73	-53.67
121	-72.24	-78.29	-53.24
122	-72.07	-75.88	-53.67
123	-71.22	-79.79	-55.32
124	-71.23	-79.73	-57.52
125	-73.04	-75.03	-69.14

126	-73.47	-82.54	-66.72
127	-72.6	-76.45	-64.54
128	-72.13	-75.94	-60.22
129	-72.24	-78.3	-57.56
130	-71.92	-74.5	-55.28
131	-72.11	-78.05	-54.17
132	-70.21	-80.75	-54.14
133	-73.5	-74.2	-56.61
134	-71.93	-79.05	-55.53
135	-71.22	-75.22	-54.27
136	-72	-78.01	-53.14
137	-70.9	-75.63	-51.67
138	-71.21	-74.05	-50.41
139	-70.18	-78.03	-53.24
140	-69.91	-80.01	-54.01
141	-73.43	-73.79	-56.72
142	-71.82	-78.88	-55.68
143	-70.99	-75.04	-54.49
144	-71.44	-77.22	-53.08
145	-70.8	-74.91	-51.86
146	-71.2	-73.93	-50.9
147	-70.9	-74.88	-50.41
148	-70.12	-77.28	-53.67
149	-69.68	-78.01	-54.14
150	-75.97	-80.8	-56.78
151	-75.09	-80.02	-57.59
152	-71.82	-75.65	-57.03
153	-72.15	-76.67	-56.1
154	-71.65	-76.86	-54.7
155	-70.57	-76.91	-53.95
156	-70.88	-75.72	-52.78
157	-70.17	-74.2	-51.86
158	-70.86	-75.54	-51.67
159	-69.65	-77.94	-55.32
160	-68.99	-78.08	-55.44
161	-73.8	-77.12	-57.71
162	-74.49	-78.55	-58.48
163	-72.17	-78.53	-57.5
164	-71.57	-74.04	-56.39
165	-71.39	-79	-55.53
166	-70.72	-77.56	-54.69
167	-70.57	-76.45	-53.95
168	-69.65	-74.46	-53.08
169	-70.89	-76	-53.14
170	-69.58	-77.81	-57.52

171	-68.96	-79.48	-56.78
172	-74.05	-78.98	-59.53
173	-73.71	-79.51	-59.4
174	-71.57	-79.02	-58.08
175	-71.92	-73.83	-57.13
176	-70.63	-77.8	-56.48
177	-70.49	-74.41	-55.53
178	-70.23	-77.05	-54.7
179	-69.56	-75.14	-54.49
180	-70.25	-77.27	-54.27
181	-68.95	-76.01	-59.31
182	-68.52	-73.67	-58.33
183	-73.85	-78.55	-61.61
184	-73.85	-80.79	-61.13
185	-68.25	-74.72	-61.5
186	-67.78	-73.07	-59.96
187	-70.62	-73.87	-60.87
188	-70.21	-73.02	-59.88
189	-69.97	-74.49	-59.14
190	-69.1	-73.3	-58.33
191	-69.43	-75.3	-57.64
192	-69.77	-75.5	-57.2
193	-68.97	-74.42	-57.05
194	-67.99	-74.76	-63.4
195	-67.33	-72.26	-61.88
196	-70.14	-73.34	-61.25
197	-69.76	-75.7	-60.37
198	-69.53	-74.61	-59.59
199	-69.14	-72.9	-59.21
200	-69.09	-74.69	-58.69
201	-69.63	-74.33	-58.35
202	-67.23	-79.71	-65.74
203	-66.85	-76.53	-63.65
204	-69.6	-71.32	-61.68
205	-69.5	-77.85	-60.99
206	-69.19	-72.36	-60.33
207	-68.92	-72.75	-59.79
208	-68.78	-74.59	-59.37
209	-69.04	-75.59	-59.11
210	-66.52	-79.56	-66.96
211	-66.25	-77.96	-64.9
212	-68.47	-70.98	-63.19
213	-68.01	-73.98	-62.41
214	-68.04	-71.42	-61.68
215	-67.84	-72.72	-61.13

216	-67.59	-73.15	-60.67
217	-68.35	-74.57	-60.39
218	-68.19	-74.69	-60.31
219	-66.17	-76.83	-68.98
220	-65.86	-75.96	-66.44
221	-68.3	-70.26	-63.55
222	-68.07	-73.7	-62.88
223	-68.08	-71.45	-62.31
224	-67.31	-72.5	-61.84
225	-67.08	-72.73	-61.45
226	-67.35	-74.41	-61.24
227	-67.93	-74.16	-61.17
228	-65.77	-76.47	-70.84
229	-65.5	-73.73	-68.02
230	-72.02	-76.1	-74.63
231	-71.99	-74.55	-72.38
232	-67.65	-74.49	-70.86
233	-67.89	-71.21	-63.8
234	-67.5	-70.98	-63.21
235	-67.48	-71.44	-62.71
236	-67.21	-71.46	-62.5
237	-67.01	-71.75	-62.19
238	-67.14	-74.73	-62.01
239	-67	-73.58	-61.95
240	-65.06	-78.81	-72.31
241	-64.85	-72.79	-69.2
242	-72.11	-75.14	-75.2
243	-71.16	-78.96	-73.76
244	-67.32	-73.71	-72.35
245	-64.29	-71.54	-70.17
246	-65.33	-77.27	-74.26
247	-63.85	-70.59	-71.33
248	-70.49	-76	-79.16
249	-65.84	-77.43	-77.1
250	-64.66	-74.06	-75.76
251	-63.04	-74.66	-72.51
252	-70.37	-73.9	-80.57
253	-65.46	-74.44	-78.43
254	-65.64	-71.17	-76.8
255	-65.8	-71.65	-75.7
256	-63.94	-72.79	-76.33
257	-62.44	-74.33	-74.06
258	-69.05	-74.78	-81.6
259	-64.82	-73.74	-79.67
260	-65.18	-70.79	-77.81

261	-65.45	-72	-76.59
262	-63.3	-69.06	-77.91
263	-63.23	-75.2	-74.59
264	-63.87	-72.76	-83.12
265	-64.24	-71.55	-80.92
266	-64.49	-70.84	-78.94
267	-65.11	-71.91	-77.97
268	-62.58	-69.15	-78.72
269	-62.98	-72.27	-84.7
270	-63.1	-71.15	-82.23
271	-63.09	-69.76	-80.06
272	-61.5	-71.37	-80.42
273	-62.48	-71.19	-83.61
274	-60.62	-71.12	-80.86
275	-59.45	-71.85	-81.3
276	-58.04	-72.42	-83.17
277	-56.77	-71.49	-83.56
278	-55.66	-70.79	-83.94
279	-55.07	-68.94	-85.07
280	-55.63	-68.31	-85.39
281	-56.73	-67.97	-87.55
282	-58.01	-66.89	-87.87
283	-65.6	-65.23	-73.27
284	-64.71	-64.55	-73.1
285	-63.42	-64.26	-73.02
286	-62.14	-64.63	-72.92
287	-61.31	-65.06	-72.91
288	-61.14	-64.51	-72.92
289	-59.42	-66.33	-88.19
290	-59.62	-67.99	-84.1
291	-60.39	-67.83	-81.6
292	-61.21	-68	-79.98
293	-61.68	-70.6	-90.41
294	-62.41	-68.92	-88.22
295	-62.83	-69.31	-86.8
296	-60.51	-66.35	-88.47
297	-60.92	-67.2	-84.4
298	-61.15	-67.55	-81.9
299	-61.75	-68.34	-80.26
300	-62.37	-69.57	-90.68
301	-62.71	-68.72	-88.49
302	-63.2	-68.91	-87.6
303	-61.46	-65.55	-88.76
304	-61.72	-65.59	-84.69
305	-62.11	-67.64	-82.18

306	-62.55	-70.54	-81.34
307	-62.76	-69.97	-92.62
308	-63.27	-69.27	-89.86
309	-63.64	-67.57	-87.86
310	-62.57	-65.1	-89.04
311	-62.72	-65.47	-84.97
312	-62.97	-66.99	-83.5
313	-63.04	-69.26	-81.62
314	-63.41	-69.25	-80.18
315	-63.75	-69.91	-90.12
316	-64.09	-68.02	-89.12
317	-63.21	-65.77	-89.32
318	-63.33	-65.03	-86.69
319	-63.52	-67.09	-83.77
320	-63.66	-68.87	-81.87
321	-63.96	-68.93	-80.44
322	-64.25	-68.92	-91.57
323	-64.52	-68.83	-89.36
324	-63.87	-65.77	-91.96
325	-69.73	-61.79	-76.88
326	-69.02	-61.4	-76.73
327	-69.81	-61.45	-76.51
328	-68.54	-60.74	-76.41
329	-68.05	-60.81	-76.33
330	-67.95	-60.61	-76.27
331	-64.58	-64.39	-92.22
332	-64.71	-63.88	-87.21
333	-65.56	-67.98	-83.6
334	-66.03	-68.06	-92.4
335	-66.24	-66.33	-91.32
336	-70.03	-61.36	-77.12
337	-69.38	-61.34	-76.97
338	-68.76	-60.8	-76.76
339	-69.25	-60.58	-76.66
340	-68.84	-60.46	-76.58
341	-68.4	-60.33	-76.52
342	-67.99	-60.02	-76.47
343	-65.28	-64.02	-92.47
344	-65.45	-63.32	-87.46
345	-66.04	-67.05	-83.84
346	-66.12	-67.45	-82.21
347	-66.38	-68.6	-94.3
348	-66.61	-66.1	-91.53
349	-69.95	-60.79	-77.36
350	-70.53	-60.83	-77.12

351	-69.24	-60.45	-77
352	-68.93	-60.39	-76.9
353	-69.48	-60.23	-76.77
354	-68.61	-60	-76.72
355	-68.81	-59.69	-76.72
356	-65.76	-63.71	-92.7
357	-65.89	-63.61	-88.55
358	-66.35	-67.47	-84.06
359	-66.54	-67.61	-83.24
360	-66.83	-66.87	-81.8
361	-66.9	-66.04	-91.76
362	-70.01	-60.8	-77.59
363	-69.46	-60.42	-77.35
364	-69.38	-60.14	-77.23
365	-69.4	-59.9	-77.07
366	-69.46	-60.21	-77.01
367	-69.01	-59.73	-76.96
368	-68.65	-59.38	-76.95
369	-66.17	-63.55	-92.93
370	-65.09	-62.66	-88.77
371	-70.74	-67.01	-84.3
372	-66.94	-68.18	-83.47
373	-66.99	-65.98	-82.03
374	-67.12	-66.34	-93.18
375	-70.53	-60.16	-77.71
376	-69.98	-60.15	-77.58
377	-70.23	-59.71	-77.46
378	-69.73	-59.51	-77.3
379	-69.3	-59.4	-77.24
380	-69.03	-59.24	-77.19
381	-69.96	-58.73	-77.19
382	-66.8	-62.63	-93.16
383	-65.47	-62.66	-89
384	-71.06	-66.9	-85.56
385	-67.4	-66.33	-83.67
386	-67.48	-65.93	-82.96
387	-67.65	-65.89	-93.37
388	-70.42	-59.82	-77.93
389	-69.99	-59.68	-77.8
390	-69.65	-59.51	-77.61
391	-70.23	-59.05	-77.53
392	-69.82	-58.83	-77.46
393	-70.37	-58.42	-77.41
394	-69.6	-58.71	-77.41
395	-67.03	-62.4	-93.39

396	-66.09	-62.12	-91.04
397	-70.83	-59.42	-78.14
398	-71.02	-59.34	-78.01
399	-70.57	-59.22	-77.83
400	-70.56	-58.67	-77.75
401	-70.5	-58.19	-77.68
402	-69.76	-58.55	-77.63
403	-66.51	-62.21	-93.61
404	-66.61	-61.23	-91.26
405	-71.44	-59.21	-78.35
406	-71.15	-59.04	-78.14
407	-70.69	-58.46	-78.04
408	-70.39	-58.3	-77.96
409	-70.62	-58.13	-77.89
410	-70.47	-57.51	-77.85
411	-69.85	-57.43	-77.84
412	-66.97	-61.38	-93.82
413	-66.91	-60.91	-91.47
414	-72.82	-58.1	-78.86
415	-72.22	-57.78	-78.63
416	-71.71	-57.46	-78.53
417	-71.2	-57.13	-78.44
418	-71.7	-56.89	-78.38
419	-71.53	-56.63	-78.33
420	-71.66	-56.46	-78.32
421	-67.36	-61.19	-94.86
422	-67.43	-60.2	-91.68
423	-72.37	-57.51	-78.95
424	-72.82	-57.19	-78.83
425	-72.03	-56.93	-78.73
426	-71.52	-56.49	-78.65
427	-71.66	-56.28	-78.58
428	-72.16	-56.05	-78.53
429	-71.9	-55.75	-78.53
430	-67.72	-60.18	-95.07
431	-67.83	-59.79	-91.88
432	-72.11	-57.02	-79.15
433	-72.81	-56.88	-79.03
434	-71.63	-56.51	-78.93
435	-71.78	-56	-78.85
436	-71.59	-55.72	-78.78
437	-71.87	-55.42	-78.73
438	-68.04	-59.42	-95.27
439	-68.13	-58.85	-92.08
440	-72.64	-56.85	-79.34

441	-72.18	-56.36	-79.22
442	-72.31	-55.82	-79.12
443	-72.08	-55.28	-79.04
444	-72.14	-54.8	-78.97
445	-68.48	-58.65	-95.46
446	-68.66	-58.08	-92.27
447	-73.39	-60.48	-106.06
448	-73.54	-60.11	-86.59
449	-74.1	-60.1	-85.75
450	-71.39	-60.19	-85.03
451	-72.59	-56.54	-79.53
452	-72.75	-55.86	-79.41
453	-72.42	-55.12	-79.24
454	-72.3	-54.64	-79.17
455	-72.95	-54.11	-79.12
456	-72.34	-53.86	-79.11
457	-71.15	-53.65	-79.08
458	-69.4	-57.57	-99.04
459	-68.64	-57.26	-92.45
460	-73.66	-59.47	-106.25
461	-73.71	-59.46	-87.81
462	-74.63	-59.3	-85.94
463	-73.95	-59.41	-85.21
464	-74.07	-56.33	-79.71
465	-72.16	-55.76	-79.52
466	-71.73	-54.67	-79.43
467	-73.59	-53.67	-79.36
468	-73.06	-53.27	-79.31
469	-73.82	-52.88	-79.3
470	-71.5	-52.8	-79.27
471	-69.51	-56.5	-99.22
472	-69.03	-55.57	-92.63
473	-74.4	-58.43	-106.4
474	-73.59	-58.53	-88
475	-73.95	-58.44	-87.02
476	-74.67	-59.38	-85.39
477	-74.23	-56.25	-79.8
478	-72.65	-55.33	-79.7
479	-72.14	-54.4	-79.61
480	-73.45	-53.38	-79.54
481	-73.32	-52.29	-79.49
482	-73.93	-52.09	-79.48
483	-71.69	-52	-79.45
484	-69.55	-54.42	-99.4
485	-69.29	-54.43	-92.81
486	-74.76	-57.28	-106.59
487	-74.07	-57.65	-88.14
488	-74.48	-61.72	-87.2
489	-75.35	-61.83	-86.36
490	-69.63	-53.13	-99.58
491	-69.86	-53.2	-92.99
492	-70.05	-51.26	-100.59
493	-70.02	-52.22	-95.55
494	-74.79	-55.43	-106.94
495	-75.16	-56.75	-104.5
496	-75.42	-56.14	-87.81
497	-77.63	-58.47	-86.98
498	-74.48	-48.27	-80.34
499	-73.31	-47.19	-80.28
500	-74.05	-46.52	-80.24
501	-73.1	-47.1	-80.24
502	-71.7	-48.28	-80.24
503	-70.06	-50.06	-100.76
504	-70.44	-50.74	-95.72
505	-75	-57.07	-107.11
506	-76.99	-57.96	-104.96
507	-75.74	-58.59	-87.98
508	-76.34	-59.2	-87.14
509	-70.69	-55.97	-100.93
510	-70.62	-58.29	-95.89
511	-75.86	-57.12	-110.25
512	-76.13	-56.32	-105.12
513	-75.28	-56.54	-88.14
514	-76.64	-57.4	-87.31
515	-74.87	-51.99	-80.89
516	-74.81	-51.61	-80.84
517	-73.85	-52.09	-80.84
518	-71.2	-55.29	-101.09
519	-71.11	-57.46	-96.05
520	-72.25	-58.7	-93.7
521	-77.77	-60.78	-111.26
522	-77.28	-53.55	-81.32
523	-74.36	-53.29	-81.27
524	-74.52	-53.21	-81.27
525	-76.47	-54.03	-81.48
526	-74.75	-53.42	-81.43
527	-75.52	-53.62	-81.43

APPENDIX F
People Presence Effect on IPS Accuracy

IPS Accuracy affected by people (NLOS) using the MRM Database						
The affected Access Point						
AP1	AP2	AP3	AP1, AP2	AP1, AP3	AP2, AP3	AP1, AP2, AP3
0.333333	0.333333	0.333333	0.333333	0.333333	0.333333	0.333333
0.666667	0.666667	0.666667	0.666667	0.745356	0.666667	0.666667
0.745356	0.745356	0.745356	0.745356	0.745356	0.745356	0.745356
0.745356	0.745356	0.745356	0.745356	0.745356	0.745356	0.745356
0.666667	0.666667	0.666667	0.666667	0.666667	0.666667	0.666667
0.745356	1.054093	2.357023	1.054093	2.108185	2.108185	2.108185
0.333333	0.333333	1.374369	0.333333	1.374369	0.333333	1.374369
1.20185	0.666667	0.666667	1.20185	1.20185	0.666667	0.333333
2.134375	0.471405	2.134375	2.134375	2.134375	2.134375	2.134375
0.333333	0.333333	0.333333	1.795055	0.333333	0.333333	1.795055
2.236068	0.333333	2.333333	2.357023	3.073181	0.333333	2.357023
0.333333	0.745356	0.745356	0.745356	0.333333	0.745356	0.333333
0.471405	0.333333	0.333333	0.333333	0.333333	0.333333	0.333333
2.333333	0.666667	2.333333	2.333333	2.333333	0.666667	2.333333
0.333333	0.333333	0.333333	0.333333	0.333333	0.333333	0.333333
0.745356	0.745356	0.745356	0.745356	0.745356	0.745356	0.745356
0.333333	0.745356	0.745356	1.374369	0.333333	0.745356	1.374369
2.687419	0.333333	0.333333	2.687419	0.333333	0.333333	0.333333
0.333333	0.333333	0.333333	0.333333	0.333333	0.333333	0.333333
0.745356	0.745356	0.745356	0.745356	0.942809	0.745356	0.942809
0.471405	0.471405	0.471405	0.471405	0.471405	0.471405	0.471405
2.108185	0.333333	2.108185	2.108185	2.108185	2.108185	2.108185
0.333333	0.333333	0.333333	0.333333	0.333333	0.333333	0.333333
0.666667	1.333333	0	0.666667	0	1.333333	0.666667
0.333333	4	0.333333	4	0.333333	5.666667	5.666667
0.471405	0.745356	0.471405	0.745356	0.471405	0.745356	0.745356
0.333333	0.333333	0.333333	0.333333	0.333333	0.333333	0.333333
0.745356	0.745356	0.745356	0.745356	0.745356	0.745356	0.745356
0.942809	0.471405	0.942809	0.942809	0.942809	0.471405	0.942809
0.745356	0.745356	0.745356	0.745356	0.745356	0.745356	0.745356
0.333333	1.20185	0.333333	1.20185	2.333333	1.20185	2.333333
0.333333	0.333333	0.333333	0.333333	0.333333	0.333333	1
0.471405	0.471405	0.471405	0.471405	0.471405	0.471405	0.471405
0.745356	0.745356	0.745356	0.745356	0.745356	0.745356	0.745356
0.666667	0.333333	0.666667	0.333333	0.666667	0.333333	0.333333
1.054093	1.054093	0.333333	1.054093	1.054093	1.054093	1.054093
0.745356	0.745356	0.745356	1.490712	1.490712	1.490712	1.490712
0.745356	1	1.20185	1.054093	0.745356	1	1.054093
0.745356	0.666667	0.745356	1.054093	1.20185	1.054093	1.054093

IPS Accuracy affected by people (NLOS) using the MRM Database						
The affected Access Point						
AP1	AP2	AP3	AP1, AP2	AP1, AP3	AP2, AP3	AP1, AP2, AP3
1.699673	0	0	1.699673	0	0	0
1.490712	1.666667	2.666667	1.666667	1.490712	3.59011	3.59011
0	3.073181	0	3.073181	0	3.073181	3.073181
0.333333	0.333333	0.333333	0.333333	0.333333	0.333333	0.333333
0.471405	0.471405	0.471405	0.471405	0.471405	0.471405	0.471405
0.471405	0.471405	0.471405	0.471405	0.471405	0.471405	0.471405
0.745356	0.745356	0.745356	0.745356	0.745356	0.745356	0.745356
0.745356	0.745356	0.745356	0.745356	0.745356	0.745356	0.745356
0	0	0	0	0	0	0
0.745356	0.745356	0.745356	0.333333	0.745356	0.745356	0.745356
0	2.828427	2.357023	2.828427	2.357023	2.357023	2.357023
Mean						
0.763039	**0.769501**	**0.792019**	**1.05725**	**0.847388**	**0.944369**	**1.102993**

IPS Accuracy affected by people (NLOS) using the ARM-RT database						
The affected Access Point						
AP1	AP2	AP3	AP1, AP2	AP1, AP3	AP2, AP3	AP1, AP2, AP3
1.20185	1.20185	1.20185	1.20185	1.20185	1.20185	1.20185
0.942809	0.942809	0.942809	0.942809	0.942809	0.471405	0.471405
0.471405	0.471405	0.471405	0.471405	0.471405	0.471405	0.471405
0.942809	0.942809	1.20185	0.942809	1.20185	1.943651	1.943651
0.745356	1.054093	1.333333	1.666667	1.666667	1.054093	1.490712
1.374369	1.374369	1.374369	1.374369	0.666667	0.666667	0.666667
1.20185	0.333333	1.20185	1.20185	1.20185	1.20185	2.134375
0.333333	0.333333	1.20185	0.333333	1.20185	1.20185	0.333333
1.374369	2	1.374369	2	1.374369	2	2
0.745356	0.745356	0.745356	0.745356	0.745356	0.745356	0.745356
1.374369	1.374369	1.374369	1.374369	2.236068	1.374369	1.666667
1	0.333333	1.795055	1	1.374369	1.795055	1.054093
0.333333	0.666667	0.333333	0.333333	1.20185	0.333333	0.333333
1	1	1	1	1	1	1
4.068852	0.333333	0.942809	4.242641	4.268749	4.268749	5
1.20185	0.666667	0.666667	0.666667	0.666667	0.666667	0.666667
2.687419	2.687419	1.374369	2.687419	1.374369	1.374369	1.374369
1.20185	1.374369	1.374369	1.943651	1.374369	2.357023	2.981424
1	1	1	1	1	1	1
2.134375	1	1	2.134375	1	1	1
0.745356	0.745356	0.745356	0.745356	0.745356	0.745356	0.745356
1.414214	1.414214	1.414214	1.414214	1.414214	1.414214	1.414214
1.054093	3.72678	3.72678	1.054093	1.054093	3.72678	1.054093
1	1	1	1	1	1	1

IPS Accuracy affected by people (NLOS) using the ARM-RT database						
The affected Access Point						
AP1	AP2	AP3	AP1, AP2	AP1, AP3	AP2, AP3	AP1, AP2, AP3
1.374369	2	1.374369	1.374369	1.374369	2	1.374369
0.333333	0.333333	1	1	0.333333	1	1
0	0	0	0	0	0	0
0	0	0	0	0	0	0
1	1	0	1	0	1	0
0.666667	0.666667	0.666667	0.666667	0.666667	0.666667	0.666667
1	1	1	1	1	1	1
2	2	1.20185	2	2.027588	0.942809	2.687419
1	1	1	1	1	2	1
2.426703	2.426703	1.20185	2.108185	2.108185	1.20185	2.108185
0	0	0	0	0	1	0
1.20185	1.20185	0.471405	1.20185	0.471405	0.471405	0.471405
0.666667	0.666667	1.490712	0.666667	0.666667	1.490712	0.666667
3.666667	3.666667	2.333333	1	4	1	3
1	1	1	1	1	1	1
1.885618	1.885618	0.745356	3.282953	2.134375	3.14466	4.346135
0.745356	0.745356	0.745356	0.745356	0.745356	0.745356	0.745356
1	1	1	1	1	1	1
1	1	1	1	1	1	1
0	0	0	0	0	0	0
1	1	1	1	1	1	1
1	1	1.666667	1	1.666667	1.666667	1.666667
1.374369	1.374369	1.374369	1.374369	1.374369	1.374369	1.374369
1.20185	1.20185	1.20185	1.20185	1.20185	1.20185	3.399346
0.745356	0.745356	0.745356	0.745356	0.745356	0.745356	0.745356
1	1	2.134375	1.943651	2.134375	2.134375	2.134375
Mean						
1.13676	**1.092726**	**1.062998**	**1.175757**	**1.160707**	**1.236002**	**1.282706**

IPS Accuracy affected by people (NLOS) using the ARM-MW database						
The affected Access Point						
AP1	AP2	AP3	AP1, AP2	AP1, AP3	AP2, AP3	AP1, AP2, AP3
0.745356	0.745356	0.745356	0.745356	0.471405	0.471405	0.471405
1.490712	1.490712	1.490712	1.490712	1.490712	1.490712	1.490712
0.666667	0.666667	0.666667	0.666667	0.666667	0.666667	0.666667
2.134375	1.885618	2.848001	2.134375	2.848001	2.848001	3.073181
1	0.333333	1	0.333333	1	1	1
2	1.333333	2	2	2.981424	2.981424	2.981424
1.490712	1.054093	1.885618	2.236068	1.054093	1.885618	2.687419
1.054093	1.054093	2.236068	1.054093	2.236068	2.236068	2.236068
1.414214	1.414214	1.414214	1.414214	1.414214	1.414214	1.490712

IPS Accuracy affected by people (NLOS) using the ARM-MW database						
The affected Access Point						
AP1	AP2	AP3	AP1, AP2	AP1, AP3	AP2, AP3	AP1, AP2, AP3
1.699673	1.699673	1.490712	1.699673	1.374369	1.374369	1.699673
0.745356	0.745356	1.374369	0.745356	0.942809	0.942809	0.942809
0	1	2	0	1	1	1
0.745356	0.745356	0.745356	0.745356	0.745356	0.745356	0.745356
1.699673	1.699673	1.490712	1.699673	1.490712	1.490712	1.490712
1.490712	1.490712	1.490712	1.490712	1.490712	1.490712	1.490712
1.666667	2.426703	1.885618	2.687419	1.414214	1.885618	1.414214
1.490712	1.490712	1.666667	2.236068	1.666667	1.666667	1.666667
2.687419	2.687419	1.795055	2.687419	3	1.795055	3.018462
1.490712	1.490712	0.942809	1.490712	1.490712	0.942809	1.490712
1	1	1	1	1	1	1
0.666667	0.666667	0.471405	0.666667	0	0.471405	0
1	1	0.745356	1.943651	0.942809	0.942809	1.414214
1.20185	1.20185	1	1.20185	1	1.20185	1.374369
2.748737	2.108185	2	7.063207	2.108185	2.108185	7.063207
1.414214	1.414214	0.745356	2.236068	1.414214	0.745356	1.414214
1	1	1	1	1.414214	1	1.414214
0.942809	0.942809	0.942809	0.942809	0.942809	0.942809	0.942809
1.414214	1.414214	1.414214	1.414214	1.414214	1.414214	1.414214
2	1	2	2	3	2	3
1	1	1	1	1	1	1
1	1	1	1	1	1	1
1.490712	2.236068	0.745356	2.867442	1.490712	2.134375	2.828427
1.374369	2.134375	0.745356	2.236068	1.374369	1.490712	2.236068
1.490712	2.134375	0.942809	2.134375	1.490712	2.134375	2.134375
1	2	1	1	1	1	1
1.414214	1.414214	1.414214	1.414214	1	1.414214	1.414214
1.795055	1.795055	1.795055	1.795055	2.357023	1.795055	1.795055
2.981424	1.943651	1.414214	3.162278	3.72678	1.943651	3.162278
1	0.942809	0.942809	0.942809	1	0.942809	1
1.374369	1.374369	1.374369	1.374369	1.374369	1.374369	1.374369
0.745356	1.795055	1.414214	1.414214	0.745356	1.414214	1.414214
2	1.414214	1.414214	1.414214	4.772607	1.414214	2.848001
0.942809	1.699673	0.942809	1.699673	0.942809	1.699673	1.699673
1.795055	2.333333	1.795055	2	1.795055	2	2
1	1	1	1	1	1	1
1	1	1	1	1	1	1
1	1	1	1.054093	1	1.374369	1.795055
0.942809	1.054093	0.942809	1	1	1	1.490712
1	1	1	1	1	1	1.374369
1	1	1	1	1	1	1
Mean						

IPS Accuracy affected by people (NLOS) using the ARM-MW database						
The affected Access Point						
AP1	AP2	AP3	AP1, AP2	AP1, AP3	AP2, AP3	AP1, AP2, AP3
1.328956	**1.369459**	**1.287421**	**1.570689**	**1.461687**	**1.385737**	**1.693219**

IPS Accuracy affected by people (LOS) using the MRM database						
The affected Access Point						
AP1	AP2	AP3	AP1, AP2	AP1, AP3	AP2, AP3	AP1, AP2, AP3
3	0.333333	1.666667	3	2.134375	1.666667	2.134375
2.538591	0.666667	0.745356	2.538591	1.943651	0.666667	1.943651
1.699673	0.745356	3	1.699673	3.681787	3	3.681787
2.867442	1.333333	2.357023	2.687419	2.687419	3	2.687419
1.374369	2.108185	1.666667	2.687419	2.027588	1.374369	4.176655
3.771236	2.403701	4.533824	3.771236	5.734884	4.807402	5.547772
1.054093	1.666667	2.403701	2.538591	2.426703	4.176655	5.077182
1.666667	2.538591	3.681787	2.108185	6.146363	3.800585	7.45356
3.59011	5.906682	8.43274	4.642796	2.748737	6.119187	5.676462
1.054093	0.745356	3.480102	2.603417	4.176655	3.605551	0.333333
1.333333	4.678556	4.242641	1.885618	5.754226	2.981424	4.21637
2.848001	1.666667	1.795055	1.490712	1.666667	2.687419	0.471405
1.333333	2.333333	4.714045	3.349959	2.108185	1.20185	2.333333
4.242641	1.20185	6.798693	4.123106	11.02018	3.14466	10.34945
5.374838	2.426703	3.399346	11.00505	7.310571	2.687419	6.565905
4.630815	1.054093	6	12.45436	8.975275	2.748737	8.666667
1.414214	5.962848	1.054093	11.74261	8.956686	8.800253	16.99673
12.07385	13.0384	10.58825	9.333333	5.426274	8.013877	17.97838
1.374369	2.027588	8.013877	2.687419	2.027588	3.59011	8.806563
12.98289	9.024658	2.538591	15.0037	10.12148	0.333333	15.69855
3.800585	1.795055	6.262765	6.009252	12.22475	7.007932	6.798693
0.471405	3.282953	0.666667	2.134375	8.569973	2.687419	3.72678
2.426703	2.666667	1.333333	3.073181	4.123106	1.054093	4.955356
4.333333	5.754226	1	3.333333	4.642796	0.666667	3.399346
1.795055	8.975275	4.176655	4.268749	8.006941	6.871843	3.299832
2.981424	10.46688	3.666667	13.37078	5.830952	4.176655	2.426703
4.714045	7.67391	1.333333	11.72367	2.357023	3.282953	7.490735
5.547772	2.357023	2.357023	3.72678	5.754226	1.943651	4.013865
2.603417	6.036923	3.605551	7.378648	2.426703	2.357023	3.399346
3.431877	2.357023	3.72678	8.333333	2.236068	3.14466	3.431877
2.403701	4.472136	4.678556	3.14466	4.533824	4.533824	6.871843
3.431877	4.027682	3.605551	4.013865	6.200358	4.533824	5.18545
3	4.853407	0.666667	0.942809	3	4.176655	3
4.013865	2.603417	2.603417	5.34374	9.803627	5.497474	3.14466
9.545214	0.942809	4.333333	3.480102	8.944272	1.943651	9.261629
5.426274	1.699673	2.748737	3.431877	7.615773	0.666667	7.90218

IPS Accuracy affected by people (LOS) using the MRM database						
The affected Access Point						
AP1	AP2	AP3	AP1, AP2	AP1, AP3	AP2, AP3	AP1, AP2, AP3
3.681787	6.411795	4.630815	3.681787	3.800585	4.472136	2.236068
1.490712	0.666667	1.374369	2.603417	5.830952	3.018462	7.031674
2.981424	1.333333	3.282953	4.268749	4.921608	4.068852	1.490712
2.108185	8.117197	0.745356	1.699673	1.054093	4.484541	1.666667
4.013865	5.088113	6.708204	2.236068	11.14052	4.630815	4.714045
4	6.411795	10.46688	5.374838	10.46688	6.741249	5.374838
0.745356	4	4.853407	6.082763	6.839428	3.480102	3.14466
0.471405	3.299832	4.346135	3.018462	10.12148	7.490735	9.803627
1.666667	1.490712	2.603417	5.270463	1.943651	3.543382	3.282953
0.745356	3.800585	2.236068	5.385165	3.299832	8.006941	6.009252
2.666667	2.687419	0.471405	3.887301	0.666667	2.134375	0.666667
0	3.349959	0	1.699673	0	4	5.821416
2.981424	4.666667	3.681787	2.538591	5.547772	4.666667	3.800585
5.374838	2.426703	8.439326	6.798693	6.960204	5.906682	6.960204
Mean						
3.261576	**3.711568**	**3.634352**	**4.79216**	**5.318787**	**3.791922**	**5.422144**

IPS Accuracy affected by people (LOS) using the ARM-RT database						
The affected Access Point						
AP1	AP2	AP3	AP1, AP2	AP1, AP3	AP2, AP3	AP1, AP2, AP3
3.073181	0.471405	1.20185	0.471405	1.20185	0.942809	0.745356
0.942809	0.745356	0.745356	0.745356	0.471405	0.745356	0.471405
0.471405	0.745356	0.745356	0.745356	0.942809	0.745356	0.942809
2.357023	2.108185	2.426703	2.108185	3.073181	2.748737	2.108185
3.073181	2.108185	1.666667	3.333333	3.073181	1.885618	3.299832
0.666667	0.666667	3.800585	2.687419	2.134375	4.176655	4.176655
2.687419	2.687419	3.543382	4.013865	3.800585	3.771236	4.533824
3.333333	2.687419	2.236068	0.942809	3.333333	2.828427	4.642796
2.108185	2.603417	5.897269	4.714045	4.472136	6.599663	6.146363
2.687419	1.20185	3.431877	3.431877	4.955356	4.268749	5.467073
3.018462	4.772607	4.176655	3.72678	0.333333	6.960204	6.146363
3.666667	3.771236	7.063207	5.934831	6.472163	7.007932	8.359957
2.687419	1	6.146363	3.666667	5.426274	4.484541	6.128259
3.800585	5	7.031674	0.666667	7.007932	2.848001	4.955356
6.472163	4.013865	5.754226	3.162278	9.15302	3.480102	4.268749
2.236068	1.20185	0.745356	1.699673	5.333333	3.333333	3.72678
7.490735	2.426703	4.714045	5.270463	7.45356	3.073181	8.724168
3	1.943651	3.162278	5.426274	2.108185	1.699673	1.699673
3.681787	2.333333	9.055385	2.333333	2.687419	7.695598	4
8.232726	3.349959	2.108185	7.086764	1.666667	1.490712	2.603417
9.171211	1	7.45356	6.324555	2.426703	1.795055	3.333333

IPS Accuracy affected by people (LOS) using the ARM-RT database						
The affected Access Point						
AP1	AP2	AP3	AP1, AP2	AP1, AP3	AP2, AP3	AP1, AP2, AP3
2.666667	0.745356	2.848001	3.333333	2.666667	1.943651	3.14466
3	0	6.082763	4.013865	2.357023	6.082763	0
6.674995	5.426274	1	7.401201	3.543382	2.748737	3.666667
2.236068	2.027588	15.83947	3.073181	2.236068	2.108185	2.236068
3.681787	0.471405	3	4.123106	3.771236	2	3.800585
1.699673	0.666667	0	2	2.027588	0	0
1.333333	1	1	1	2	1	2
2.687419	1	1	2	2	0.333333	1
2.828427	2	0	2.867442	2	0	0
0	2.333333	1	1	0.333333	1	1
5.09902	3.399346	2.236068	6.616478	7.695598	3.073181	5.734884
1.490712	3	1.666667	4.346135	4.013865	3	2.108185
7.666667	0.745356	1.414214	6.749486	11.35292	1.414214	5.676462
4.714045	2	0	5.821416	5.676462	1.666667	4.123106
3.59011	17.39093	0.471405	17.46425	6.128259	0.471405	10.76001
2.748737	4.642796	2.357023	6.036923	2.748737	4.642796	1.699673
8	6.036923	3.681787	0.333333	8.724168	4.055175	4.123106
6	8.02773	1.699673	2.333333	4.384315	7.401201	1.490712
12.72792	4.772607	8.333333	10.63015	11.08051	10.20349	10.93415
1.943651	0	0.745356	0	0.745356	1	0
0	5	1.414214	6.146363	1.943651	5.705748	5.696002
1	1.943651	1	2.426703	1.414214	1.943651	1.943651
0	0.745356	0	1.666667	0	1.666667	1.666667
1	1	1	1.414214	1	0.942809	1.943651
3	0.471405	0.471405	1.666667	2.666667	1	0.471405
1.666667	4	2.236068	3	1.885618	3.162278	3.162278
1.795055	7.923243	3.399346	8.498366	3.399346	7.520343	7.781745
0.333333	8.232726	0.745356	5.270463	1	7.803133	5.696002
1.490712	6.128259	2.134375	6.871843	2.134375	6.128259	2.848001
Mean						
3.318669	**2.959388**	**2.997651**	**3.931937**	**3.569123**	**3.251972**	**3.62376**

IPS Accuracy affected by people (LOS) using the ARM-MW database						
The affected Access Point						
AP1	AP2	AP3	AP1, AP2	AP1, AP3	AP2, AP3	AP1, AP2, AP3
4.772607	1.374369	6.119187	4.333333	4.333333	5.547772	6.368324
7.063207	1.333333	3.018462	7.063207	7.063207	4.853407	4.384315
1.374369	8.749603	3.162278	1.943651	1.943651	3.162278	3.333333
1.054093	3.59011	3.480102	0.666667	0.666667	3.399346	4.472136
2.687419	2.134375	5.676462	4.533824	4.533824	7.845735	9.055385
1.374369	2.981424	2.236068	2.333333	2.333333	9.42809	10.04988

IPS Accuracy affected by people (LOS) using the ARM-MW database						
The affected Access Point						
AP1	AP2	AP3	AP1, AP2	AP1, AP3	AP2, AP3	AP1, AP2, AP3
14.55259	12.97005	5.270463	15.93389	15.93389	9.29755	14.64392
2.134375	2.236068	3.72678	2.828427	2.828427	4.921608	6.324555
2.687419	2.687419	3.681787	3.162278	3.162278	5.906682	7.45356
3.605551	3.605551	2.687419	3.543382	3.543382	5.934831	7.15697
2.828427	2.828427	5	2.867442	2.867442	4.055175	6.749486
8.749603	8.956686	4.533824	9.689628	9.689628	4.921608	14.76106
0.745356	0.745356	2.357023	0.745356	0.745356	1.699673	3
3.333333	2.666667	4	4.384315	4.384315	6.871843	7.781745
1.490712	1.490712	0.745356	1.490712	1.490712	1.490712	1.943651
2.357023	2.357023	3	2.426703	2.426703	3.59011	3.605551
3.14466	2.981424	3.72678	5	5	5.270463	8.339997
9.480975	7.60117	5	10.5935	10.5935	3.282953	15.892
2.357023	1.795055	2.134375	3.681787	3.681787	2	6.036923
1.333333	2.426703	1.414214	2.426703	2.426703	5.374838	4.630815
13.66667	7.695598	3.162278	15.29343	15.29343	9.171211	20.46678
14.4722	8.439326	3.605551	15.3912	15.3912	9.871395	21.187
2.134375	2.748737	4.346135	3.299832	3.299832	4.346135	3.14466
11	11.392	10.5251	22.66912	22.66912	11.45523	19.10497
11.33823	5.705748	1.414214	20.377	20.377	11.45523	17.20788
2	1.414214	12.33784	12.0185	7.195678	10.46688	13.67073
4	3.72678	18.02776	12.4052	8.653837	9.285592	16.71991
0.745356	1.414214	18	1.943651	18.24829	6.472163	6.548961
6.324555	1.666667	5.676462	13.42055	9.803627	5.044249	13.92041
2	1	1	2	2	1	2
0	1.699673	3	1	12.26558	1	9.243616
4	5.270463	1.414214	4.533824	5.656854	3.771236	4.472136
3.605551	4.472136	2.867442	4.242641	7.007932	4.242641	4.242641
4.123106	5.830952	2.236068	5.656854	6.666667	5.467073	5.656854
3.333333	6	1	6	14.55259	5.374838	14.67045
3.480102	6.082763	4.346135	6.082763	13.6178	4.027682	13.74369
4.666667	4.123106	2.357023	0	5.374838	3.681787	3.605551
8.485281	6.574361	5.174725	6	9.339284	1.666667	9.15302
4.123106	7.071068	5.18545	2.538591	13.09792	3.800585	13.09792
3.72678	3.901567	2.236068	3.72678	11.74261	4.384315	5.656854
0.666667	6.699917	0.745356	3.162278	2.666667	4.346135	0.666667
6.082763	3	6.082763	8.062258	7.363574	8.062258	8.062258
0.745356	7.363574	0.942809	4.346135	1	5.705748	3.399346
1.20185	6.699917	1.374369	5.830952	6	5.934831	5.09902
1	1	1	1	1	1	1
1	3.162278	1	3.59011	1	2.687419	4.027682
1.490712	6.574361	7.071068	2.236068	1.699673	7.81025	10.29563
1.795055	7.81025	6.403124	6.749486	2	9.006171	10.20349

IPS Accuracy affected by people (LOS) using the ARM-MW database						
The affected Access Point						
AP1	AP2	AP3	AP1, AP2	AP1, AP3	AP2, AP3	AP1, AP2, AP3
1.795055	2.981424	3.72678	9.735388	7.95124	6.839428	8.498366
3.771236	11.82277	8.800253	11.57104	8.537499	11.60938	10
Mean						
4.078009	**4.577108**	**4.320591**	**6.090635**	**7.022417**	**5.556824**	**8.495002**

APPENDIX G
Initial and Adapted Error

Table G.1 Initial Position and Initial Error

No.	Real Position		People Position			Initial RSSI			Initial Position		Initial Error
	x	y	AP1	AP2	AP3	AP1	AP2	AP3	x	y	
3	2	13	LOS	LOS	LOS	-90	-88	-70	3.67	12.33	2.13
20	4	12	LOS	LOS	LOS	-85	-87	-75	3	13.67	1.94
23	4	9	NLOS	NLOS	NLOS	-86	-84	-61	4.33	11	2
35	6	13	LOS	LOS	LOS	-88	-86	-75	3.67	14.3	2.7
37	6	11	NLOS	NLOS	NLOS	-82	-78	-63	6.3	10.3	0.75
47	7	10	NLOS	NLOS	NLOS	-84	-80	-63	6.67	12.3	2.3
54	8	9	NLOS	NLOS	NLOS	-82	-76	-56	8	9.33	0.33
70	11	11	NLOS	NLOS	NLOS	-78	-83	-59	10.3	10	1.20
85	13	9	NLOS	NLOS	NLOS	-79	-77	-55	11.3	9	1.67
93	14	7	NLOS	NLOS	NLOS	-68	-75	-51	17	7.67	3
104	15	6	NLOS	NLOS	NLOS	-73	-75	-53	16.3	7.67	2.13
112	16	8	NLOS	NLOS	NLOS	-72	-78	-48	17.7	8.67	1.79
116	17	14	NLOS	LOS	NLOS	-78	-84	-57	16.7	13	1.05
120	17	10	LOS	LOS	NLOS	-78	-83	-50	16	7.33	2.85
121	17	9	LOS	LOS	NLOS	-78	-83	-49	16	7.33	1.94
139	19	7	LOS	LOS	NLOS	-71	-82	-46	17.7	7.67	1.49
148	20	7	LOS	LOS	NLOS	-67	-81	-47	17.3	7	2.67
150	20	5	NLOS	NLOS	NLOS	-76	-77	-49	17	7.67	4.01
156	21	11	NLOS	NLOS	NLOS	-74	-76	-55	23.3	11	2.33
168	22	10	NLOS	NLOS	LOS	-71	-76	-59	23	9.67	1.05
194	25	7	NLOS	NLOS	NLOS	-64	-77	-56	26	6.33	1.20
202	26	7	NLOS	NLOS	LOS	-64	-77	-59	29.3	6.33	2.90
222	29	14	NLOS	NLOS	LOS	-68	-76	-67	29.3	13	1.05
223	29	13	NLOS	NLOS	NLOS	-69	-76	-65	29.7	12	1.20
228	29	7	NLOS	NLOS	NLOS	-67	-71	-62	31	7.33	2.03
242	30	5	NLOS	NLOS	LOS	-73	-74	-68	30	7.67	2.67
253	33	4	LOS	LOS	NLOS	-67	-78	-69	32	6.67	2.85
254	33	3	LOS	LOS	NLOS	-68	-77	-72	34.7	3.33	1.7
276	40	7	NLOS	NLOS	LOS	-54	-68	-70	38.3	6	1.94
279	43	7	NLOS	LOS	LOS	-51	-69	-76	45.7	8	2.85
280	44	7	NLOS	LOS	NLOS	-53	-70	-73	40.7	5	2.89
293	47	3	NLOS	NLOS	NLOS	-62	-68	-75	47	5.33	2.33
298	48	5	NLOS	NLOS	NLOS	-62	-66	-73	47.3	4	1.20
304	49	6	LOS	NLOS	LOS	-63	-66	-72	49	4	2
307	49	3	NLOS	LOS	NLOS	-61	-67	-74	47	3.33	2.03

No.	Real Position		People Position			Initial RSSI			Initial Position		Initial Error
	x	y	AP1	AP2	AP3	AP1	AP2	AP3	x	y	
310	50	7	LOS	NLOS	LOS	-66	-61	-71	51	6.33	1.20
316	50	1	NLOS	NLOS	LOS	-66	-73	-83	48	1	2
317	51	7	LOS	NLOS	LOS	-64	-60	-71	53	6	2.24
339	54	12	NLOS	LOS	NLOS	-74	-67	-74	57	13.33	3.28
340	54	11	NLOS	LOS	NLOS	-73	-64	-73	55.3	10.67	1.37
345	54	4	NLOS	LOS	NLOS	-69	-72	-80	52	7	3.61
346	54	3	NLOS	LOS	NLOS	-71	-70	-82	56.7	3.67	2.75
347	54	2	NLOS	LOS	NLOS	-67	-70	-77	53	2.67	1.20
349	55	15	NLOS	LOS	NLOS	-76	-70	-75	57	13.33	2.60
350	55	14	NLOS	LOS	NLOS	-77	-65	-76	55.7	14.67	0.94
356	55	7	LOS	NLOS	LOS	-67	-57	-78	57.3	9	3.07
364	56	13	NLOS	LOS	NLOS	-76	-64	-76	55.7	14.67	1.7
366	56	11	NLOS	NLOS	NLOS	-72	-64	-75	57.3	12.33	1.89
377	57	13	NLOS	LOS	NLOS	-76	-63	-76	55.7	14.67	2.13
378	57	12	NLOS	LOS	NLOS	-75	-67	-75	57	13.33	1.33
396	58	6	LOS	LOS	LOS	-66	-63	-80	56.7	5	1.67
409	60	11	NLOS	NLOS	NLOS	-72	-62	-80	61	11.33	1.05
426	62	12	NLOS	LOS	NLOS	-76	-61	-79	62	14	2
433	63	14	NLOS	NLOS	NLOS	-75	-62	-80	60	13.33	3.07
438	63	7	NLOS	NLOS	NLOS	-64	-54	-79	60	7.33	3.02
460	65	4	NLOS	NLOS	NLOS	-72	-55	-81	65.7	3	1.20
467	66	12	NLOS	LOS	NLOS	-79	-55	-79	65	10.67	1.67
484	67	7	LOS	NLOS	LOS	-73	-46	-84	68	5.33	1.94
490	68	7	LOS	NLOS	LOS	-70	-49	-80	67	9	2.24
491	68	6	LOS	NLOS	LOS	-72	-44	-83	68	7	1
499	70	11	NLOS	LOS	NLOS	-79	-47	-82	66.7	10.67	2.95
508	71	7	NLOS	NLOS	NLOS	-75	-53	-86	70.7	3.67	3.35
515	72	11	NLOS	NLOS	NLOS	-77	-53	-84	72.3	10	1.05
516	72	10	NLOS	LOS	NLOS	-76	-59	-83	71.3	7.67	2.43
522	73	11	LOS	NLOS	LOS	-81	-51	-88	73	10	1
Average of accuracy in initial position											2.04

Table G.2 Adapted position and adapted error

No.	Adapted RSSI			Adapted Position		Adapted Error
	AP1	AP2	AP3	x	y	
3	-85	-83	-65	2.3	13	0.33
20	-80	-82	-70	3.33	12	0.67
23	-85.5	-83.5	-60.5	3.67	9.67	0.75
35	-83	-81	-70	5.3	13.3	0.75
37	-81.5	-77.5	-62.5	6	10.67	0.33
47	-83.5	-79.5	-62.5	6	10.3	1
54	-81.5	-75.5	-55.5	8	9.3	0.33
70	-77.5	-82.5	-58.5	11	11.33	0.34
85	-78.5	-76.5	-54.5	13	9.3	0.33
93	-67.5	-74.5	-50.5	14.67	6.3	0.94
104	-72.5	-74.5	-52.5	14.67	6.33	0.48
112	-71.5	-77.5	-47.5	16.33	8	0.34
116	-77.5	-80	-56.5	16.67	13.67	0.48
120	-73	-78	-49.5	16.67	10	0.34
121	-73	-78	-48.5	16.33	8.67	0.75
139	-66	-77	-45.5	19.67	6.67	0.75
148	-63	-77	-46.5	20.33	6.67	0.48
150	-75.5	-76.5	-48.5	18.33	7.33	2.87
156	-73.5	-75.5	-54.5	21.33	10.33	0.75
168	-70.5	-75.5	-54	22	10.33	0.34
194	-62.5	-75.5	-55.5	25.67	6.67	0.75
202	-63.5	-76.5	-54	26	6.67	0.34
222	-67.5	-75.5	-62	29.33	14.67	0.75
223	-68.5	-75.5	-64.5	29	13.33	0.34
228	-66.5	-70.5	-61	29	6.67	0.34
242	-72.5	-73.5	-63	29.67	6.33	1.38
253	-63	-73	-68.5	32.67	3.67	0.48
254	-63	-72	-71.5	33.67	3.67	0.95
276	-53.5	-67.5	-70	40.67	7	0.67
279	-50.5	-64	-71	42.67	7	0.34
280	-52.5	-65	-72.5	44	7	0
293	-61.5	-67.5	-74.5	47	3.33	0.34
298	-61.5	-65.5	-72.5	48.33	5.33	0.48
304	-59	-65.5	-68	49	6.33	0.34
307	-60.5	-62	-73.5	48.33	3.33	0.75
310	-61	-60.5	-66	50.33	6.67	0.48
316	-66	-73	-82	50.3	1.3	0.47
317	-59	-59.5	-66	50.33	6.67	0.75
339	-72.5	-61	-73.5	54	11.67	0.34
340	-72.5	-59	-72.5	54	11.33	0.34

No.	Adapted RSSI			Adapted Position		Adapted Error
	AP1	AP2	AP3	x	y	
345	-67.5	-67	-79.5	54.33	3.33	0.75
346	-66	-69.5	-77	54.67	3	0.67
347	-66.5	-65	-76.5	54	3	1
349	-75.5	-64	-75.5	55.67	14.67	0.75
350	-76.5	-60	-75.5	55.67	14	0.67
356	-62	-56.5	-73	55	6.67	0.34
364	-75.5	-59	-75.5	56	13.33	0.34
366	-71.5	-63.5	-74.5	56.33	11.67	0.75
377	-75.5	-58	-75.5	56.33	13.33	0.75
378	-74.5	-62	-74.5	57.67	11.67	0.75
396	-61	-58	-75	58	6	0
409	-71.5	-61.5	-79.5	60.67	11	0.67
426	-75.5	-56	-78.5	62	12	0
433	-74.5	-61.5	-79.5	62.33	14	0.67
438	-63.5	-53.5	-78.5	63	6.67	0.34
460	-71.5	-55	-80.5	64.33	3.33	0.95
467	-78.5	-50	-78.5	65.67	12.33	0.48
484	-68	-45.5	-79	67.33	7.33	0.48
490	-65	-48.5	-75	68.33	6.33	0.75
491	-67	-43.5	-78	68.33	6.67	0.75
499	-78.5	-42	-81.5	70	11	0
508	-74.5	-52.5	-85.5	71.33	6.33	0.75
515	-76.5	-52.5	-83.5	72.33	10.67	0.48
516	-75.5	-54	-82.5	72	10	0
522	-76	-50.5	-83	72.33	10.67	0.75
Average of accuracy in adapted/accurate position						0.57

APPENDIX H
Ray Tracing Script on MATLAB


```
% PART ONE
% It is the interface that creates the variables


clear all
clc

%% Ray Tracing Engine Parameters

optimizationMode = 0;              % if 1, then reduces the Rx mesh size to measurement
locations only
plotMode = 1;                      % Ray Tracing engine plot mode
demoMode = 1;                      % Ray Tracing Engine Plot Mode

losFlag = 1;                       % whether or not calculate LoS
reflectionFlag = 1;                % whether or not calculate First reflections
secondReflectionFlag = 1;
reflectExaggerationFac = 1e0;      % Must be 1 unless to emphasize reflection for
demonstration purposes

disableIncidentAngle = 0;          % 1 Disables the incident angle calculation, if
disableIncidentAngle= 1
solidIncidentAngle = 45;           % if disableIncidentAngle =1, then assign this which
overwrites all the incident angles! This is unnecessary feature
polarizationSwap = 1;              % (See notes in HOW THIS WORSK)
                                   % 1, Applies TE to walls and TM to ceiling. 0
applies TM to the walls and TE to the ceiling


imageRSSIScale = 5;                % increase this if number of meshes nodes are small
(skala warna RSSI)
grayScaleImage = 0;


freq = 24e5;                      % frequency in hertz
lightVel = 3e8;                    % kecepatan gelombang EM
lambda = lightVel./freq;
refDistance = 1;                   % Reference distance from Tx (1 meter)
FPSLRefLoss = 0;


antennaGainRes = 40;
antennaEffiLoss = -11.5;           % dB antenna efficiency, missmatch and loss all
together

ceilingEnable = 1;                 % if = 1, Allowing to define ceiling and floor
manually

groundLevel = 0;
ceilingLevel = 3;                  % Height of the ceiling
```

```
mesh_.xNodeNum = 81; %Razak3 =81
mesh_.yNodeNum = 81;
% increase the size for better resolution and especially if you're increasing the
frequency
mesh_.zNodeNum = 1;


%% Antenna Gain pattern calculation

[TxAntennaGainAE] = AntennaTemp (antennaGainRes,demoMode) + antennaEffiLoss; %
TxAntennaGainAE needs to be in dB
RxAntennaGainAE = TxAntennaGainAE;


% Location of the transmitter (s)

Tx.xyz = [8,43,2.9  ];

% power of the transmitter dB(m)
Tx.power =  [-30]; % Ray Power at 1m in dB

% Defining the boundary of the analysis (something like a boundary condition)
boundary = [
            0,80 %RAZAK3
            0,80
            0,3
            ];


% Walls to be defined in a clockwise or counter clockwise manner
%% CLOCK WISE WALL DEFINITION

% Reads the structure from an excel file (see in this code section at the
% top)
% [wallxyz1, wallxyz2, wallxyz3, wallxyz4,wallX,wallY,wallZ] = CSV23D_V1(demoMode,
groundLevel,ceilingLevel,Tx.xyz);
[wallxyz1, wallxyz2, wallxyz3, wallxyz4,wallX,wallY,wallZ] = CSV23D_V1(demoMode,
groundLevel,Tx.xyz);

wall.xyz1 = wallxyz1;
wall.xyz2 = wallxyz2;
wall.xyz3 = wallxyz3;
wall.xyz4 = wallxyz4;

wall.X = wallX;
wall.Y = wallY;
wall.Z = wallZ;


% Define the ceiling of the structure manually if required walls can be
% defined the same fashion
```

```
if ceilingEnable == 1

    ceillFloor.xyz1 = [
                       0,0,ceilingLevel%RAZAK3 sd
                       0,19,ceilingLevel
                       0,37,ceilingLevel
                       0,0,groundLevel
                       0,19,groundLevel
                       0,37,groundLevel%RAZAK3
                        ];

    ceillFloor.xyz2 = [
                        8.5,0,ceilingLevel%RAZAK3
                        12,19,ceilingLevel
                        16,37,ceilingLevel
                        8.5,0,groundLevel
                        12,19,groundLevel
                        16,37,groundLevel%RAZAK3
                        ];

    ceillFloor.xyz3 = [
                        11,19,ceilingLevel%RAZAK3
                        15,37,ceilingLevel
                        16,80,ceilingLevel
                        11,19,groundLevel
                        15,37,groundLevel
                        16,80,groundLevel%RAZAK3
                        ];

    ceillFloor.xyz4 = [
                        0,19,ceilingLevel%RAZAK3
                        0,37,ceilingLevel
                        0,72,ceilingLevel
                        0,19,groundLevel
                        0,37,groundLevel
                        0,72,groundLevel%RAZAK3
                        ];
else

    ceillFloor.xyz1 = [];
    ceillFloor.xyz2 = [];
    ceillFloor.xyz3 = [];
    ceillFloor.xyz4 = [];

end
%=========================================================================
% Relative permittivity of falls can be defined here individually
ep=5.3;
%RAZAK3
kc=6.38;
bt=5.86
```

```
tb=2.7;
wall.relativePerm = [
                        kc;kc;tb;kc;bt;kc;bt;bt% outer wall 1 sd 8 RAZAK
                        ;tb;bt;tb;bt;tb%wall 9 sd 13 RAZAK
                        ;tb;tb;tb;bt;bt;bt;bt;tb%14 sd 21 RAZAK
                        ;kc;kc;tb;tb;tb;tb%22 sd 27 RAZAK
                        ;bt;bt;tb;tb;tb;tb;tb;tb%28 sd 35 RAZAK
                        ;tb;tb;tb;tb;bt;kc%RAZAK
                        ;ep;ep;ep;ep%Er people
                        ;3.08;3.08;3.08;1.5;1.5;1.5%Er lantai & ceiling RAZAK
                        ];
%=========================================================================

%% Adding Ceillilng and Floor to the structure
for i = 1:size(ceillFloor.xyz1,1)

    wall.xyz1 = [wall.xyz1;ceillFloor.xyz1(i,:)];
    wall.xyz2 = [wall.xyz2;ceillFloor.xyz2(i,:)];
    wall.xyz3 = [wall.xyz3;ceillFloor.xyz3(i,:)];
    wall.xyz4 = [wall.xyz4;ceillFloor.xyz4(i,:)];

end


%===================================
% PART TWO
% 3D Ray Tracing Engin
%===================================
% Producing Plan as Image
% finding linear mapping that maps:
% boundary(1,1) ----> 1
% boundary(1,2) ----> mesh.xNodeNum .* imageRSSIScale
% map = alpha .* (x) + beta, where alpha is the expantion fac & beta is shift
alpha.x = (1 - mesh_.xNodeNum .* imageRSSIScale)./(boundary(1,1) - boundary(1,2));
beta.x  = 1 - (boundary(1,1) .* alpha.x);

alpha.y = (1 - mesh_.yNodeNum .* imageRSSIScale)./(boundary(2,1) - boundary(2,2));
beta.y  = 1 - (boundary(2,1) .* alpha.y);


imageBoundary(1,:) = round(alpha.x .* boundary(1,:) + beta.x)
imageBoundary(2,:) = round(alpha.y .* boundary(2,:) + beta.y)

% Shifting all the walls and Tx position
imageWalls.x = (reshape(round((alpha.x .* [wall.xyz1(:,1); wall.xyz2(:,1);wall.xyz3(:,1)⤷
wall.xyz4(:,1)]) + beta.x),size(wall.xyz1,1),4));
imageWalls.y = (reshape(round((alpha.y .* [wall.xyz1(:,2); wall.xyz2(:,2);wall.xyz3(:,2)⤷
wall.xyz4(:,2)]) + beta.y),size(wall.xyz1,1),4));
imageTx.xy(:,1) = round((alpha.x .* Tx.xyz(:,1)) + beta.x);
imageTx.xy(:,2) = round((alpha.y .* Tx.xyz(:,2)) + beta.y);
```

```
%structImage awal
structImage = false(imageBoundary(2,2),imageBoundary(1,2));

%update structImage (pada komponen matrik tertentu 0 diganti 1)
if exist('measurementLocationXyz','var')
    measLoc.xy(:,1) = round((alpha.x .* measurementLocationXyz(:,1)) + beta.x);
    measLoc.xy(:,2) = round((alpha.y .* measurementLocationXyz(:,2)) + beta.y);
    for i = 1:size(measurementLocationXyz,1)
        structImage(measLoc.xy(i,1),measLoc.xy(i,2)) = 1;
    end
end


for i = 1:size(Tx.xyz,1)
    structImage(imageTx.xy(i,1),imageTx.xy(i,2)) = 1;
end

% structImage =  imdilate(structImage,strel('disk',3));

if exist('MATLABStructMode','var')
    if MATLABStructMode == 1
        for j = 1:(size(wall.xyz1,1) - size(ceillFloor.xyz1,1))
            for i = 1:3
                 [wallC,wallR] = bresenham(imageWalls.x(j,i),imageWalls.y(j,i)↙
imageWalls.x(j,i+1),imageWalls.y(j,i+1));%LOS between Tx &Rx
                for k = 1:numel(wallC)
                    structImage(wallC(k),wallR(k)) = 1;
                end
            end
        end
    end
else
    for j = 1:size(wall.xyz1,1)
        for i = 1:3
             [wallC,wallR] = bresenham(imageWalls.x(j,i),imageWalls.y(j,i),imageWalls↙x
(j,i+1),imageWalls.y(j,i+1));%LOS between Tx &Rx
             for k = 1:numel(wallC)
                 structImage(wallC(k),wallR(k)) = 1;
             end
        end
    end
end


structImage = structImage(1:imageBoundary(1,2),1:imageBoundary(2,2));
structImage = imrotate(structImage,90);


if demoMode ==1
    figure
    imshow(structImage)
```

```
end

%% Defining a Finite Panel (wall)

for i = 1:size(wall.xyz1,1)
    wall.minMax.x(i,:) = [min([wall.xyz1(i,1),wall.xyz2(i,1),wall.xyz3(i,1),wall.xyz4(i,
1)]),...
        max([wall.xyz1(i,1),wall.xyz2(i,1),wall.xyz3(i,1),wall.xyz4(i,1)])];
    wall.minMax.y(i,:) = [min([wall.xyz1(i,2),wall.xyz2(i,2),wall.xyz3(i,2),wall.xyz4(i,
2)]),...
        max([wall.xyz1(i,2),wall.xyz2(i,2),wall.xyz3(i,2),wall.xyz4(i,2)])];
    wall.minMax.z(i,:) = [min([wall.xyz1(i,3),wall.xyz2(i,3),wall.xyz3(i,3),wall.xyz4(i,
3)]),...
        max([wall.xyz1(i,3),wall.xyz2(i,3),wall.xyz3(i,3),wall.xyz4(i,3)])];
end



%% 3D Formation of the Structure
if demoMode == 1
    figure
    wall.X = [wall.xyz1(:,1)';wall.xyz2(:,1)';wall.xyz3(:,1)';wall.xyz4(:,1)'];
    wall.Y = [wall.xyz1(:,2)';wall.xyz2(:,2)';wall.xyz3(:,2)';wall.xyz4(:,2)'];
    wall.Z = [wall.xyz1(:,3)';wall.xyz2(:,3)';wall.xyz3(:,3)';wall.xyz4(:,3)'];
    wall.C = zeros(size(wall.X));
    fill3(wall.X, wall.Y, wall.Z,wall.C)
    hold on
    for i = 1:size(Tx.xyz,1)
        plot3(Tx.xyz(i,1),Tx.xyz(i,2),Tx.xyz(i,
3),'LineStyle','none','Marker','*','Color','Red');
    end
    pause(eps) % to show the 3D structure
    xlabel('X')
    ylabel('Y')
    zlabel('Z')
end

    if ~isequal(size(wall.xyz1,1), size(wall.relativePerm,1))
        disp(sprintf(['Error: Geometry & setting dimension mismatch!\nsize(wall.xyz1)=[,'
num2str(size(wall.xyz1)),...
            ']\nsize(wall.relativePerm)=[',num2str(size(wall.relativePerm)),']\nFirst
dimmensions must be of the same size']))
        return
    end
% end


%% Claculating Fresnel Coefficients for Walls

for i = 1:size(wall.xyz1,1)
```

```
    [wall.TE.refFac(i,:),wall.TE.transFac(i,:),wall.TM.refFac(i,:),wall.TM.transFac(i,:)]
= ...
        FresnelCoefficients(1,wall.relativePerm(i,1),0:90,0);

%     disableIncidentAngle =0; % 1 is disabling incident angle.


    if disableIncidentAngle == 1
        wall.TE.refFac(i,:) = repmat(wall.TE.refFac(i,solidIncidentAngle),1,91);
        wall.TE.transFac(i,:) = repmat(wall.TE.transFac(i,solidIncidentAngle),1,91);
        wall.TM.refFac(i,:) = repmat(wall.TM.refFac(i,solidIncidentAngle),1,91);
        wall.TM.transFac(i,:) = repmat(wall.TM.transFac(i,solidIncidentAngle),1,91);
    end


end
    if disableIncidentAngle == 1
%         solidIncidentAngle = 45; % will use this angle for incidence instead
        disp('Angle of incidence is disabled!')
    end


%% Meshing The Boundary Volume
if numel(linspace(boundary(3,1),boundary(3,2),mesh_.zNodeNum)) == 1
    try
        zplaneHeight = Rx.xyz(1,3);
    catch
        zplaneHeight = str2num(str2mat(inputdlg('Please assign the RX simulation
height:','Heigh Assignment')));
    end
    [X,Y,Z] = ndgrid(linspace(boundary(1,1),boundary(1,2),mesh_.xNodeNum),...
    linspace(boundary(2,1),boundary(2,2),mesh_.yNodeNum),...
    zplaneHeight);

else

    [X,Y,Z] = ndgrid(linspace(boundary(1,1),boundary(1,2),mesh_.xNodeNum),...
        linspace(boundary(2,1),boundary(2,2),mesh_.yNodeNum),...
        linspace(boundary(3,1),boundary(3,2),mesh_.zNodeNum));
end


if optimizationMode == 1
    Rx.xyz = Rx.xyz(locationIndex,:);
else
    Rx.xyz = [reshape(X,[],1,1),reshape(Y,[],1,1),reshape(Z,[],1,1)];
end


if demoMode == 1
    plot3(Rx.xyz(:,1),Rx.xyz(:,2),Rx.xyz(:,3),'LineStyle','none','Marker','.');
```

```
    view(2)
end


% Distance Of TX(s) From Every Mesh Node (RXi), Its vector and unit vector
for i = 1:size(Tx.xyz,1)
    RxTx.vec.xyz(:,1:3,i) = repmat(Tx.xyz(i,:),size(Rx.xyz,1),1) - Rx.xyz;
    RxTx.dist(:,1,i) = sqrt(sum(RxTx.vec.xyz(:,1:3,i).^2,2));
    RxTx.unitVec.xyz(:,1:3,i) = RxTx.vec.xyz(:,1:3,i) ./ repmat(RxTx.dist(:,1,i),1,3);
end


%% EQUATING THE PANELS (WALLS) IN 3D
% Find Walls Normals
wall.normal.xyz = (cross(wall.xyz2 - wall.xyz1,wall.xyz3 - wall.xyz1,2));
wall.unitNormal.xyz = wall.normal.xyz ./ repmat(sqrt(sum(wall.normal.xyz.^2,2)),1,3);



for i = 1:size(Tx.xyz,1)
    % Finding Projection of Tx on each panel https://en.wikipedia.org/wiki/Line%E2%80%
93plane_intersection
    Tx.wallProj.xyz(:,:,i) = repmat((dot((wall.xyz1 - repmat(Tx.xyz(i,:),size(wall.xyz1,
1),1)),wall.unitNormal.xyz,2)...
        ./dot(wall.unitNormal.xyz,wall.unitNormal.xyz,2)),1,3).* wall.unitNormal.xyz +
repmat(Tx.xyz(i,:),size(wall.unitNormal.xyz,1),1);
    % Calculating the reflection (mirror) of Tx accross each panel
    Tx.wallReflec.xyz(:,:,i) = repmat(Tx.xyz(i,:),size(wall.unitNormal.xyz,1),1) + 2.*
(Tx.wallProj.xyz(:,:,i) - repmat(Tx.xyz(i,:),size(wall.unitNormal.xyz,1),1));
end


%% Calculating the Second Image of Tx across each wall (every Tx.WallReflec should be
images across all walls).

for i = 1:size(wall.xyz1,1) % only works for first Tx

    % Tx.secondProjWallj.xyz(:,:,x) contains the projections of wall x-th Tx.wallReflec.
xyz (x,:,1)
    Tx.secondProjWallj.xyz(:,:,i) = repmat((dot((wall.xyz1 - repmat(Tx.wallReflec.xyz
(i,:,1),size(wall.xyz1,1),1)),wall.unitNormal.xyz,2)...
        ./dot(wall.unitNormal.xyz,wall.unitNormal.xyz,2)),1,3).* wall.unitNormal.xyz +
repmat(Tx.wallReflec.xyz(i,:,1),size(wall.unitNormal.xyz,1),1);% only works for 1 TX so
(:,:,1)

    Tx.secondReflecWallj.xyz(:,:,i) = repmat(Tx.wallReflec.xyz(i,:,1),size(wall.
unitNormal.xyz,1),1) + 2.* (Tx.secondProjWallj.xyz(:,:,i) - repmat(Tx.wallReflec.xyz(i,
1),size(wall.unitNormal.xyz,1),1));

end
%%
```

```
% Line Vector Between TxReflection & Rx
for i = 1:size(Tx.xyz,1) %
    for j = 1:size(Tx.wallReflec.xyz,1)
        % 4th dimension represents the Tx
        Rx2TxRefl.vec.xyz(:,1:3,j,i) = repmat(Tx.wallReflec.xyz(j,:,i),size(Rx.xyz,1),1)
- Rx.xyz;
        % 3rd dimension represents Tximage across the wall which the reflection took
place
        Rx2TxRefl.dist(:,1,j,i) = sqrt(sum(Rx2TxRefl.vec.xyz(:,1:3,j,i).^2,2));
        Rx2TxRefl.unitVec.xyz(:,1:3,j,i) = Rx2TxRefl.vec.xyz(:,1:3,j,i) ./ repmat
(Rx2TxRefl.dist(:,1,j,i),1,3);
%         Rx2TxRefl.dist(:,1 = sqrt(sum(Rx2TxRefl.xyz.^2,2));
    end
end


%% Calculating LOS Component
if losFlag == 1

    for i = 1:size(Tx.xyz,1)
        % beam angle is measured in relation to the origin, unit vectors of
        % [1,0,0],[0,1,0],[0,0,1]. This depends on the orientation of the TX
        losBeamAngle.Tx.Ele(:,i) = asind(-RxTx.vec.xyz(:,3,i) ./ sqrt(sum(RxTx.vec.xyz
(:,:,i).^2,2)));  % Elevation angle (between beam and Z plane not it's normal) -90<ele<90
degrees
        losBeamAngle.Tx.Azi(:,i) = atan2(-RxTx.vec.xyz(:,2,i),-RxTx.vec.xyz(:,1,i)) *
(180/pi); % Azimuth angle (between x and beam) -180<azi<180

        losBeamAngle.Tx.Ele(find(isnan(losBeamAngle.Tx.Ele(:,i)) == 1),i) = 0;% if nan
turns the beam angle to 0
        losBeamAngle.Tx.Zen(:,i) = abs(90-losBeamAngle.Tx.Ele(:,i)); % Zenith angle is
calculated and used to find the antenna gain
        losBeamAngle.Tx.Azi(find(isnan(losBeamAngle.Tx.Azi(:,i)) == 1),i) = 0;% Azimuth
angle is unlikely to be nan due to use of atan2
        losBeamAngle.Tx.ZenIndex(:,i) = (losBeamAngle.Tx.Zen(:,i)./180).* (antennaGainRes
- 1) + 1; % between 1 to Resolution
        losBeamAngle.Tx.AziIndex(:,i) = ((losBeamAngle.Tx.Azi(:,i) + 180)./360).*
(antennaGainRes - 1) + 1; % between 1 to Resolution

        losBeamAngle.Rx.Ele(:,i) = -1 .* losBeamAngle.Tx.Ele(:,i);
        losBeamAngle.Rx.Zen(:,i) = abs(90 - losBeamAngle.Rx.Ele(:,i));
        losBeamAngle.Rx.Azi(:,i) = atan2(RxTx.vec.xyz(:,2,i),RxTx.vec.xyz(:,1,i)) *
(180/pi);
        losBeamAngle.Rx.Azi(find(isnan(losBeamAngle.Rx.Azi(:,i)) == 1),i) = 0;% Azimuth
angle is unlikely to be nan due to use of atan2
        losBeamAngle.Rx.ZenIndex(:,i) = (losBeamAngle.Rx.Zen(:,i)./180).* (antennaGainRes
- 1) + 1; % between 1 to Resolution
        losBeamAngle.Rx.AziIndex(:,i) = ((losBeamAngle.Rx.Azi(:,i) + 180)./360).*
(antennaGainRes - 1) + 1; % between 1 to Resolution
    end
```

```
    Tx2RxWalljd = zeros(size(wall.xyz1,1),1);
    Tx2RxWalljxyz = zeros(size(wall.xyz1,1),3);
    Tx2RxVec = zeros(size(Tx.xyz,1),3);
    Tx2RxIntersectingWalls = zeros(size(Tx2RxWalljd));
    Rx.LosRssi = zeros(size(Rx.xyz,1),1);

    for k = 1:size(Rx.xyz,1)
        for i = 1:size(Tx.xyz,1)
            Tx2RxVec(i,:) = Rx.xyz(k,:) - Tx.xyz(i,:);% i index is not really needed-
            Tx2RxIntersectingWalls = zeros(size(Tx2RxWalljd));
            incidentAngle = zeros(size(Tx2RxWalljd));
            tempFresnelCoeff = ones(size(Tx2RxWalljd));
            for j = 1:size(wall.xyz1,1)
                % find intersection with each wall and validate it
                Tx2RxWalljd(j) = dot(wall.xyz1(j,:) - Tx.xyz(i,:), wall.normal.xyz(j,:),
2) ./ dot(Tx2RxVec(i,:) , wall.normal.xyz(j,:),2);% Scalar value of the line between TX
& Rx
                if (Tx2RxWalljd(j)<1 && Tx2RxWalljd(j)>0)
                    Tx2RxWalljxyz(j,:) = Tx2RxWalljd(j) .* Tx2RxVec(i,:) + Tx.xyz(i,:);%
Intersection point with wall j
                    if (prod(wall.minMax.x(j,:) - Tx2RxWalljxyz(j,1),2) < eps) && (prod
(wall.minMax.y(j,:) - Tx2RxWalljxyz(j,2),2) < eps) && (prod(wall.minMax.z(j,:)
Tx2RxWalljxyz(j,3),2) < eps)
                        % At this point the intersection is definite
                        Tx2RxIntersectingWalls(j) = 1;
                        % Angle between the beam and intersecting wall
                        incidentAngle(j) = acosd(abs(dot(wall.normal.xyz(j,:),Tx2RxVec
(i,:),2)./...
                            (sqrt(sum(wall.normal.xyz(j,:).^2,2)) .* sqrt(sum(Tx2RxVec
(i,:).^2,2)))));
                        if j < (size(wall.xyz1,1) - size(ceillFloor.xyz1,1) + 1)% checks
if it's wall or ceiling
                            if polarizationSwap == 1 %% Polarization check for walls
                                tempFresnelCoeff (j) = wall.TE.transFac(j,(round
(incidentAngle(j))+1));  % Invoking Temporary Transmission Coefficients for walls
                            elseif polarizationSwap == 0
                                tempFresnelCoeff (j) = wall.TM.transFac(j,(round
(incidentAngle(j))+1));  % Invoking Temporary Transmission Coefficients for walls
                            end
                        else
                           % Polarizaton check for ceiling
                            if polarizationSwap == 1
                                tempFresnelCoeff (j) = wall.TM.transFac(j,(round
(incidentAngle(j))+1));  % Invoking Temporary Transmission Coefficients for Ceiling
                            elseif polarizationSwap == 0
                                tempFresnelCoeff (j) = wall.TE.transFac(j,(round
(incidentAngle(j))+1));  % Invoking Temporary Transmission Coefficients for Ceiling
                            end
                        end
                    end
```

```
            end
        end
%

% 1 - This only measures the loss not the received power so it only works for
%     one TX at the moment.
% 2-  log(FresnelCoeff) need to be subtracted as it procudes negative number, log(0:1)=
0
            Rx.LosRssi(k) = Rx.LosRssi(k) + 10.^((Tx.power(i) - (FPSLRefLoss + 20 *
log10(4*pi*((RxTx.dist(k,1,i) >= refDistance) .* RxTx.dist(k,1,i) + (RxTx.dist(k,1,i) <
refDistance)*refDistance) .* freq ./ lightVel)...
                - 10.*log10(prod(tempFresnelCoeff))) + (TxAntennaGainAE(round
(losBeamAngle.Tx.AziIndex(k,i)),round(losBeamAngle.Tx.ZenIndex(k,i)))) +...
                (RxAntennaGainAE(round(losBeamAngle.Rx.AziIndex(k,i)),round
(losBeamAngle.Rx.ZenIndex(k,i))))/10) .* complex(cos(2*pi*freq*RxTx.dist(k,1,i)
/lightVel + pi) , sin(2*pi*freq*RxTx.dist(k,1,i)./lightVel + pi));
%             Rx.LosRssi(k) = 10.^(Rx.LosRssi(k)./10) .* complex(cos(2*pi*freq*RxTx.
dist(k,1,i)./lightVel + pi) , sin(2*pi*freq*RxTx.dist(k,1,i)./lightVel + pi)); %
converting to linear and multiply by complex carrier
        end
    end

else
    Rx.LosRssi = zeros(size(Rx.xyz,1),1);
end



timestimes = 0;

%% Calculating Multipath & Reflection Components

if reflectionFlag == 1
    for k = 1:size(Rx.xyz,1)
        Rx.reflecjRssi = zeros(size(Tx.wallReflec.xyz,1),size(Tx.xyz,1));
        for i = 1:size(Tx.xyz,1)
            for j = 1:size(Tx.wallReflec.xyz) % this is same as size(wall.xyz1,1)
                TxRef2Rx.vec.xyz = Rx.xyz(k,:) - Tx.wallReflec.xyz(j,:,i);
                TxRef2RxRefwallIntd = dot(wall.xyz1(j,:) - Tx.wallReflec.xyz(j,:,i),
wall.normal.xyz(j,:),2) ./ dot(TxRef2Rx.vec.xyz, wall.normal.xyz(j,:),2);

%                 tempReflecCoeff = 1; % This is in case there is no reflection

                if (TxRef2RxRefwallIntd < 1 && TxRef2RxRefwallIntd > 0)% d checks the
reflection possibility from TxImage j
                    reflectPointj = TxRef2RxRefwallIntd .* TxRef2Rx.vec.xyz + Tx.
wallReflec.xyz(j,:,i);
                    % xyz check the reflection possibility from TxImage j
                    if(prod(wall.minMax.x(j,:) - reflectPointj(1,1),2) < eps) && (prod
(wall.minMax.y(j,:) - reflectPointj(1,2),2) < eps) && (prod(wall.minMax.z(j,:) -
reflectPointj(1,3),2) < eps)
```

```
                        % At this point there is a path for reflection, now
                        % 1- Find the reflection coefficient
                        % 2- Count the walls between reflection paths

                        % 1- Finding Reflection Coefficient
                         tempReflecAngle = acosd(abs(dot(TxRef2Rx.vec.xyz,wall.normal.xyz
(j,:),2) ./ ((sqrt(sum(TxRef2Rx.vec.xyz.^2,2)) .* sqrt(sum(wall.normal.xyz(j,:).^2))))));
                        if  j < (size(wall.xyz1,1) - size(ceillFloor.xyz1,1) + 1)% if
panel is a wall
                            if polarizationSwap == 1
                                tempReflecCoeff = wall.TE.refFac(j,(round
(tempReflecAngle)+1));
                            else
                                tempReflecCoeff = wall.TM.refFac(j,(round
(tempReflecAngle)+1));
                            end
                        else % if panel is either ceiling or floor
                            if polarizationSwap == 1
                                tempReflecCoeff = wall.TM.refFac(j,(round
(tempReflecAngle)+1));
                            else
                                tempReflecCoeff = wall.TE.refFac(j,(round
(tempReflecAngle)+1));
                            end
                        end


                        % 2- now that there is reflection, lets find the walls between
the reflection paths
                         Tx2ReflectPointj = reflectPointj - Tx.xyz(i,:);
                         reflectPointj2Rx = Rx.xyz(k,:) - reflectPointj;
                         Tx2ReflectPointjDist = sqrt(sum(Tx2ReflectPointj.^2,2));
                         reflectPointj2RxDist = sqrt(sum(reflectPointj2Rx.^2,2));

                         Tx2ReflectPointIntersecWall  = zeros(size(wall.xyz1,1),1);
                         reflectPointj2RxIntersecWall = zeros(size(wall.xyz1,1),1);

                        % There is reflection so find the antenna gain and
                        % beam departure angle, departure angle for
                        % reflections, is the angle between reflection
                        % point of the reflecting wall and the TX image.

                         depBeamAngle.Ele = asind(Tx2ReflectPointj(1,3) ./ sqrt(sum
(Tx2ReflectPointj.^2,2)));  % Elevation angle (between beam and Z plane not it's normal)
-90<ele<90 degrees
                         depBeamAngle.Azi = atan2(Tx2ReflectPointj(1,2),Tx2ReflectPointj
(1,1)) * (180/pi); % Azimuth angle (between x and beam) -180<azi<180

                        if isnan(depBeamAngle.Ele)
                             depBeamAngle.Ele = 0;% if nan turns the beam angle to 0
                        end
```

```
                        depBeamAngle.Zen = abs(90-depBeamAngle.Ele); % Zenith angle is
calculated and used to find the antenna gain

                        if isnan(depBeamAngle.Azi)
                            depBeamAngle.Azi = 0;% Azimuth angle is unlikely to be nan
due to use of atan2
                        end

                        depBeamAngle.ZenIndex = (depBeamAngle.Zen /180).* (antennaGainRes
- 1) + 1; % between 1 to antennaGainRes
                        depBeamAngle.AziIndex = ((depBeamAngle.Azi + 180)/360).*
(antennaGainRes - 1) + 1; % between 1 to Resolution


                        % Also Calculating the Angle of Arrival
                        arrBeamAngle.Ele = asin(-reflectPointj2Rx(1,3) ./ sqrt(sum
(reflectPointj2Rx.^2,2)));
                        arrBeamAngle.Azi = atan2(-reflectPointj2Rx(1,2),-reflectPointj2Rx
(1,1)) * (180/pi);

                        if isnan(arrBeamAngle.Ele)
                            arrBeamAngle.Ele = 0;% if nan turns the beam angle to 0
                        end

                        arrBeamAngle.Zen = abs(90-arrBeamAngle.Ele); % Zenith angle is
calculated and used to find the antenna gain

                        if isnan(arrBeamAngle.Azi)
                            arrBeamAngle.Azi = 0;% Azimuth angle is unlikely to be nan
due to use of atan2
                        end

                        arrBeamAngle.ZenIndex = (arrBeamAngle.Zen /180).* (antennaGainRes
- 1) + 1; % between 1 to antennaGainRes
                        arrBeamAngle.AziIndex = ((arrBeamAngle.Azi + 180)/360).*
(antennaGainRes - 1) + 1; % between 1 to Resolution


                        % a- Find Walls Between TX to Reflection point
                        tempTx2ReflpointTransCoeff = ones(size(wall.xyz1,1),1);
                        tempReflpoint2RxTransCoeff = ones(size(wall.xyz1,1),1);
                        for s = 1:size(wall.xyz1,1)
                            % Finding Scalar value of intersection lines
                            Tx2ReflectPointjWallsd = dot(wall.xyz1(s,:) - Tx.xyz(i,:),
wall.normal.xyz(s,:),2)./dot(Tx2ReflectPointj,wall.normal.xyz(s,:),2);
                            reflectPointj2Rxd = dot(wall.xyz1(s,:) - reflectPointj,wall.
normal.xyz(s,:),2) ./ dot(reflectPointj2Rx,wall.normal.xyz(s,:),2);
                            % Checking for finite plane intersection
                            if (Tx2ReflectPointjWallsd < 1 && Tx2ReflectPointjWallsd > 0
&& abs(Tx2ReflectPointjWallsd - 1) > eps)
```

```
                                Tx2ReflectPointjWallsxyz = Tx2ReflectPointjWallsd .*
Tx2ReflectPointj + Tx.xyz(i,:);
                               if(prod(wall.minMax.x(s,:) - Tx2ReflectPointjWallsxyz
(1,1),2) < eps) && (prod(wall.minMax.y(s,:) - Tx2ReflectPointjWallsxyz(1,2),2) < eps) &&
(prod(wall.minMax.z(s,:) - Tx2ReflectPointjWallsxyz(1,3),2) < eps)
                                    % At this point wall s in between
                                     Tx2ReflectPointIntersecWall(s) = 1;
                                     intercepWallsIncAngle.Tx2ReflPoint(s) = acosd(abs(dot
(wall.normal.xyz(s,:),Tx2ReflectPointj,2)./...
                                     (sqrt(sum(wall.normal.xyz(s,:).^2,2)) .* sqrt(sum
(Tx2ReflectPointj.^2,2)))));
                                    if  s < (size(wall.xyz1,1) - size(ceillFloor.xyz1,1)
+ 1) % Transmission Coeffs for the intercepting walls between TX and refl point
                                        if polarizationSwap == 1
                                            tempTx2ReflpointTransCoeff(s) = wall.TE.
transFac(round(intercepWallsIncAngle.Tx2ReflPoint(s))+1);
                                        else
                                            tempTx2ReflpointTransCoeff(s) = wall.TM.
transFac(round(intercepWallsIncAngle.Tx2ReflPoint(s))+1);
                                        end
                                    else % if panel is a wall
                                        if polarizationSwap == 1
                                            tempTx2ReflpointTransCoeff(s) = wall.TM.
transFac(round(intercepWallsIncAngle.Tx2ReflPoint(s))+1);
                                        else
                                            tempTx2ReflpointTransCoeff(s) = wall.TE.
transFac(round(intercepWallsIncAngle.Tx2ReflPoint(s))+1);
                                        end
                                    end
                                end
                            end

                            % b- Find finite walls Between Reflection point and RX. if
below has complicated rule, as the reflectPointj2Rxd tend to
                            % be smaller than matlab's epsilon and sometimes a little bi
smaller than epsilon but bigger than epsm
                            if (reflectPointj2Rxd < 1 && reflectPointj2Rxd > 0 && abs
(reflectPointj2Rxd - 1) > eps && not(reflectPointj2Rxd < epsm))
                                reflectPointj2Rxxyz = reflectPointj2Rxd .*
reflectPointj2Rx + reflectPointj;
                               if(prod(wall.minMax.x(s,:) - reflectPointj2Rxxyz(1,1),2)
< eps) && (prod(wall.minMax.y(s,:) - reflectPointj2Rxxyz(1,2),2) < eps) && (prod(wall.
minMax.z(s,:) - reflectPointj2Rxxyz(1,3),2) < eps)
                                    % At this point wall s in between (reflection poin
to Rx)
                                     reflectPointj2RxIntersecWall(s,1) = 1;
                                     intercepWallsIncAngle.ReflPoint2Rx(s) = acosd(abs(dot
(wall.normal.xyz(s,:),reflectPointj2Rx,2)./...
                                     (sqrt(sum(wall.normal.xyz(s,:).^2,2)) .* sqrt(sum
(reflectPointj2Rx.^2,2)))));
                                    if  s < (size(wall.xyz1,1) - size(ceillFloor.xyz1,1
```

```
+ 1) % Transmission Coeffs for the intercepting walls between TX and refl point
                                        if polarizationSwap == 1
                                            tempReflpoint2RxTransCoeff(s) = wall.TM.
transFac(round(intercepWallsIncAngle.ReflPoint2Rx(s))+1);
                                        else
                                            tempReflpoint2RxTransCoeff(s) = wall.TM.
transFac(round(intercepWallsIncAngle.ReflPoint2Rx(s))+1);
                                        end
                                    else % if panel is either ceiling or floor
                                        if polarizationSwap == 1
                                            tempReflpoint2RxTransCoeff(s) = wall.TM.
transFac(round(intercepWallsIncAngle.ReflPoint2Rx(s))+1);
                                        else
                                            tempReflpoint2RxTransCoeff(s) = wall.TE.
transFac(round(intercepWallsIncAngle.ReflPoint2Rx(s))+1);
                                        end
                                    end

                                end
                            end
                        end % end of for S

                        % found number of walls between reflection paths.
                        % calculate the received signal at Rx from
                        % reflection point on wall j

                         Rx.reflecjRssi(j,i) = 10^((Tx.power(i,:) - (FPSLRefLoss
20*log10(4*pi*(Tx2ReflectPointjDist+reflectPointj2RxDist) .* freq ./ lightVel))
(10*log10(prod(tempTx2ReflpointTransCoeff))) ...
                            + (10*log10(tempReflecCoeff)) + (10*log10(prod
(tempReflpoint2RxTransCoeff))) + (TxAntennaGainAE(round(depBeamAngle.AziIndex),round
(depBeamAngle.ZenIndex))) + ...
                             (RxAntennaGainAE(round(arrBeamAngle.AziIndex),round
(arrBeamAngle.ZenIndex))))/10) ...
                             .* complex(cos(2*pi*freq* Rx2TxRefl.dist(k,1,j,i)./lightVel
pi) , sin(2*pi*freq*Rx2TxRefl.dist(k,1,j,i)./lightVel + pi));

                    end % end of if reflection exist
                end % end of d check for reflection
            end% end of for j
        end % end of for i
        Rx.ReflecRssi(k,1) = sum(sum(Rx.reflecjRssi,1),2);
    end
else
    Rx.ReflecRssi = zeros(size(Rx.xyz,1),1);
end


%% Caclulating Second Reflections (Only works for one Tx).
if secondReflectionFlag == 1
```

```
    Rx.SecondRefRSSI = zeros(size(Rx.xyz,1),1);
    for i = 1:size(Rx.xyz,1)
        Rx.SeconReflWallJRSSI = zeros(size(wall.xyz1,1),1);
        for j = 1:size(Tx.secondReflecWallj.xyz,3)

            %Initializing Parameters for Tx to First Reflection ponit
            Tx2FirstReflPintIntersecWalls = zeros(size(wall.xyz1,1),1);% logs the wall
between Tx and first reflection point on wall J
            Tx2FirstReflPintTransCoeff = ones(size(wall.xyz1,1),1);% logs the Trans
coeff of the wall between the Tx and the first reflection point
            %Initializing Parameters for First to Second Reflection ponit
            first2SecondReflPintIntersecWalls = zeros(size(wall.xyz1,1),1);
            first2SecondReflPintTransCoeff = ones(size(wall.xyz1,1),1);
            %Initializing Parameters for SECOND to Rx path
            second2RxIntersecWalls = zeros(size(wall.xyz1,1),1);
            second2RxReflPintTransCoeff = ones(size(wall.xyz1,1),1);

            Rx.SecondReflWallKRSSI = zeros(size(wall.xyz1,1),1);

            for k = 1:size(Tx.secondReflecWallj.xyz,1)
                if (sum(Tx.secondReflecWallj.xyz(k,:,j) ~= Tx.xyz) ~= 0)% checks if the
Tx.secondReflecWallj lies on the Tx
                    TxSecondRef2Rx.vec.xyz = Rx.xyz(i,:) - Tx.secondReflecWallj.xyz(k,:,
j);
                    TxSecondRef2Rx.dist = sqrt(sum(TxSecondRef2Rx.vec.xyz.^2,2));
                    % Find intersection of Tx.secondReflecWallj with wall k
                     TxSecndRef2wallKIntd = dot(wall.xyz1(k,:) - Tx.secondReflecWallj.xyz
(k,:,j), wall.normal.xyz(k,:),2) ./ dot(TxSecondRef2Rx.vec.xyz, wall.normal.xyz(k,:),2);
                    if (TxSecndRef2wallKIntd < 1 && TxSecndRef2wallKIntd > 0)% check if
there is intersection between the TxSecondreflection and the wall K
                        secondReflectPointK = TxSecndRef2wallKIntd .* TxSecondRef2Rx.
vec.xyz + Tx.secondReflecWallj.xyz(k,:,j);
                        % now check if secondReflectPointK actually lies on the finite
plane(wall) K
                        if (prod(wall.minMax.x(k,:) - secondReflectPointK(1,1),2) < eps
&& (prod(wall.minMax.y(k,:) - secondReflectPointK(1,2),2) < eps) && (prod(wall.minMax.z
(k,:) - secondReflectPointK(1,3),2) < eps)
                            % At this point there is a path for second reflection, now
chekc if there is a valid
                            % path for first reflection (LOS between first reflection
and secondReflectPointK intersects with wall j
                             TxRefj2secondReflectPointK.vec.xyz = secondReflectPointK -
Tx.wallReflec.xyz(j,:);
                             TxRefj2SecondReflectPointKWalljIntd = dot(wall.xyz1(j,:) -
Tx.wallReflec.xyz(j,:), wall.normal.xyz(j,:),2) ./ dot(TxRefj2secondReflectPointK.vec.
xyz, wall.normal.xyz(j,:),2); % Find the intersection of wall j with
TxRef2secondReflectPointK

                            if (TxRefj2SecondReflectPointKWalljIntd < 1 &&
TxRefj2SecondReflectPointKWalljIntd > 0)% check if there is intersection
                                % now that there is intersection
```

```
                                firstReflecPointj = TxRefj2SecondReflectPointKWalljInt
.* TxRefj2secondReflectPointK.vec.xyz + Tx.wallReflec.xyz(j,:);
                               if (prod(wall.minMax.x(j,:) - firstReflecPointj(1,1),2
< eps) && (prod(wall.minMax.y(j,:) - firstReflecPointj(1,2),2) < eps) && (prod(wall.
minMax.z(j,:) - firstReflecPointj(1,3),2) < eps)% check if the intersection lies on a
finite plane
                                % At this point there is a path for second & first
reflections,
                                % 1- Find the reflection coefficient for both first
and second reflections
                                % 2- Count the walls between reflection paths

                                % 1- Finding Reflection Coefficient
                                 tempSecondReflecAngle = acosd(abs(dot
(TxSecondRef2Rx.vec.xyz,wall.normal.xyz(k,:),2) ./ ((sqrt(sum(TxSecondRef2Rx.vec.xyz.^2,
2)) .* sqrt(sum(wall.normal.xyz(k,:).^2))))));
                                 tempFirstReflecAngle  = acosd(abs(dot
(TxRefj2secondReflectPointK.vec.xyz,wall.normal.xyz(j,:),2) ./ ((sqrt(sum
(TxRefj2secondReflectPointK.vec.xyz.^2,2)) .* sqrt(sum(wall.normal.xyz(j,:).^2))))));

                                % Second Reflection factors baised on wall K for
second reflections
                               if  k < (size(wall.xyz1,1) - size(ceillFloor.xyz1,1)
+ 1) % if panel is a wall
                                   if polarizationSwap == 1
                                        tempSecondReflecCoeff = wall.TE.refFac(k,
(round(tempSecondReflecAngle)+1));
                                   else
                                        tempSecondReflecCoeff = wall.TM.refFac(k,
(round(tempSecondReflecAngle)+1));
                                   end
                               else % if panel is either ceiling or floor
                                   if polarizationSwap == 1
                                        tempSecondReflecCoeff = wall.TM.refFac(k,
(round(tempSecondReflecAngle)+1));
                                   else
                                        tempSecondReflecCoeff = wall.TE.refFac(k,
(round(tempSecondReflecAngle)+1));
                                   end
                               end


                               % First Reflection factors baised on wall j for
second reflections
                                if  j < (size(wall.xyz1,1) - size(ceillFloor.xyz1,1)
+ 1) % if panel is a wall
                                   if polarizationSwap == 1
                                        tempFirstReflecCoeff = wall.TE.refFac(j,

(round(tempFirstReflecAngle)+1));
                                   else
                                        tempFirstReflecCoeff = wall.TM.refFac(j,
```

```
(round(tempFirstReflecAngle)+1));
                                    end
                                else % if panel is either ceiling or floor
                                    if polarizationSwap == 1
                                        tempFirstReflecCoeff = wall.TM.refFac(j,
(round(tempFirstReflecAngle)+1));
                                    else
                                        tempFirstReflecCoeff = wall.TE.refFac(j,
(round(tempFirstReflecAngle)+1));
                                    end
                                end

                                % The path of second reflection breaks down into 2
parts. Tx to First Reflection point. First to second
                                % Reflection point. Second reflection point to RX
For each path, walls in between need ot be checked

                                 Tx2FirstReflPoint.vec.xyz = firstReflecPointj - Tx.
xyz;
                                 firstReflPoint2SecondReflPoint.vec.xyz
secondReflectPointK - firstReflecPointj;
                                 secondReflPoint2Rx.vec.xyz = Rx.xyz(i,:)
secondReflectPointK;

                                % checking number of walls between TX and
firstReflectionPoint
                                for l = 1:size(wall.xyz1,1) % checking number of
walls between TX and firstReflectionPoint
                                    if (l ~= j) % unecessary, only for safety
measures as intersection D for same wall is zero.
                                        wallLIntdTx2FirstReflPoint = dot(wall.xyz1
(l,:) - Tx.xyz, wall.normal.xyz(l,:),2) ./ dot(Tx2FirstReflPoint.vec.xyz, wall.normal.xyz
(l,:),2);
                                        if (wallLIntdTx2FirstReflPoint < 1 &&
wallLIntdTx2FirstReflPoint > 0)
                                            wallLintTx2Tx2FirstReflPoint
wallLIntdTx2FirstReflPoint .* Tx2FirstReflPoint.vec.xyz + Tx.xyz;
                                            if (prod(wall.minMax.x(l,:)
wallLintTx2Tx2FirstReflPoint(1,1),2) < eps) && (prod(wall.minMax.y(l,:)
wallLintTx2Tx2FirstReflPoint(1,2),2) < eps) && (prod(wall.minMax.z(l,:)
wallLintTx2Tx2FirstReflPoint(1,3),2) < eps)
                                                % now wall L is in between. Find the
angle of incidence and transmission coefficient
                                                Tx2FirstReflPintIntersecWalls(l,1)
1; % logging the wall in between
                                                tempWallInterceptingAngle(l) = acosd
(abs(dot(wall.normal.xyz(l,:),Tx2FirstReflPoint.vec.xyz,2)./..
                                                (sqrt(sum(wall.normal.xyz(l,:).^2,2))
.* sqrt(sum(Tx2FirstReflPoint.vec.xyz.^2,2)))));% finds the angle between
                                                if  l < (size(wall.xyz1,1) - size
(ceillFloor.xyz1,1) + 1) % Transmission Coeffs for the intercepting walls between TX and
```

```
refl point
                                                    if polarizationSwap == 1
                                                        Tx2FirstReflPintTransCoeff(l)
= wall.TE.transFac(round(tempWallInterceptingAngle(l))+1);
                                                    else
                                                        Tx2FirstReflPintTransCoeff(l)
= wall.TM.transFac(round(tempWallInterceptingAngle(l))+1);
                                                    end
                                                else % if panel is either ceiling or
floor
                                                    if polarizationSwap == 1
                                                        Tx2FirstReflPintTransCoeff(l)
= wall.TM.transFac(round(tempWallInterceptingAngle(l))+1);
                                                    else
                                                        Tx2FirstReflPintTransCoeff(l)
= wall.TE.transFac(round(tempWallInterceptingAngle(l))+1);
                                                    end
                                                end
                                            end % if (prod(wall.minMax.x(j,:)
wallLintTx2Tx2FirstReflPoint(1,1),2) < eps) && (prod(wall.minMax.y(j,:)
wallLintTx2Tx2FirstReflPoint(1,2),2) < eps) && (prod(wall.minMax.z(j,:)
wallLintTx2Tx2FirstReflPoint(1,3),2) < eps)
                                        end % if (wallLintdTx2FirstReflPoint < 1 &&
wallLintdTx2FirstReflPoint > 0).
                                    end % if (l ~= j)
                                end % for l = 1:size(wall.xyz1,1)



                                % checking number of walls between the
FIRSTReflectionPoint and SECONDreflection point
                                for l = 1:size(wall.xyz1,1) % First Reflection Pint
to Second
                                    wallLIntdFirstRefl2SecondReflPoint = dot(wall.
xyz1(l,:) - firstReflecPointj, wall.normal.xyz(l,:),2) ./ dot
(firstReflPoint2SecondReflPoint.vec.xyz, wall.normal.xyz(l,:),2);
                                    if (wallLIntdFirstRefl2SecondReflPoint < 1 &&
wallLIntdFirstRefl2SecondReflPoint > 0)
                                        wallLIntFirstRefl2SecondReflPoint
wallLIntdFirstRefl2SecondReflPoint .* firstReflPoint2SecondReflPoint.vec.xyz
firstReflecPointj;
                                        if (prod(wall.minMax.x(l,:)
wallLIntFirstRefl2SecondReflPoint(1,1),2) < eps) && (prod(wall.minMax.y(l,:)
wallLIntFirstRefl2SecondReflPoint(1,2),2) < eps) && (prod(wall.minMax.z(l,:)
wallLIntFirstRefl2SecondReflPoint(1,3),2) < eps)
                                            % now wall L is in between. Find the
angle of incidence and transmission coefficient

                                            first2SecondReflPintIntersecWalls(l,1)
1; % logging the wall in between
                                            tempWallInterceptingAngle(l) = acosd(abs
```

```
(dot(wall.normal.xyz(l,:),firstReflPoint2SecondReflPoint.vec.xyz,2)./..
                                                (sqrt(sum(wall.normal.xyz(l,:).^2,2)) ↙
sqrt(sum(firstReflPoint2SecondReflPoint.vec.xyz.^2,2)))));% finds the angle between
                                               if  l < (size(wall.xyz1,1) - size↙
(ceillFloor.xyz1,1) + 1) % Transmission Coeffs for the intercepting walls between TX and ↙
refl point
                                                   if polarizationSwap == 1
                                                       first2SecondReflPintTransCoeff(l) ↙
= wall.TE.transFac(round(tempWallInterceptingAngle(l))+1);
                                                   else
                                                       first2SecondReflPintTransCoeff(l) ↙
= wall.TM.transFac(round(tempWallInterceptingAngle(l))+1);
                                                   end
                                               else % if panel is either ceiling or↙
floor
                                                   if polarizationSwap == 1
                                                       first2SecondReflPintTransCoeff(l) ↙
= wall.TM.transFac(round(tempWallInterceptingAngle(l))+1);
                                                   else
                                                       first2SecondReflPintTransCoeff(l) ↙
= wall.TE.transFac(round(tempWallInterceptingAngle(l))+1);
                                                   end
                                               end

                                           end % if (prod(wall.minMax.x(j,:) ↙
wallLintTx2Tx2FirstReflPoint(1,1),2) < eps) && (prod(wall.minMax.y(j,:) ↙
wallLintTx2Tx2FirstReflPoint(1,2),2) < eps) && (prod(wall.minMax.z(j,:) ↙
wallLintTx2Tx2FirstReflPoint(1,3),2) < eps)
                                       end % if (wallLintdTx2FirstReflPoint < 1 && ↙
wallLintdTx2FirstReflPoint > 0).

                                   end % for l = 1:size(wall.xyz1,1)



                                  % checking number of walls between the SECOND ↙
reflection point to the RX.
                                   for l = 1:size(wall.xyz1,1) % SECOND to RX
                                       if (l ~= k) % To Avoid the Same wall that the↙
second Reflection is bouncing of! Although this is for safety really
                                           wallLIntdSecondRef2Rx = dot(wall.xyz1(l,:) ↙
Rx.xyz(i,:), wall.normal.xyz(l,:),2) ./ dot(secondReflPoint2Rx.vec.xyz, wall.normal.xyz↙
(l,:),2);
                                           if (wallLIntdSecondRef2Rx < 1 && ↙
wallLIntdSecondRef2Rx > 0)
                                               wallLIntSecondRef2Rx ↙
wallLIntdSecondRef2Rx .* secondReflPoint2Rx.vec.xyz + secondReflectPointK;
                                               if (prod(wall.minMax.x(l,:) ↙
wallLIntSecondRef2Rx(1,1),2) < eps) && (prod(wall.minMax.y(l,:) - wallLIntSecondRef2Rx↙
(1,2),2) < eps) && (prod(wall.minMax.z(l,:) - wallLIntSecondRef2Rx(1,3),2) < eps)
                                                   % now wall L is in between. Find the↙
```

```
angle of incidence and transmission coefficient

                                                    second2RxIntersecWalls(1,1) = 1;%
logging the wall in between
                                                    tempWallInterceptingAngle(1) = acosd
(abs(dot(wall.normal.xyz(l,:),secondReflPoint2Rx.vec.xyz,2)./..
                                                   (sqrt(sum(wall.normal.xyz(l,:).^2,2))
.* sqrt(sum(secondReflPoint2Rx.vec.xyz.^2,2)))));% finds the angle between
                                                  if  l < (size(wall.xyz1,1) - size
(ceillFloor.xyz1,1) + 1) % Transmission Coeffs for the intercepting walls between TX and
refl point
                                                    if polarizationSwap == 1
                                                        second2RxReflPintTransCoeff
(l) = wall.TE.transFac(round(tempWallInterceptingAngle(l))+1);
                                                    else
                                                        second2RxReflPintTransCoeff
(l) = wall.TM.transFac(round(tempWallInterceptingAngle(l))+1);
                                                    end
                                                  else % if panel is either ceiling or
floor
                                                    if polarizationSwap == 1
                                                        second2RxReflPintTransCoeff
(l) = wall.TM.transFac(round(tempWallInterceptingAngle(l))+1);
                                                    else
                                                        second2RxReflPintTransCoeff
(l) = wall.TE.transFac(round(tempWallInterceptingAngle(l))+1);
                                                    end
                                                  end

                                              end % if (prod(wall.minMax.x(j,:)
wallLintTx2Tx2FirstReflPoint(1,1),2) < eps) && (prod(wall.minMax.y(j,:)
wallLintTx2Tx2FirstReflPoint(1,2),2) < eps) && (prod(wall.minMax.z(j,:)
wallLintTx2Tx2FirstReflPoint(1,3),2) < eps)
                                            end % if (wallLintdTx2FirstReflPoint < 1 &&
wallLintdTx2FirstReflPoint > 0).
                                        end % if (l ~= k)
                                    end % for l = 1:size(wall.xyz1,1)

                                   % There is reflection so find the antenna gain and
                                   % beam departure angle, departure angle for
                                   % reflections, is the angle between reflection
                                   % point of the reflecting wall and the TX image.

                                    depBeamAngle.Ele = asind(Tx2FirstReflPoint.vec.xyz
(1,3) ./ sqrt(sum(Tx2FirstReflPoint.vec.xyz.^2,2))); % Elevation angle (between beam and
Z plane not it's normal) -90<ele<90 degrees
                                    depBeamAngle.Azi = atan2(Tx2FirstReflPoint.vec.xyz
(1,2),Tx2FirstReflPoint.vec.xyz(1,1)) * (180/pi);% Azimuth angle (between x and beam)
-180<azi<180

                                   if isnan(depBeamAngle.Ele)
```

```
                                depBeamAngle.Ele = 0;% if nan turns the beam angle
to 0
                                end

                                depBeamAngle.Zen = abs(90-depBeamAngle.Ele); %
Zenith angle is calculated and used to find the antenna gain

                                if isnan(depBeamAngle.Azi)
                                depBeamAngle.Azi = 0;% Azimuth angle is unlikely to
be nan due to use of atan2
                                end

                                depBeamAngle.ZenIndex = (depBeamAngle.Zen /180)
(antennaGainRes - 1) + 1; % between 1 to antennaGainRes
                                depBeamAngle.AziIndex = ((depBeamAngle.Azi + 180)
/360).* (antennaGainRes - 1) + 1; % between 1 to Resolution


                                % Also Calculating the Angle of Arrival
                                arrBeamAngle.Ele = asin(-secondReflPoint2Rx.vec.xyz
(1,3) ./ sqrt(sum(secondReflPoint2Rx.vec.xyz.^2,2)));
                                arrBeamAngle.Azi = atan2(-secondReflPoint2Rx.vec.xyz
(1,2),-secondReflPoint2Rx.vec.xyz(1,1)) * (180/pi);

                                if isnan(arrBeamAngle.Ele)
                                arrBeamAngle.Ele = 0;% if nan turns the beam angle
to 0
                                end

                                arrBeamAngle.Zen = abs(90-arrBeamAngle.Ele); %
Zenith angle is calculated and used to find the antenna gain

                                if isnan(arrBeamAngle.Azi)
                                arrBeamAngle.Azi = 0;% Azimuth angle is unlikely to
be nan due to use of atan2
                                end

                                arrBeamAngle.ZenIndex = (arrBeamAngle.Zen /180)
(antennaGainRes - 1) + 1; % between 1 to antennaGainRes
                                arrBeamAngle.AziIndex = ((arrBeamAngle.Azi + 180)
/360).* (antennaGainRes - 1) + 1; % between 1 to Resolution


                                % Calculating the Second Reflection of Wall 1:K for
First Reflection being of wall J
                                Rx.SecondReflWallKRSSI(k) = 10^((Tx.power
(FPSLRefLoss + 20*log10(4*pi*(TxSecondRef2Rx.dist) .* freq ./ lightVel)) + (10*log10(prod
(Tx2FirstReflPintTransCoeff)))...
                                + (10*log10(tempFirstReflecCoeff)) + (10*log10(prod
(first2SecondReflPintTransCoeff))) + (10*log10(tempSecondReflecCoeff)) + (10*log10(prod
(second2RxReflPintTransCoeff))) + (TxAntennaGainAE(round(depBeamAngle.AziIndex),round
```

```
(depBeamAngle.ZenIndex))) + ...
                                    (RxAntennaGainAE(round(arrBeamAngle.AziIndex),round
(arrBeamAngle.ZenIndex)))/10) ...
                                    .* complex(cos(2*pi*freq*TxSecondRef2Rx.dist
/lightVel) , sin(2*pi*freq*TxSecondRef2Rx.dist./lightVel));

                                end % if (prod(wall.minMax.x(j,:) - secondReflectPointK
(1,1),2) < eps) && (prod(wall.minMax.y(j,:) - secondReflectPointK(1,2),2) < eps) && (prod
(wall.minMax.z(j,:) - secondReflectPointK(1,3),2) < eps) % check if the intersection lies
on a finite plane
                            end % if (TxRefj2SecondReflectPointKWalljIntd < 1 &&
TxRefj2SecondReflectPointKWalljIntd > 0)
                        end %(prod(wall.minMax.x(j,:) - secondReflectPointK(1,1),2)
eps) && (prod(wall.minMax.y(j,:) - secondReflectPointK(1,2),2) < eps) && (prod(wall.
minMax.z(j,:) - secondReflectPointK(1,3),2) < eps)
                    end %(TxSecndRef2wallKIntd < 1 && TxSecndRef2wallKIntd > 0)
                   % check the validity of the first projection being on the wall
                end % if Tx.secondReflecWallj ~= Tx.xyz
            end % for k = size(Tx.secondReflecWallj.xyz,1)
            Rx.SeconReflWallJRSSI(j) = sum(Rx.SecondReflWallKRSSI);
        end % for j = 1:size(Tx.secondReflecWallj.xyz,3)
        Rx.SecondRefRSSI(i,1) = sum(Rx.SeconReflWallJRSSI);
    end % for i = 1:size(Rx.xyz,1)
else % if secondReflectionFlag == 1
    Rx.SecondRefRSSI = zeros(size(Rx.xyz,1),1);
end % if secondReflection == 1


%% Line Of Sight Propagation Map Only
if losFlag == 1
    Rx.TotalRSSI = 10*log10(abs(Rx.LosRssi));
    Rx.TotalRSSI(find(isinf(Rx.TotalRSSI) == 1)) = 0;

    imageRSSI = zeros(mesh_.yNodeNum,mesh_.xNodeNum,3);
    if mesh_.zNodeNum ~= 1
        zplaneHeight =  linspace(boundary(3,1),boundary(3,2),mesh_.zNodeNum);
    end

    if plotMode == 1
        for i = 1:mesh_.zNodeNum
            Rx.TotalRSSILayer(:,i) = (Rx.TotalRSSI(((i-1)*(mesh_.xNodeNum.*mesh_
yNodeNum)+1):(i*(mesh_.xNodeNum.*mesh_.yNodeNum))));
            imageRSSI = mat2gray(reshape(Rx.TotalRSSILayer(:,i),mesh_.yNodeNum,mesh_
xNodeNum));

            figure
            colormap gray
            imageRSSIScaled = imresize(imrotate(imageRSSI,90),imageRSSIScale);
        %     structImageScaled = imresize(structImage,[size(imageRSSIScaled,1),size
(imageRSSIScaled,2)]);
            imageRSSIScaledOverlayed = imoverlay(imageRSSIScaled,structImage,[0,0,0]);
```

```
            imshow(rgb2gray(imageRSSIScaledOverlayed));
        %     [min(abs(Rx.TotalRSSILayer(:,i))),max(abs(Rx.TotalRSSILayer(:,i)))]
            colorbarLabels = min((Rx.TotalRSSILayer(:,i))) + (0:5) .* ((max(Rx.TotalRSSILayer(:,i))-min(Rx.TotalRSSILayer(:,i)))./5);
            colorbar('YTickLabel',num2str((colorbarLabels'),'%10.1f'));
            title(['LOS Only @ Z-Plane height of ',num2str(zplaneHeight(i),'%10.2f'),';Tx Power = ',num2str(Tx.power')]);

            if grayScaleImage == 0
                colormap(gca,'jet');
            end
        end
    end
end

%% Reflection Propagation Map Only
if reflectionFlag == 1
    Rx.TotalRSSI = 10*log10(abs(Rx.ReflecRssi));
    Rx.TotalRSSI(find(isinf(Rx.TotalRSSI) == 1)) = 0;
    Rx.TotalRSSI(find((Rx.TotalRSSI) == 0)) = min(min(Rx.TotalRSSI));

    imageRSSI = zeros(mesh_.yNodeNum,mesh_.xNodeNum,3);
    if mesh_.zNodeNum ~= 1
        zplaneHeight =  linspace(boundary(3,1),boundary(3,2),mesh_.zNodeNum);
    end

    if plotMode == 1
        for i = 1:mesh_.zNodeNum
            Rx.TotalRSSILayer(:,i) = (Rx.TotalRSSI(((i-1)*(mesh_.xNodeNum.*mesh_.yNodeNum)+1):(i*(mesh_.xNodeNum.*mesh_.yNodeNum))));
            imageRSSI = mat2gray(reshape(Rx.TotalRSSILayer(:,i),mesh_.yNodeNum,mesh_.xNodeNum));

            figure
            colormap gray
            imageRSSIScaled = imresize(imrotate(imageRSSI,90),imageRSSIScale);
        %     structImageScaled = imresize(structImage,[size(imageRSSIScaled,1),size(imageRSSIScaled,2)]);
            imageRSSIScaledOverlayed = imoverlay(imageRSSIScaled,structImage,[0,0,0]);
            imshow(rgb2gray(imageRSSIScaledOverlayed));
        %     [min(abs(Rx.TotalRSSILayer(:,i))),max(abs(Rx.TotalRSSILayer(:,i)))]
            colorbarLabels = min((Rx.TotalRSSILayer(:,i))) + (0:5) .* ((max(Rx.TotalRSSILayer(:,i))-min(Rx.TotalRSSILayer(:,i)))./5);
            colorbar('YTickLabel',num2str((colorbarLabels'),'%10.1f'));
            title(['First Reflections Only@ Z-Plane height of ',num2str(zplaneHeight(i),'%10.2f'),'; Tx Power = ',num2str(Tx.power')]);

            if grayScaleImage == 0
                colormap(gca,'jet');
            end
        end
```

```
    end
end



%% Second Reflection Propagation Map Only
if secondReflectionFlag == 1
    Rx.TotalRSSI = 10*log10(abs(Rx.SecondRefRSSI));
    Rx.TotalRSSI(find(isinf(Rx.TotalRSSI) == 1)) = 0;
    Rx.TotalRSSI(find((Rx.TotalRSSI) == 0)) = min(min(Rx.TotalRSSI));

    imageRSSI = zeros(mesh_.yNodeNum,mesh_.xNodeNum,3);
    if mesh_.zNodeNum ~= 1
        zplaneHeight =  linspace(boundary(3,1),boundary(3,2),mesh_.zNodeNum);
    end

    if plotMode == 1
        for i = 1:mesh_.zNodeNum
            Rx.TotalRSSILayer(:,i) = (Rx.TotalRSSI(((i-1)*(mesh_.xNodeNum.*mesh_.↙
yNodeNum)+1):(i*(mesh_.xNodeNum.*mesh_.yNodeNum))));
            imageRSSI = mat2gray(reshape(Rx.TotalRSSILayer(:,i),mesh_.yNodeNum,mesh_.↙
xNodeNum));

            figure
            colormap gray
            imageRSSIScaled = imresize(imrotate(imageRSSI,90),imageRSSIScale);
            % To Take care of the Blackage
            blackageMask = (imageRSSI == 1);
            blackageMaskScaled = imresize(imrotate(blackageMask,90),imageRSSIScale);
            blackageMaskScaled = blackageMaskScaled | structImage;
        %     structImageScaled = imresize(structImage,[size(imageRSSIScaled,1),size↙
(imageRSSIScaled,2)]);
            imageRSSIScaledOverlayed = imoverlay(imageRSSIScaled,blackageMaskScaled,↙
[0,0,0]);
%             imageRSSIScaledOverlayed = imoverlay(imageRSSIScaledOverlayed,↙
blackageMaskScaled,[0,0,0])
            imshow(rgb2gray(imageRSSIScaledOverlayed));
        %     [min(abs(Rx.TotalRSSILayer(:,i))),max(abs(Rx.TotalRSSILayer(:,i)))]
            colorbarLabels = min((Rx.TotalRSSILayer(:,i))) + (0:5) .* ((max(Rx↙
TotalRSSILayer(:,i))-min(Rx.TotalRSSILayer(:,i)))./5);

            colorbar('YTickLabel',num2str((colorbarLabels'),'%10.1f'));
            title(['Second Reflections Only@ Z-Plane height of ',num2str(zplaneHeight↙
(i),'%10.2f'),'; Tx Power = ',num2str(Tx.power)]);

            if grayScaleImage == 0
                colormap(gca,'jet');
            end
        end
    end
end
```

```
%% Reflection & Line Of Signt Propagation Map
Rx.TotalRSSI = 10*log10(abs(Rx.LosRssi + (reflectExaggerationFac * Rx.ReflecRssi) ↙
(reflectExaggerationFac * Rx.SecondRefRSSI) ));
Rx.TotalRSSIloss = 10*log10(abs(Rx.LosRssi));
Rx.TotalRSSIref1 = 10*log10(abs(reflectExaggerationFac * Rx.ReflecRssi ));
Rx.TotalRSSIref2 = 10*log10(abs(reflectExaggerationFac * Rx.SecondRefRSSI));

P=Rx.TotalRSSI;
P0=Rx.TotalRSSIloss;
errorP=P-P0;
mseP=immse(P,P0);

imageRSSI = zeros(mesh_.yNodeNum,mesh_.xNodeNum,3);
if mesh_.zNodeNum ~= 1
    zplaneHeight =  linspace(boundary(3,1),boundary(3,2),mesh_.zNodeNum);
end

if plotMode == 1
    for i = 1:mesh_.zNodeNum
        Rx.TotalRSSILayer(:,i) = (Rx.TotalRSSI(((i-1)*(mesh_.xNodeNum.*mesh_.yNodeNum) ↙
+1):(i*(mesh_.xNodeNum.*mesh_.yNodeNum))));
        imageRSSI = mat2gray(reshape(Rx.TotalRSSILayer(:,i),mesh_.yNodeNum,mesh_ ↙
xNodeNum));

        figure
        colormap gray
        imageRSSIScaled = imresize(imrotate(imageRSSI,90),imageRSSIScale);
    %     structImageScaled = imresize(structImage,[size(imageRSSIScaled,1),size ↙
(imageRSSIScaled,2)]);
        imageRSSIScaledOverlayed = imoverlay(imageRSSIScaled,structImage,[0,0,0]);
        imshow(rgb2gray(imageRSSIScaledOverlayed));
    %     [min(abs(Rx.TotalRSSILayer(:,i))),max(abs(Rx.TotalRSSILayer(:,i)))]
        colorbarLabels = min((Rx.TotalRSSILayer(:,i))) + (0:5) .* ((max(Rx.TotalRSSILayer ↙
(:,i))-min(Rx.TotalRSSILayer(:,i)))./5);
        colorbar('YTickLabel',num2str((colorbarLabels'),'%10.1f'));
        title(['Z-Plane height of ',num2str(zplaneHeight(i),'%10.2f'),'; LOS = ',num2str ↙
(losFlag),'; Reflec = ',num2str(reflectionFlag),'; Tx Power = ',num2str(Tx.power')]);

        if grayScaleImage == 0
            colormap(gca,'jet');
        end
    end
end
```

LIST OF PUBLICATIONS

INDEXED JOURNALS (PUBLISHED)

No.	Paper	Index
1	**Firdaus,** Noor Azurati Ahmad, and Shamsul Sahibuddin. 2017. "Indoor Positioning System based Wi-Fi Fingerprinting for Dynamic Environment." In Journal of Engineering and Applied Sciences	Scopus (Q3)
2	**Firdaus**, Noor Azurati Ahmad, Shamsul Sahibuddin, "Indoor Positioning System Based on WLAN Fingerprint and User Orientations with Minimum Computation Time" In TELKOMNIKA	Scopus (Q2)
3	**Firdaus**, Noor Azurati Ahmad, Shamsul Sahibuddin, "Accurate Indoor-Positioning Model Based on People Effect and Ray-Tracing Propagation" In SENSORS	ISI (Q1)
4	**Firdaus**, Noor Azurati Ahmad, Shamsul Sahibuddin, Adi Azlan, and Iyad H Alshami. "A Review of Hybrid Indoor Positioning System Using WLAN Fingerprint and Image Processing" In International Journal of Electrical and Computer Engineering Systems	Scopus (Q4)

CONFERENCES (PUBLISHED)

No.	Paper	Index
1	**Firdaus**; Ahmad, N.A.; Sahibuddin, S. Adapted WLAN Fingerprint Indoor Positioning System (IPS) Based on User Orientations. In *Recent Trends in Information and Communication Technology*; Springer: Berlin, Germany, 2017; pp. 226–236.	Springer, ISI
2	**Firdaus**; Ahmad, N.A.; Sahibuddin, S. *Effect of People around User to WLAN Indoor Positioning System Accuracy*. In Proceedings of the Second Palestinian International Conference on Information and Communication Technology (PICICT 2017), Gaza, Palestine, 8-9 May 2017; pp. 17–21.	IEEE, Scopus
3	**Firdaus,** Noor Azurati Ahmad, Shamsul Sahibuddin, Rudzidatul Akmam Dziyauddin. *Modelling the Effect of Human Body around User on Signal Strength and Accuracy of Indoor Positioning*. In Proceedings of 3rd International Conference on Smart Sensors and Application (*ICSSA*). Kuala Lumpur, Malaysia on the 7-9th April 2020	IEEE, Scopus

COPY RIGHT

Human model for dynamic changes in indoor positioning system (LY2019008898)